



Therapeutic stapled peptides: Efficacy and molecular targets

Yulei Li^{a,*}, Minghao Wu^{c,1}, Yinxue Fu^{a,1}, Jingwen Xue^a, Fei Yuan^a, Tianci Qu^a, Anastassia N. Rissanou^e, Yilin Wang^d, Xiang Li^{b,*}, Honggang Hu^{c,*}

^a School of Pharmaceutical Sciences & Institute of Materia Medica, Shandong First Medical University & Shandong Academy of Medical Sciences, Jinan, Shandong 250117, China

^b School of Pharmacy, Second Military Medical University, 325 Guohe Road, Shanghai, 200433, China

^c School of Medicine, Shanghai University, 99 Shangda Road, Shanghai 200444, China

^d Department of Hepatic Surgery, Fudan University Shanghai Cancer Center, Department of Oncology, Shanghai Medical College, Fudan University, 131 Dong'an Road, Shanghai 200032, China

^e Theoretical & Physical Chemistry Institute, National Hellenic Research Foundation, 48 Vassileos Constantinou Avenue, Athens 11635, Greece

ARTICLE INFO

Key words:

Staple peptide
Therapeutic peptide drug
 α -helical peptide
Targets

ABSTRACT

Peptide stapling, by employing a stable, preformed alpha-helical conformation, results in the production of peptides with improved membrane permeability and enhanced proteolytic stability, compared to the original peptides, and provides an effective solution to accelerate the rapid development of peptide drugs. Various reviews present peptide stapling chemistries, anchoring residues and one- or two-component cyclization, however, therapeutic stapled peptides have not been systematically summarized, especially focusing on various disease-related targets. This review highlights the latest advances in therapeutic peptide drug development facilitated by the application of stapling technology, including different stapling techniques, synthetic accessibility, applicability to biological targets, potential for solving biological problems, as well as the current status of development. Stapled peptides as therapeutic drug candidates have been classified and analysed mainly by receptor- and ligand-based stapled peptide design against various diseases, including cancer, infectious diseases, inflammation, and diabetes. This review is expected to provide a comprehensive reference for the rational design of stapled peptides for different diseases and targets to facilitate the development of therapeutic peptides with enhanced pharmacokinetic and biological properties.

1. Introduction

Peptides play a significant role in the advancement of the modern pharmaceutical industry, as well as in the fields of biological and

chemical sciences [1]. To date, about 80 peptide drugs on the global market have been utilised for the treatment of various diseases, including cancer, diabetes, osteoporosis, and viral infections. The search for new peptide therapeutics has steadily continued, with approximately

Abbreviations: RCM, ring-closing metathesis; PPI, protein-protein interaction; HDP, host defense peptide; CuAAC, CuI-catalyzed azide-alkyne cycloaddition; Ugi-4CRs, Ugi four-component reactions; CD, circular dichroism; Hyp, hydroxyproline; Hle, homoleucine; DAC, Diels-Alder [4+2] cycloaddition; MCR, multicomponent reaction; SPs, stapled peptides; BH, Bcl-2 homology; TCF, T cytokine; CBD, β -catenin binding structural domain; EGFR, epidermal growth factor receptor; HER2, human epidermal growth factor 2; AMP, antimicrobial peptide; Mag2, magainin 2; StAMP, stapled AMP; TA, toxin-antitoxin; RNase, ribonuclease; RNAP, RNA polymerase; 6-HB, 6-helix bundle; RBD, receptor-binding domain; HACE2, host cellular angiotensin-converting enzyme 2 receptor; NTD, N-terminal structural domain; CTD, C-terminal structural domain; CA, capsid; CHR, C-terminal heptapeptide repeat region; NHR, N-terminal heptapeptide repeat region; IN, integrase; PIC, pre-integration complex; RSV, respiratory syncytial virus; EBOV-GP2, Ebola virus transmembrane glycoprotein 2; HR, heptapeptide repeat regions; GLP-1, glucagon-like peptide-1; VIP, vasoactive intestinal peptide; VPAC2, vasoactive intestinal peptide receptor 2; GIP, glucose-dependent insulin stimulating peptide; PPAR γ , peroxisome proliferator-activated receptor γ ; GK, glucokinase; PKCa, protein kinase C- α ; IL-1 β , interleukin-1 β ; IL-17, interleukin-17A; SARS-CoV-2, severe acute respiratory syndrome coronavirus 2; NHDF, normal human dermal fibroblast; GSK-3 β , glycogen synthase kinase-3 β ; RANK, nuclear factor- κ B receptor activating factor; RANKL, nuclear factor- κ B receptor activating factor ligand; PTH, parathyroid hormone; PTHrP, parathyroid hormone-related protein; VAMP2, Vesicle Associated Membrane Protein 2; TNF- α , Tumor necrosis factor- α .

* Corresponding authors.

E-mail addresses: fengyunliyu@sina.com (Y. Li), xiangli@smmu.edu.cn (X. Li), hhu66@shu.edu.cn (H. Hu).

¹ These authors made equal contributions to this work.

<https://doi.org/10.1016/j.yphrs.2024.107137>

Received 6 December 2023; Received in revised form 6 March 2024; Accepted 6 March 2024

Available online 23 March 2024

1043-6618/© 2024 The Authors. Published by Elsevier Ltd. This is an open access article under the CC BY-NC-ND license (<http://creativecommons.org/licenses/by-nc-nd/4.0/>).

150 peptides currently in clinical development and > 400 peptides in preclinical studies [2–4]. Over the past 60 years, the number of peptide therapeutics on the market has steadily increased, and peptide sales have continued to rise, along with the expansion of the therapeutic market [4]. Although there has been progress in the development of peptide drugs in recent years, their limitations, which include short circulation time, poor cellular penetration, and conformational flexibility, decrease their affinity to specific targets and hinder their rapid development. To overcome these limitations of peptides as therapeutic agents, several chemical modification strategies have been developed [5–11]. These approaches include N-terminal capping, D-amino acid substitution, pegylation, lipidation, and macrocyclization [4,12–14].

Macrocyclisation improves cell permeability and provides enhanced protein hydrolytic stability. However, the clinical application of cyclic peptides remains challenging, prompting researchers to extensively investigate their physicochemical properties [15,16]. The stapling strategy is one of the most common methods of macrocyclisation strategy, which enhances the peptide α -helical conformation [17]. In general, the peptide stapling method is a strategy that involves the cross-linking of the side chain of the amino acid residue to the terminus of the peptide or the side chain of the amino acid residue to the side chain of the amino acid residue in the native peptide [12,18–22]. The two amino acids selected or replaced are located on the same helical face, and their side chains can be covalently cross-linked to each other. [23–26] For every 3.6 residues in α -helices, $i/i+3$, $i/i+4$ (one-turn staple), $i/i+7$ (two-turn staple), and $i/i+11$ (three-turn staple) positions are aligned along the same helical face, and the covalent connection of these side chains can stabilize the helical conformation (Fig. 1 A). Several chemical reactions have been employed in the development of peptide stapling (Fig. 1B) [27]. The all-hydrocarbon stapling strategy is considered one of the most promising approaches for addressing undruggable targets. The term stapled peptide was first introduced by Verdine et al. (2000). They synthesised several olefin tethers-containing α,α -disubstituted unnatural amino acids and determined the optimal side chain length and the stereochemical properties of ring-closing metathesis (RCM), catalysed by ruthenium in linear peptides [28]. Subsequently, Blackwell and Grubbs expanded on this pioneering work by using Grubbs catalysts to establish a staple between two *O*-allylserine residues of a linear peptide through RCM reaction [29].

In addition to all-hydrocarbon stapling, a growing number of stapling strategies utilising different forms of macrocyclisation chemistry have been developed over the past 20 years. With the rapid development of peptide stapling strategies, they have been increasingly used in drug research. The stapling strategy has two main aspects. On the one hand, it is used to design drugs with well-defined drug targets, including intracellular and extracellular targets, mainly for regulating protein-protein interactions (PPIs) (Fig. 2A) [27,30–33]. Up to 40% of PPIs occur between a protein domain and a short peptide structural region, while about 60% of peptides bind to the protein in helical or helical-like

conformations. Peptides that are involved in these PPIs are potential lead candidates for the development of PPI inhibitors [34]. Furthermore, stapled helical peptides have attracted much attention because of their increased affinity with target proteins, the enhanced cell penetration, and proteolytic resistance. In contrast, stapling strategies have been applied to peptides of natural products that have broad-spectrum activity and are widely found in nature, including endogenous host defence peptides (HDPs) and exogenous toxin peptides (Fig. 2B) [35–41]. These peptides mainly use electrostatic interactions to bind to negatively charged cell membranes and further disrupt them due to their active effects. There are three types of transmembrane pore models: barrel-stave pore, toroidal pore, and carpet model [42–44]. The use of stapling strategies to address the challenges associated with the undruggable properties of peptides has resulted in significant progress in the field of stapled peptide-based therapeutics. This progress has led to advancement in drug research.

In this review, we briefly introduce the reported peptide stapling technologies for drug development in terms of their synthetic availability, potential to solve biological problems, and current status of development. Furthermore, recent advances in the development of stapled peptides as therapeutic drug candidates have been classified and analysed mainly by receptor- and ligand-based stapled peptide design against different diseases, including cancer, infectious diseases, inflammation, diabetes, and others (Fig. 3 and Fig. 4). The purpose of this review is to provide a comprehensive reference for the rational design of stapled peptides for the treatment of different diseases and protein targets, including the choice of different anchored amino acids and various functional cross-linkers. This will facilitate the development of therapeutic peptides with higher synthetic efficiencies and improved biochemical and pharmacokinetic properties.

2. Stapling techniques

The initial peptide side chain cyclisation method mainly uses the reaction between natural amino acids, such as lysine, to form the amide bond with glutamic acid or aspartic acid side chain (Fig. 5A) [45]. Currently, many new stapling methods have emerged to synthesize stapled peptides using unnatural amino acids, natural amino acids, or a combination of unnatural and natural amino acids (Fig. 5) [28,29,46]. These methods involve a variety of chemical reactions, not only to enrich the structure of the stapled peptide, but also to identify α -helix-mediated inhibitors for PPIs. The stapling method with the most significant impact in this field is an all-hydrocarbon stapling strategy that utilizes olefin-bearing unnatural amino acid residues for the design of natural peptides for the treatment of a wide variety of diseases [21,27, 47]. A summary of each methodology and some examples are provided below.

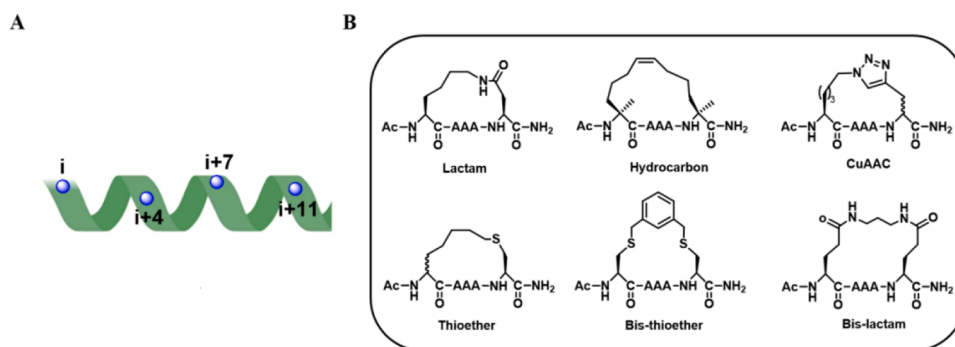


Fig. 1. (A) Amino acid residues on the same helical face are shown in green with i , $i + 4/7/11$ spacing. (B) Stapling strategies by utilising different macrocyclisation chemistry.

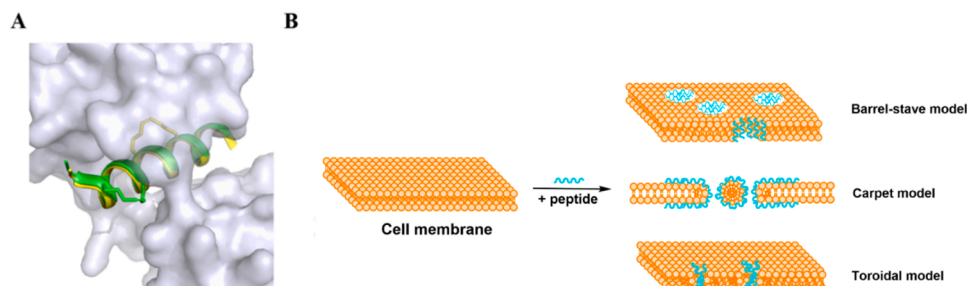


Fig. 2. (A) Regulation model of stapled peptides in PPI. (B) Three kinds of transmembrane pore models, including barrel-stave pore, toroidal pore, and carpet model.

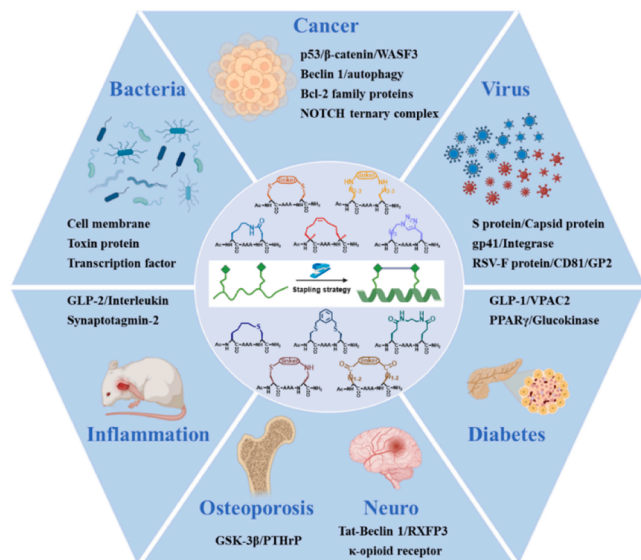


Fig. 3. Stapled peptides for the treatment of various diseases.

2.1. Lactamization

The first stapling strategy of peptides is to form a lactam bridge between the existing amino acid residues Lys and Asp or Glu (Fig. 5A) [48]. Many studies characterized by lactamization have investigated amide bonds with different side chain lengths and localization to optimize the helix stability of different peptide systems [21,49–51]. Although both Asp-Lys and Lys-Asp lactam bridges improve helical stability, Lys-Asp lactamization is preferred because of its improved helix-inducing effect. In addition, the *i, i+4* spacing is the optimal helically constrained structure in stapled peptides with lactam, Lys, and Asp/Glu residues. This configuration cannot be achieved through one-component stapling reactions at the *i, i+7* position [52]. In addition to the lactamization

between Lys and Asp/Glu, two Lys can also act as stapling amino acids in peptide stapling mediated by two-component lactamization (Fig. 5H). Two NHS ester-containing functional cross-linkers were linked to the amino groups of the initialised Lys-Lys residues to provide the bi-lactam-containing stapled peptide [53–55]. The optimal peptide helical stability obtained using the Lys-Lys initialized stapling strategy through lactamization positively correlated with the crosslinkers possessing appropriate rigidity and length. However, high reaction efficiency and reduced byproducts are the main bottlenecks of this stapling method. Similar to Lys-Lys as stapling residues, Glu-Glu-anchored paired residues can also generate a bi-lactam staple through the formation of bisamide (Fig. 5I) [32,56–60]. In addition, Ugi four-component reactions (Ugi-4CRs) were adopted to synthesize Asp-Asp or Glu-Glu stapled peptides, and the results suggested that Glu-Glu stapled peptides had higher helical stability and binding activity than Asp-Asp stapled peptides [32]. In the Glu-Glu or Asp-Asp initialized stapling strategy, the systematic chemical selectivity for other amino acids was not investigated. However, high Ugi staple diversity is a promising strategy for modulating the pharmacological properties and activity of peptides [32].

2.2. Ring-closing metathesis (RCM)

RCM consists of coupling between two terminal alkenes, which results in the formation of a macrocycle connected by a double bond while losing an ethylene molecule (Fig. 5C) [27,47,61]. Both amino acid assembly and RCM reactions were performed on a solid support, and the simple operation procedures make this classical stapling method widely used for various peptide sequences. All-hydrocarbon stapling chemistry based on the RCM reaction has been widely used as a potential therapeutic strategy for designing effective peptide inhibitors. They can target extracellular/intracellular PPIs with shallow binding surfaces, which were previously considered undruggable using small molecular ligands [22,62]. This strategy has also been widely used to improve the enzymatic stability, the broad-spectrum activity, the therapeutic effects, and the drug resistance of linear peptides for cancer and infectious diseases [38–40].

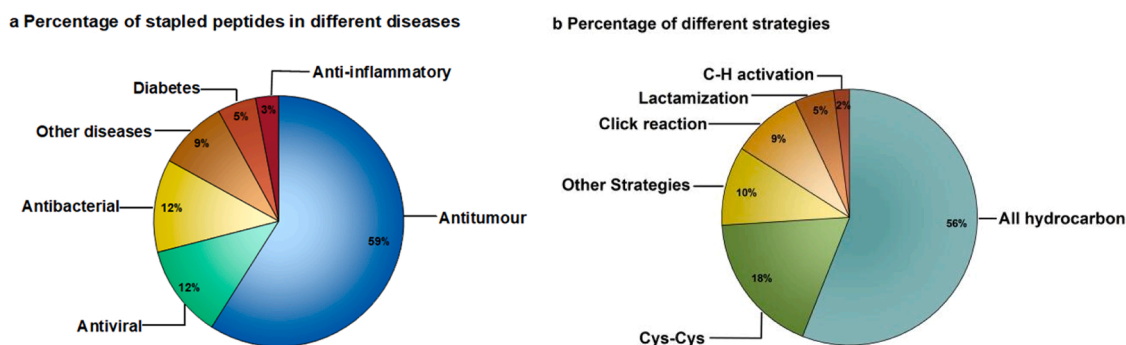


Fig. 4. Application of staple peptides in various diseases.

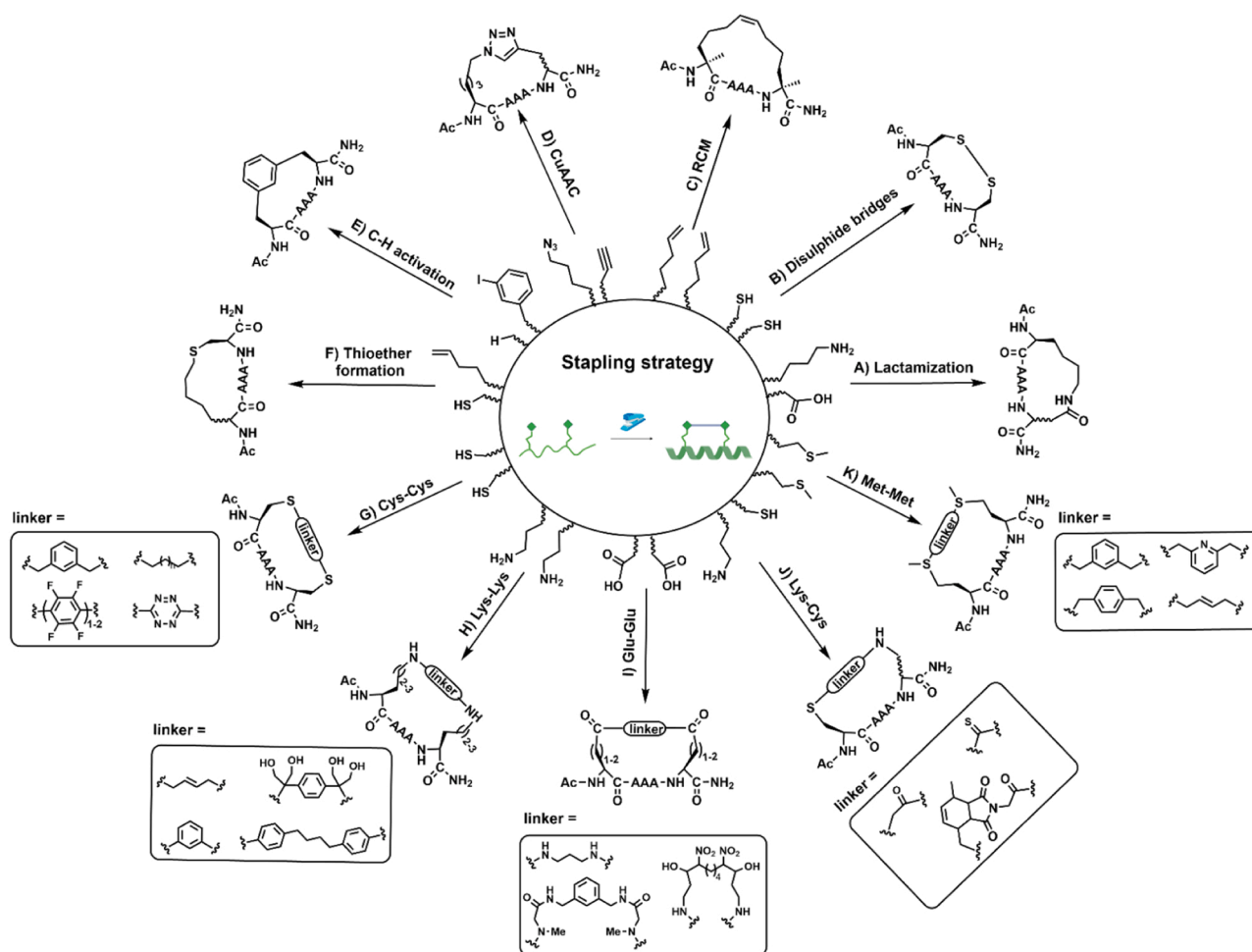


Fig. 5. Representative one-component and multi-component stapling strategies for the preparation of stapled peptides. (A) Lactamisation. (B) Disulphide bridge between two Cys residues. (C) Ring-closing metathesis. (D) Copper(I)-catalysed azide-alkyne cycloaddition. (E) Pd-catalysed C-H activation. (F) Thioether formation. (G) Cys-Cys initialized stapling strategy. (H) Lys-Lys initialised stapling strategy. (I) Glu-Glu initialised stapling strategy. (J) Lys-Cys initialised stapling strategy. (K) Met-Met initialised stapling strategy.

2.3. Cu(I)-catalysed azide-alkyne cycloaddition (CuAAC)

CuAAC, often known as Huisgen cycloaddition or click chemistry, is a critical reaction in biochemistry. Unnatural stapling amino acids, including ω -azido- and ω -yl- α -amino acids, are necessary for the formation of triazole-staple (Fig. 5D). Chorev et al. [63] reported the creation of helical structure, for the first time, through the click chemistry at $i, i + 4$ position in a parathyroid hormone-related peptide. A comparison of side-chain lengths revealed that a staple ring with 5–6 methylene units was able to stabilize the peptide helix; in contrast, other lengths led to random coil conformations. The $i, i + 4$ spacing of paired residues L-Nle(ϵ -N3)/D-Pra is the optimal choice in one-component peptide stapling with triazole [64]. A significant advantage of the CuAAC chemistry is the high tolerance for various functional groups, so that peptides with unprotected functional groups are able to act as linear precursors for the formation of triazole-staple. Given its high biocompatibility and efficiency, CuAAC is the preferred strategy for peptide stapling [52,65].

2.4. C-H activation

C-H activation reaction is employed for the formation of a C(sp³)-C(sp²) bond between the aryl groups in the iodine-containing Phe and the β -carbon in Ala with phthaloyl-protected amino acid (Fig. 5E) [66–68]. Liquid-phase cyclisation of various tetrapeptides by using

C-terminal *m*-iodine-containing phenylalanine and N-terminal Ala showed that the C-H activation reaction tolerated almost all natural amino acids containing common protected or unprotected groups. It is worth noting that this C-H activation stapling reaction has good conversions in the solid phase when transferred from solution. Furthermore, staples with 6- or 7-atom-length at the $i, i + 3$ or $i, i + 4$ positions can be obtained through the C-H activation reaction on the resin, where the paired residues Ala-Phe are not located at the N-terminal or C-terminal, respectively [69]. This strategy enables direct stapling through the C-H activation reaction of complex peptides and lays a foundation for the stapling of novel peptides.

2.5. Cys-Cys initialized stapling strategy

The Cys-Cys initialized stapling strategy mainly involves Cys-alkylation and Cys-arylation, which can be easily and conveniently obtained by cross-linking two thiols with suitable bifunctional agents (Fig. 5G) [70]. Cys-Cys stapled peptide synthesis typically begins with conventional solid-phase assembly and cleavage with global deprotection to provide an unprotected peptide precursor, followed by two thiol cyclisations in solutions with suitable bifunctional linkers. Reducing reagents (TCEP, GSH, and DTT) are generally co-incubated with linear peptide precursors containing Cys before stapling to avoid additional oxidation [71,72]. Although an extra synthetic step and possibly one additional purification step may be required for Cys-Cys

initialised stapling strategy, this approach offers the advantage of avoiding the use of expensive unnatural amino acids or amino acids which contain orthogonal protecting group [73]. Another significant advantage of the Cys-Cys initialized stapling strategy is the ability to easily modify and functionalise stapled peptides using a facile-modified crosslinker.

2.6. Other strategies

While the most established techniques utilize the five aforementioned stapling strategies, other stapling reactions also show promising applications for stapled peptide synthesis, including thioether formation (Fig. 5F) [74–77], Lys-Lys initialized *N*-alkylation or *N*-aromatisation (Fig. 5H) [78–80], Lys-Cys initialised peptide stapling (Fig. 5J), and Met-Met through chemoselective bis-alkylation (Fig. 5K) [81–84]. Several studies have highlighted the progress made in these fields [20, 21, 27, 33, 34, 47, 85]. Herein, we mainly focus on a summary and discussion of the broad application of peptide stapling in the treatment of various diseases to further promote the rational design of peptide stapling and development of stapled peptide drugs.

3. Current application of stapled peptides in diseases

3.1. Stapled peptides in the treatment of tumour

Tumours are one of the main causes of death worldwide, and chemotherapy is the most common therapeutic strategy [86–88]. Peptide drugs have higher activity and selectivity than small molecule drugs and lower cost than protein drugs [89–91]. However, the inherent nature of peptides, which makes them susceptible to enzymatic degradation, limits the clinical application of anti-tumour peptide drugs. The stapling strategy provides a promising modification solution to improve the stability and selectivity of peptide drugs (Table 1) [92–95]. In the following section, we summarise the progress in the use of stapling strategy for the development of anti-tumour drugs, offering insights for future anti-tumour peptide drug development.

3.1.1. Anti-tumour stapled peptides based on p53-MDM2

p53 is an important oncogene, and deletions and mutations in the p53 gene are important causes of tumorigenesis [113, 114]. MDM2 and MDMX negatively regulate p53 and inhibit p53 activity, leading to the occurrence of tumours [115, 116]. The peptide sequence p53_{14–29} located at the p53 *N*-terminal end can bind and regulate interactions with the hydrophobic cleft of MDM2 [117, 118]. Verdine's group [97] designed 10 stapled peptides based on p53_{14–29} using an all-hydrocarbon stapling strategy. The results showed that stapled

peptides displayed increased α -helicity. The preferred stapled peptide, SAH-p53–8 (Fig. 6a), can transmigrate through cell membranes to induce apoptosis in tumour cells. Subsequently, Verdine's group [98] conducted an in-depth study and found that SAH-p53–8 effectively inhibits MDMX activity. The stapled peptide SAH-p53–8 is a promising dual-target inhibitor of tumour suppression. Wang et al. [100] used SAH-p53–8 as a template to mutate S₅ and R₈ of the i, i+7 site previously used for cyclisation to a cysteine, which was then stapled with 1,7-octadiene or 1,8-nonadiene through thiol-ene stapling to form the stapled peptides SAH-p53–8 and SAH-p53–14. Compared to unstapled peptides, stapled peptides exhibited a higher degree of α -helicity. In addition, the potency of the inhibition of block p53-MDM2 interactions was investigated, and the stapled peptide SAH-p53–14 (Fig. 6a) with a nine-carbon linker showed the most pronounced effect, with a 3- to 4-fold enhancement over the linear peptide. Therefore, the thiol-ene stapling approach complements the classical RCM approach in the synthesis of stapled peptides.

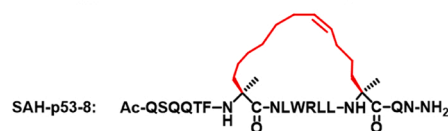
Chen et al. [119] used phage display technology to identify a peptide PDI that was 300-fold more potent than the p53_{14–29} peptide in disrupting the binding of MDM2/MDMX-p53. Chang et al. [31] optimized PDI to improve both its biological and biophysical properties using an all-hydrocarbon stapling strategy. The stapled peptide ATSP-7041 (Fig. 6b) showed significant tumour inhibitory activity *in vitro* and *in vivo*, 7-fold higher α -helicity than PDI, and 50-fold higher inhibitory activity against SJS-1 human osteosarcoma cell growth relative, compared with SAH-p53–8. However, limitations in mass production due to the presence of the unnatural Cba amino acid and the intention to obtain higher cellular activity prompted further optimisation of ATSP-7041 through Leu substitution for Cba, Ala substitution for Ser, and the addition of five Ala residues at the C-terminus. This led to the development of the clinical drug candidate ALRN-6924. ALRN-6924 (Fig. 6b) [120–124], is a stapled peptide and the first MDM2/MDMX dual inhibitor to enter the clinic, which mimics the N-terminal domain of the tumour suppressor protein p53. Based on the x-ray co-crystal structure of ALRN-6924 bound to MDMX [31] (Fig. 6b), it was discovered that Phe19, Trp23, Leu26, and Tyr22 from ALRN-6924 are key binding Residues. ALRN-6924 exhibits a high affinity for binding to both MDM2 and MDMX, leading to the activation of the cellular p53 signaling pathway. In the cell proliferation assay, penta-L-alanyl-D-alaninamide incorporation at the C-terminal moiety of ALRN-6924 enhanced the cellular potency by 3 folds, compared with ATSP-7041. Meanwhile, proteolysis of ALRN-6924 in cells produces an active metabolite, ALRN-8714 (Fig. 6b), with long-acting activity, potent binding activity to MDM2 and MDMX, and slow dissociation kinetics. Moreover, ALRN-6924 at high doses showed anticancer activity by binding to MDM2/MDMX, and at lower doses, it temporarily blocked the cell cycle

Table 1

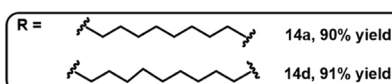
Application of stapled peptides in the treatment of tumour.

Template peptide	The target	Location	Strategy	Ref.
p53 _{14–29} : LSQETFSDLWKLLPEN	p53-MDM2	Intracellular	All hydrocarbon; Lactamization; Diels-Alder cyclization reaction; Ugi-MCR	[32,96–100]
PMI-N8A: TSFAEYWNLSP	p53-MDM2	Intracellular	All hydrocarbon; Lys-Cys	[73,93,101]
PDI: LTFEHYWAQLTS	p53-MDM2	Intracellular	<i>N</i> -arylation of lysine	[31,78]
MAML _{121–136} : β -Ala-ERLRRRIELCRRHHST	NOTCH ternary complex	Intracellular	All hydrocarbon	[102]
BID BH3: EDIIRNIARHLAQVGDSDNRSIW	Bcl-2 family proteins	Intracellular	All hydrocarbon	[46]
MCL-1 BH3: KALETLRVGDGVQRNHETAF	Bcl-2 family proteins	Intracellular	All hydrocarbon	[103]
Bcl-xL/Bak BH3: GQVGRQLAIGDDINR	Bcl-2 family proteins	Intracellular	Azobenzene mediated photoconvertible	[104]
Axin CBD: EENPESILDEHVQRVMK	β -catenin	Intracellular	All hydrocarbon	[100,105,106]
BCL9 α -helical domain 2: EENPESILDEHVQRVMK	β -catenin	Intracellular	All hydrocarbon	[107]
CYFIP1/WASF1 _(26–41) : LECVTNSTLAAIIRQL	WASF1	Intracellular	All hydrocarbon	[108]
Native-P1: RLQLELDEVEKNRKV	Beclin 1	Intracellular	All hydrocarbon	[109,110]
ATG16L1 _{13–33} : WKRHISEQLRRRDLRQL	ATG5-ATG16L1 complex	Intracellular	All hydrocarbon	[111]
K1: DATYTWEHLAWP	LC3/GABARAP	Intracellular	Cysteine stapled	[112]

Anti-tumor stapled peptide based on p53-MDM2

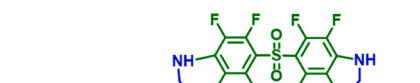
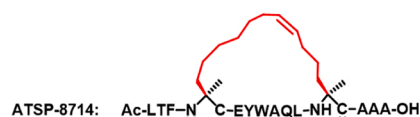
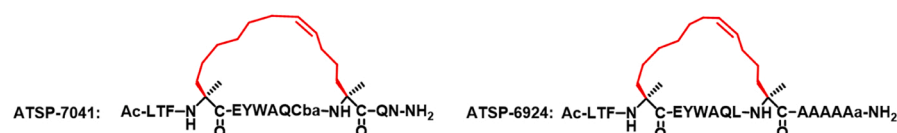
a. Design and biochemical analysis of wild-type p53₁₄₋₂₉-derived stapled peptides SAH-p53-8 and Sp53₁₄₋₂₉₋₁₄WT p53₁₄₋₂₉: Ac-LSQETFSDLWKLLEN-NH₂

Name	Helicity	Cell permeable	K _d (nM)
SAH-p53	11%	no	410±19
SAH-p53-8	85%	yes	55±11

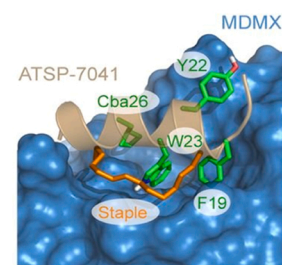
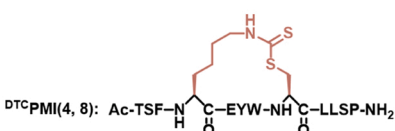
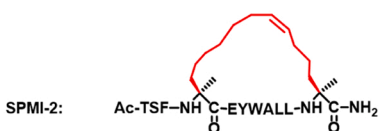
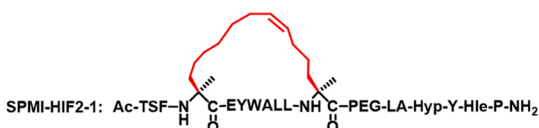


Significant increased helicity and enhanced inhibition compared to the unstapled peptide

b. Design and biochemical analysis of PDI-derived stapled peptides ATSP-7041, ATSP-6924, and SPDI-14 as inhibitors of MDM2 and MDMX

PDI: Ac-LTFEYHWAQLTS-NH₂SPDI-14: Ac-LTF-NH-C-EYWAQL-NH-C-AAAAAa-NH₂

Name	K _d (MDM2)(nM)	K _d (MDMX)(nM)
PDI	14.6	47.4
ATSP-7041	0.9	6.8
ATSP-6924	7.7±3	24.7±17
ATSP-8714	1.4	6.9
SPDI-14	68±1	/

The X-ray co-crystal structure of ALRN-6924 bound to MDMX³¹c. Design of PMI-derived stapled peptides SPMI-2 and D^{TC}PMI (4, 8), and SPMI-2-derived proTAC SMPI-HIF2-1 as inhibitors of MDM2 and MDMXPMI: Ac-TSFAEYWNLSP-NH₂D^{TC}PMI(4, 8): Ac-TSF-NH-C-EYW-NH-C-LLSP-NH₂

Name	Helicity	IC ₅₀ (μM)	K _i (MDMX)(nM)
PMI	9.77%	>100	5.2
SPMI-2	5%	28.4	180
SPMI-HIF2-1	37%	6.7	350
D ^{TC} PMI(4,8)	39.3%	27	1.9

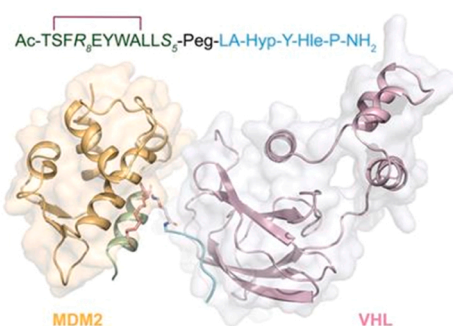
The docking study of SPMI-HIF2-1 with the target protein MDM2 and E3 ligase VHL complex⁹³

Fig. 6. Anti-tumour stapling peptide based on p53-MDM2. Reproduced with permission from Ref. [31,93].

of healthy tissues to protect the cells from the harmful effect of chemotherapy, without protecting cancer cells from p53 mutations. These results advance the use of low-dose ALRN-6924 as a protective agent against the side effects of chemotherapy in cancer patients. Additionally, the investigation of high-dose ALRN-6924 for cancer treatment continued to progress in clinical development, facilitating the

clinical application and development of other stapled peptide drugs [121–124].

To improve the pharmacodynamic and pharmacokinetic characteristics of peptide PDI, Pentelute et al. [78] utilised the lysine *N*-arylation stapling method with two lysine residues at sites *i* and *i*+7 and retained the critical residues of PDI to obtain perfluoro-aromatic stapled

peptides. The stapled peptide SPDI-14 (Fig. 6b) showed improved hydrolytic stability, compared to the linear peptides. Moreover, SPDI-14 showed improved binding, compared with the unstapled peptide, during the evaluation of the effect of the stapled peptides on protein target binding. This method solves the chemical stability problem of cysteine arylation by transforming PDI into a perfluoroaromatic *N*-arylated stapled peptide.

In a study targeting at both MDM2 and MDMX inhibitors, Brown et al. characterized the antagonist Mtide-01 by mutational analysis of amino acid residues in the peptide PMI obtained by phage display technology [125,126]. To obtain antagonists with better stability, the stapled peptide SPMI-2 (Fig. 6c) was designed using Mtide-01 as a template through the all-hydrocarbon stapling strategy [101]. The stapled peptide SPMI-2 possessed extreme and long-lasting *in vitro* p53-activating activity and showed stronger binding to MDM4 than the wild-type p53 stapled peptide SAH-p53-8. However, designing stapled PMI peptides can efficiently activate p53 signalling pathways and inhibit tumour growth *in vivo*, partly because of the rapid accumulation of MDM2 and MDMX in cancer cells. Stapled peptide-based PROTAC (SP-PROTAC), which has a high binding capacity and effectively degrades target proteins, is a novel approach for designing PROTAC. Therefore, our team [93] designed stapled peptide-based proteolytically targeted chimeras (SP-PROTACs) using PMI as a template for designing the stapled peptide SPMI with *i*, *i*+4 or *i*, *i*+7 spacing and selecting the hexapeptide HIF (LA-Hyp-Y-Hle-P) for recruiting VHL. The hydrophobic cave of VHL with the common Ile residue occupied allowed for the introduction of another residue, such as Hle, with a longer side chain, as determined through structural modeling analysis. Therefore, the introduction of Hle not only improved the binding between HIF and VHL, but also enhanced the proteolytic resistance of HIF peptide. Considering the solubility issues, different lengths of polyethylene glycol (PEG) were used as linker chains to connect SPMI and HIF to obtain a series of SP-PROTACs. Optimised SPMI-HIF2-1 (Fig. 6c) displayed more than 20-fold higher cancer cell-killing activity than the template peptide, while promoting typical MDM2 and MDMX degradation and persistent p53 activation. It exhibited superior therapeutic efficiency in subcutaneous and *in situ* colorectal cancer xenograft models, as well as an excellent pharmacokinetic profile. To examine the binding mode of SP-PROTAC with the target proteins and the E3 ligase, the researchers conducted docking studies on the ternary complex comprising SPMI-HIF2-1, MDM2/MDMX, and VHL (Fig. 6c) [93]. As shown in Fig. 6c, SPMI-HIF2-1 bridged and narrowed the distance between MDM2 and VHL. In addition, Lu's group [73] developed a new peptide-stapling strategy in which lysine-cysteine or cysteine-lysine pairs were introduced at site *i*, *i*+4 to form the dithiosemicarbamate (DTC) structure (Fig. 6c). Quantitative studies using fluorescence polarisation and surface plasmon resonance techniques showed that the binding capacity of the Lys-Cys cross-linked stapled peptide ^{DTC}PMI(4,8) to both proteins increased by an order of magnitude, compared with that of the linear peptide. The linear peptide was completely degraded within 30 min in histone G incubation experiments, whereas the half-life of ^{DTC}PMI(4,8) reached 8 h, indicating that the protein hydrolysis stability of the stapled peptide was significantly enhanced. Meanwhile, the protein imprinting results showed that the induction of p53, MDM2, and p21 in the cells increased in a dose-dependent manner after ^{DTC}PMI(4,8) treatment, suggesting that the DTC stapling strategy can help the peptides cross the cell membrane in order to play their roles. This is expected to be an important new approach for developing peptide drugs.

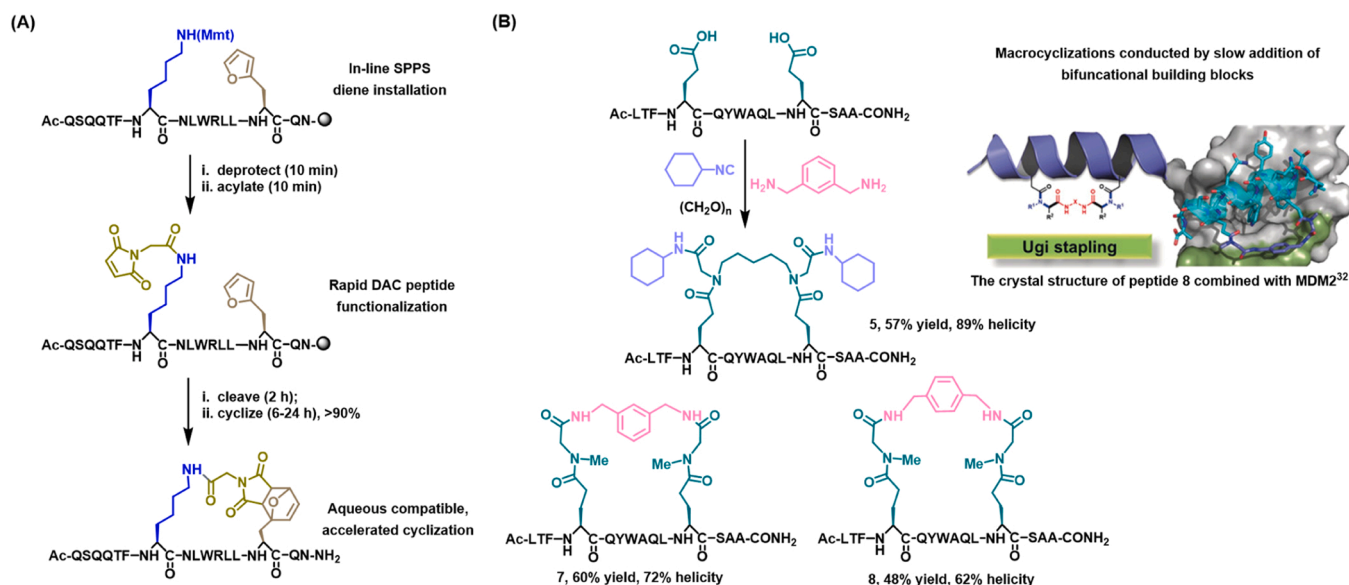
The Diels-Alder [4+2] cycloaddition (DAC) reaction is a classical reaction to construct the cyclohexene skeleton of conjugated dienes and pro-dienophiles, which proceeds quickly with excellent yield and adjustable stereochemical preferences in solid or in aqueous solution [127,128]. Moellering et al. [96] established a cyclisation bridge formed by (2-furan) alanine (AFur) and lysine at position *i*, *i*+7 of a p53-derived peptide sequence by Diels-Alder cyclisation reaction (Scheme 1A). CD results confirmed that the DAC peptide obtained using this strategy had

nearly two-fold stronger α -helical properties than the linear p53 sequence. Thus, the DAC reaction has proved to be a powerful tool for achieving large cyclisation and robust peptide stability.

The multicomponent reaction (MCR) is a versatile synthetic strategy with better stapling functionality, and stapled peptides obtained in this way can be used to generate α -helical peptides mimicking the trans-activating structural domain of p53 [32,129]. Alexander's team [32] modified the previously reported p53 by replacing Glu at position 5 with Gln to avoid its participation in cyclisation and inserting two Asp or Glu at residues 4 and 11 simultaneously to generate linear peptides 1 and 2. The generated linear peptides were subsequently converted to stapled peptides through Ugi macro cyclisation reaction, with *m*-xylene diisocyanate, methylamine, and paraformaldehyde as monofunctional groups into the stapling bridge. Eight stapled peptides (SPs) were produced with high macrocyclisation yields at positions *i* and *i*+7. Peptide 2 (Scheme 1B), containing two Glu residues, was initially selected for the macrocyclisation of double Ugi-MCR using *m*- or *p*-xylylene diisocyanates, methylamine, and paraformaldehyde as monofunctional components. Stapled peptides 7 and 8 were obtained in good yields using a designed synthesis protocol, in which the linear peptide and diisocyanate solution were slowly added separately to the reaction solution containing the preformed imine using an injection pump. A more complex experimental setup is required for the implementation of the dicarboxylic acid/diamine combination to synthesise stapled peptide 5, as it had never been used for the cyclisation of a stapled peptide [130]. Performing imines is known to increase Ugi-MCR yields [131]; hence, the diamine component is first mixed with paraformaldehyde to form imines, and then slowly, the di-imine and dicarboxylic acid-containing linear peptide solutions are added to a stirred solution of cyclohexyl isocyanide. High macrocyclisation yields were obtained for the stapled peptide 5 after 72 h of co-incubation. Alexander et al. tested the anti-MDM2 activity of SPs and found that SPs 5-8 showed high anti-MDM2/MDMX activity, demonstrating that these stapled peptides are effective dual p53-MDM2/MDMX inhibitory antagonists. To elucidate the binding mode of the SPs with their receptor, the researchers crystallized three high affinity SPs (SPs 8) with MDM2. The bound peptide 8 adopts a compact, short, two-turn α -helix conformation (Scheme 1B). Méndez's team [99] further introduced a new MCR approach through combining isonitrile-tetrazine (4+1) cycloaddition and the Ugi-MCR to produce pyrazole amide derivatives. They explored the application of this reaction for peptide stapling, focusing on linking Lys and Glu side chains at *i* and *i*+7 positions in the p53 activating peptide TSFAEYWALLS. After removing Allyl and Alloc protecting groups, they modified the Lys side chain with methyl tetrazine-NHS ester, and reacted the peptides with *n*-BNC overnight to generate stapled peptides 16 and 17. Stapled peptide 16 exhibited an α -helical secondary structure, consistent with other linear and stapled peptides in this family [132]. Additionally, fluorescein isothiocyanate-labelled stapled peptide 17 demonstrated internalization in HCT116 cells. These results showed that multicomponent stapling is an effective strategy for the development of peptide drugs.

3.1.2. Anti-tumour stapled peptides based on NOTCH ternary complexes

The ternary complex generated by the binding of the NOTCH1 receptor intracellular structural domain (ICN1) to the transcription factors CSL and MAML triggers the transcription of NOTCH target genes, leading to tumorigenesis [133,134]. The development of antagonists that act directly on the NOTCH ternary complex could inhibit cancer development. A dominant-negative fragment of the MAML protein MAML₁₂₁₋₁₃₆, expressed in human acute T-lymphoblastic leukaemia (T-ALL) cell lines, was found to antagonise NOTCH signalling and cell proliferation [135,136]. However, this fragment exhibited low proteolytic stability and limited membrane permeability. To address these problems, Moellering et al. [102] synthesised six cell-permeable and stable stapled peptides (SAHMs) derived from MAML₁₂₁₋₁₃₆ by introducing the unnatural amino acid S₅ at positions *i* and *i*+4 through RCM.



Scheme 1. (A) Schematics of DAC-5 peptide synthesis through using Diels-Alder [4+2] cycloadditions. (B) Synthesis of stapled peptides through Ugi-MCR macrocyclisation using the linear peptide containing Glu-Glu residues at positions i, i+7. Reproduced with permission from Ref. [32].

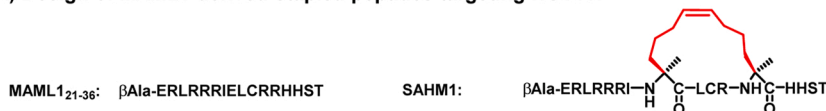
The stapled peptides had higher helicity (2–5 folds) and binding ability, and experiments on NOTCH1-related gene expression showed that the inhibitory activity of the stapled peptide SAHM1 (Fig. 7A) was 8-fold higher than that of the unmodified linear peptide MAML_{121–136}. Moreover, a comparison of the effect on the proliferation of T-ALL cells revealed that cell proliferation in the SAHM1-treated group was significantly reduced, compared with that in the MAML_{121–136}-treated group. In summary, Moellering et al. designed a stapled peptide, SAHM1, targeting NOTCH ternary complexes through an all-hydrocarbon stapling

strategy, which improved the therapeutic effect against leukaemia and provided a theoretical basis for the development of targeted therapies for NOTCH-driven cancers.

3.1.3. Anti-tumour staple peptides based on Bcl-2

Intracellular PPIs are the major control points for many signalling pathways, but they have been often proven not to be targeted by small-molecule chemistry, and they have frequently revealed an extensive, shallow, and hydrophobic protein interface. Stapling approaches, such

(A) Design of MAML1-derived stapled peptides targeting NOTCH



Name	Helicity	K _d (μM)
MAML _{121–36}	23%	/
SAHM1	94%	0.12 ± 0.02

(B) Design of anti-tumor stapled peptides targeting Bcl-2 family proteins

a. Design and biochemical analysis of BID BH3-derived stapled peptides SAHB_A



Name	Helicity	K _d (nM)	t _{1/2} (h)
BID BH3	15.7%	269	3.1
SAHB _A	87.5%	38.8	28.4

b. Design and biochemical analysis of MCL-1 BH3-derived stapled peptides MCL-1 SAHB_D



Name	K _i (μM)	K _d (nM)
MCL-1 BH3	/	245 ± 29
MCL-1 SAHB _D	0.84 ± 0.22	10 ± 3

c. Modification of Bak_{72–87} with the azobenzene crosslinker to form a photocontrollable peptide-based switch



Peptide form	K _d (nM) Bak _{72–87} ⁱ⁺⁷	K _d (nM) Bak _{72–87} ⁱ⁺¹¹
linear	134 ± 16	328 ± 19
Stapled (dark)	825 ± 157	21 ± 1
Stapled (irradiated)	42 ± 9	48 ± 10

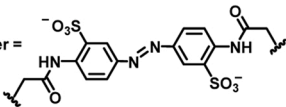
linker = 

Fig. 7. Stapled peptides based on NOTCH and Bcl family proteins. (A) Design of MAML1-derived stapled peptides targeting NOTCH. (B) Design of anti-tumour stapled peptides targeting Bcl-2 family proteins.

as hydrocarbon stapling, can enhance the properties of native peptide sequences, providing an alternative strategy for probing PPIs and manipulating biological pathways. Bcl-2 is an anti-apoptotic protein containing multiple conserved Bcl-2 homology domains (BH) that are highly expressed in some cancer cells and selectively exert anti-tumour effects [137,138]. It has been reported that an amphiphilic α -helical fragment of BH3, the homologous domain of Bcl-2, could bind to the hydrophobic region in the anti-apoptotic domain of BH1, BH2, and BH3, and regulate Bcl-2, thus promoting cell apoptosis [139]. The instability of the secondary structure of this α -helical fragment in its free state leads to increased sensitivity to proteases and difficulty in penetrating cells. To overcome this problem, Walensky et al. [46] used the α -helical peptide BID BH3 from the BH3 region of BID as a model to synthesise five stapled peptides SAHBs by using an all-hydrocarbon stapling strategy. They screened the stapled peptide SAHB_A for its growing potential in terms of helicity, enzymatic stability, binding capacity, and *in vivo* bioactivity (Figure 7Ba). Compared with the model peptide BID BH3, the stapled peptide SAHB_A increased helicity from 15.7% to 87.5%, half-life *in vitro* serum from 3.1 to 29.4 h, and K_d value from 269 to 38.8 nM.

Mcl-1 is an anti-apoptotic protein that belongs to the Bcl-2 family [140]. The overexpression of the Mcl-1 protein protects cancer cells from apoptosis and reduces the sensitivity of cancer cells to drugs, which makes the tumour resistant to a variety of treatments; this makes Mcl-1 a promising therapeutic target for tumours [141,142]. Stewart et al. [103] screened several fragments with α -helical structures in the Bcl-2 structural domain and found that the BH3 peptide sequence of Mcl-1 was an inhibitor of Mcl-1. To enhance protease resistance and cellular permeability of this fragment, an all-hydrocarbon stapling strategy was adopted. A series of stapled peptides Mcl-1 SAHB_x were synthesised, of which Mcl-1 SAHB_D (Figure 7Bb) exhibited the most desirable inhibitory activity with a K_d value of 10 ± 3 nM. Mcl-1 SAHB_D targets MCL-1, thereby neutralising its inhibitory interaction with the pro-apoptotic protein BAK and sensitising cancer cells to the caspase-dependent apoptotic pathway. Stapled-peptide lead compounds that could target this protein are currently under preclinical research.

Bcl-xL interacts with the BH3 region of proapoptotic proteins to regulate apoptosis. Designing inhibitors that target the interaction of Bcl-xL with pro-apoptotic proteins is one of the strategies that can be employed to develop innovative anti-cancer drugs [143]. Allemann et al. [104] designed and synthesized two stapled peptides Bakⁱ⁺⁷₇₂₋₈₇ and Bakⁱ⁺¹¹₇₂₋₈₇ based on the BH3 region Bak₇₂₋₈₇ of the Bcl-xL/Bak complex by introducing the photoactivatable cross-linker 3,3'-bis(sulfo)-4,4'-bis(chloroacetamido) azobenzene at the appropriately spaced cysteine residues (Figure 7Bc). Stapled peptides with stabilized helix had a high Bcl-xL binding affinity for Bakⁱ⁺⁷₇₂₋₈₇ and Bakⁱ⁺¹¹₇₂₋₈₇ with K_d of 42 ± 9 and 21 ± 1 nM, respectively, and up to 20-fold increase in affinity of their dark-adapted states with the helix-destabilized forms. Moreover, Bakⁱ⁺⁷₇₂₋₈₇ and Bakⁱ⁺¹¹₇₂₋₈₇ showed more than 200-fold increase in the selectivity in binding with Bcl-xL, compared to binding with HDM2. This study opens up the possibility of utilising such peptide-based photo-controlled switches to reversibly and selectively interfere with biomacromolecular interactions, offering an avenue for exploring and regulating cellular functions.

3.1.4. Anti-tumour staple peptide based on β -catenin

β -catenin is a key regulator in the Wnt signalling pathway; it plays a critical role in tumour invasion, metastasis, proliferation, and apoptosis [144,145]. The interaction between T cytokine (TCF) and β -catenin is a key downstream node in the Wnt pathway and plays a critical role in tumour cell growth and maintenance, and thus, the regulation of the interaction between the two can inhibit tumour growth [146,147]. Verdine's group [105] considered the β -catenin binding structural domain (CBD) in TCF4 as a candidate template peptide, but the presence of an extended linear peptide sequence that is essential for binding activity makes the CBD sequence potentially defective in terms of its

susceptibility to protein hydrolysis. Therefore, Verdine et al. [105] resumed their search for a suitable template peptide and subsequently found that the binding site of the somatodendritic axis inhibitor (Axin) in the Wnt signalling pathway to β -catenin largely overlaps with that of TCF4 and that the binding domain (CBD) of Axin to β -catenin consists only of an α -helix sequence that is not susceptible to enzymatic hydrolysis. Verdine's group [105] used Axin's CBD as a template peptide and introduced two unnatural amino acids, S5 and R8, into sites i, i+4 and i, i+7 to synthesise three stapled peptides StAx1-3 to enhance the structural stability and protein affinity of the linear peptide Axin's CBD. The results of CD and fluorescein labelling experiments showed that the stapled peptide StAx-3 (Figure 8Aa) had the largest α -helicity and exhibited a significantly enhanced affinity for β -catenin. Verdine's group selected StAx-3 for further optimisation and found that the substitution of hydrophobic residues at position 468, 480, or 481 could further enhance the peptide affinity for β -catenin, resulting in the stapled peptide StAx-3-35R (Figure 8Aa). StAx-3-35R was able to directly antagonise β -catenin and inhibited the Wnt-dependent cancer cell growth in cultured cells. In addition, Wang et al. [100] reported a two-component thiol-ene stapling strategy using the axin-stapled peptide StAx-3 as a template to synthesize a linear peptide by replacing the two S5 at sites i and i+4 previously used for stapling with cysteines and then reacting with 1,7-octadiene or 1,6-hexadiene to achieve stapled peptides. The corresponding stapled peptides were formed through a two-component thiol-ene coupling, showing that the 8-carbon linked stapled peptides exhibited similar α -helicity to the peptide StAx-3 which was synthesized using all hydrocarbon stapling strategy (Figure 8Aa). Moreover, stapled peptides can block the interaction of p53-MDM2 and kill WT p53 HCT-116 cells. These results suggest that the two-component thiol-alkene stapling strategy has the same structural features as the classical RCM stapling approach and that this convenient and versatile peptide stapling strategy can potentially be applied to the modification of natural peptides.

The stapled peptide StAx-3-35R inhibits Wnt signalling at the cellular level by binding to β -catenin. Nevertheless, it remains a challenge to drive StAx-3-35R to inhibit Wnt-dependent tumour growth efficiently *in vivo*, in part due to the rapid β -catenin accumulation in cancer [105]. To overcome the limitations of these inhibitors, our group [106] designed and synthesized a new chimeric peptide inhibitor, StAx-3-35R-VHL, based on the stapled peptide StAx-3-35R by using PROTAC (Figure 8Aa). The stapled peptide StAx-3-35R analogue was used as the part that specifically recognises β -catenin and peptide ALAPYIP was the ligand that recruits VHL ubiquitin ligase [148], the two were conjugated using 6-aminohexanoic acid as a linker to obtain a PROTAC StAx-3-35R-VHL. The StAx-3-35R-VHL showed significant degradation of β -catenin at 12 h post-treatment. In addition, StAx-3-35R-VHL maintained low levels of β -catenin for a much longer time, which suggests that StAx-3-35R-VHL is capable of achieving sustained β -catenin degradation.

BCL9 interacts with β -catenin through its α -helical homology structural domain 2 to drive β -catenin signalling, thereby enhancing tumour cell division, migration, and invasion. Therefore, the inhibition of BCL9/ β -catenin interaction may suppress tumour cell growth [149,150]. Takada et al. [107] used BCL9_{HD2} as a template to design three stapled peptides SAH-BCL9x by employing an all-hydrocarbon stapling strategy, of which SAH-BCL9B (Figure 8Ab) had the highest α -helix. SAH-BCL9B showed 5-fold increase in binding and 4-fold increase in anti-proliferative potency over the template peptide; moreover, it dissociated the natural β -catenins/BCL9 complexes, selectively inhibited Wnt transcription, and exhibited a significant anti-proliferative effect against colon cancer cells.

3.1.5. Anti-tumour stapled peptide based on syndrome protein WASF1

The syndrome protein WASF1 can promote tumour cell movement, invasion, and metabolism, and it is persistently expressed at high levels in highly invasive prostate and breast cancer cells [151]. WASF1

interacts with CYFIP1 protein to form a protein complex, where CYFIP1 stabilises the protein complex; hence, blocking the interaction between WASF1 and CYFIP1 can inhibit the function of WASF1 [108,152,153]. The crystal structure of the WASF1 complex with CYFIP1 reveals the interaction surface between the two and defines an α -helical surface at amino acids 26–41 of CYFIP1, which provides a point of contact between the two proteins (Fig. 8B) [108]. To obtain inhibitors with higher stability, Teng et al. [108] designed and synthesised the stapled peptides WAHM1 and WANM2 through hydrocarbon stapling strategy using amino acid residues at positions 26–41 at the interface of the interactions of CYFIP1 and WASF1 as a template peptide (Fig. 8B). They found that WAHM1 and WANM2 bind to CYFIP1 and prevent WASF3 from binding to CYFIP1. Treatment with WAHM1 or WAHM2 effectively inhibited cellular invasion by 50–75%, compared to cells treated with the control. The inhibition of the interaction between WASF3 and CYFIP1 by stapled peptides designed using the RCM reaction may constitute a promising strategy for preventing tumour invasion and metastasis.

3.1.6. Anti-tumour stapled peptide based on Beclin 1

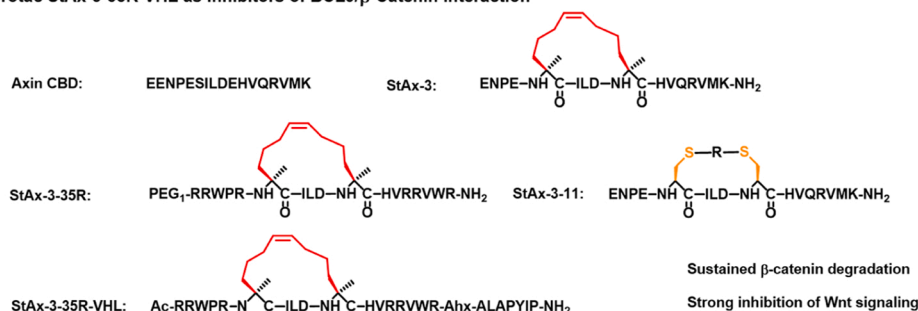
Proteins, such as human epidermal growth factor 2 (HER2) in breast cancer and epidermal growth factor receptor (EGFR) in non-small cell

lung cancer, are degraded by the cellular autophagy pathway mediated by Beclin1, leading to the inhibition of cancer cell proliferation. However, Beclin1 proteins are capable of homodimerisation within the cell, leading to a reduction in the level of cellular autophagy; therefore, targeting Beclin 1 drug design could be a promising method for treating EGFR- or HER2-driven cancers [154].

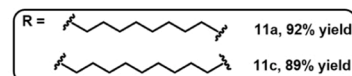
The binding interface of the Beclin1 homodimer was previously modelled by Yang et al., who selected a 15-residue fragment in the binding interface (Fig. 8C) and named it Native-P1 [109]. They predicted that the Native-P1 peptide would bind to the coiled helix structural domain of Beclin 1 to reduce Beclin-1 homodimerisation and achieve enhanced autophagy. However, this fragment suffers from certain problems, including poor structural stability; therefore, they further designed six stapled peptides (i7–01 s to i7–06 s) using Native-P1 as a template peptide and all-hydrocarbon stapling strategy [110]. The predicted binding pattern suggests that the designed i7–01 s scaffold can form stronger interactions with the Beclin 1 coiled-coil structural domain (Fig. 8C). Moreover, they modified amino acid residues based on i7–01 s and designed 75 derived stapled peptides (i7–01 s-01 to i7–01 s-75). The newly synthesised stapled peptide, i7–01 s-31 (Fig. 8C), had a binding affinity for the Beclin1 convoluted helix structural domain that was approximately 30-fold stronger than

(A) Design of anti-tumour stapled peptides targeting BCL9/ β -Catenin Complex

a. Design and biochemical analysis of Axin CBD-derived stapled peptides StAx-3, StAx-3-35R, and StAx-3-11, and StAx-3-35R derived protac StAx-3-35R-VHL as inhibitors of BCL9/ β -Catenin interaction



Name	Helicity	K _d
Axin CBD	15%	5 μ M
StAx-3	51%	60 \pm 2 nM
StAx-3-35R	/	53 \pm 9 nM



StAx-3-11a is the same helicity as StAx-3

b. The sequence of linear peptide BCL9_{HD2} and stapled peptide SAH-BCL9_B



(B) Design of anti-tumour stapled peptides targeting WASF-CYFIP1 Complex

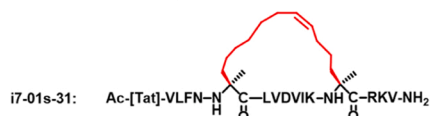
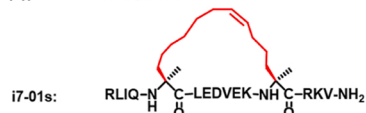
WASF³²⁶⁻⁴¹: LECVTNSTLAAIRQL



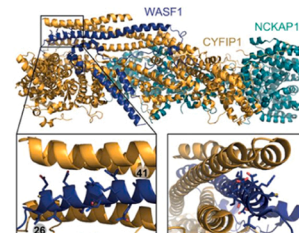
WAHM1 and WANM2 blocked the binding of WASF3 to CYFIP1; t_{1/2}(WAHM) >24 h

(C) Design of anti-tumour stapled peptides targeting Beclin 1

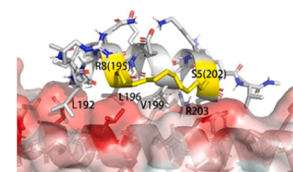
P1: RLIQELEDVEKNRQV



Name	K _d (nM)	IC ₅₀ (μ M)
i7-01s	3.21 \pm 0.28	/
i7-01s-31	0.33 \pm 0.28	27.9



The crystal structure of the WASF1 complex with CYFIP1¹⁰⁸



The predicted binding mode of the designed i7-01s scaffold and the Beclin 1 coiled-coil domain¹¹⁰

Fig. 8. Stapled peptides based on BCL9/ β -Catenin Complex, WASF-CYFIP1 complex and Beclin 1. (A) Design of anti-tumour stapled peptides targeting BCL9/ β -Catenin Complex. (B) Designing anti-tumour stapled peptides that target the WASF-CYFIP1 complex. (C) Designing anti-tumour stapled peptides that target Beclin 1.

that of the stapled peptide SP4. The optimised stapled peptide induced cell death, thereby contributing to the death of EGFR/HER2-driven cancer cells and exerting potent antiproliferative effects. Overall, the stapled peptide designed by Yang et al. to target Beclin1 may be a promising therapeutic candidate for the treatment of EGFR/HER2-driven cancers.

3.1.7. Anti-tumour stapled peptide based on autophagy-related protein

Autophagy plays an important role in maintaining cell homeostasis, and disorders of autophagy are associated with cancer [155]. Selective autophagy regulation is a promising strategy for treating cancer. In the autophagy system, autophagy-associated proteins (ATG) and Atg8 family proteins are involved in regulating signal transduction [156, 157]. The inhibition of ATG and Atg8 family protein-related PPI is an effective strategy for developing specific autophagy inhibitors for cancer treatment.

In the ATG protein, the ATG5-ATG16L1 complex is a potential target for the inhibition of autophagy [158]. Watanabe's team [111] analysed the ATG5-ATG16L1 complex crystal structure and obtained the peptide ATG16L1₁₃₋₂₉ from the α -helix region of protein ATG16L1, which can inhibit the ATG5-ATG16L1 complex formation. However, linear peptides from native proteins usually have low conformational stability, resulting in susceptibility to protease degradation. Stapled peptides 1–6 containing i, i+4 staples were synthesised using Fmoc-based SPPS and RCM catalysed by Grubbs' catalyst. Stapled peptide 1–4 showed moderate affinity for ATG5 ($K_d = 15\text{--}407$ nM). Subsequently, they added four amino acid residues, including Gln30 to Glu33 of the ATG16L1 protein, to the C-terminus of stapled peptides 1–4 to obtain the corresponding stapled peptides 7–10. The affinity of stapled peptides 7–10 to ATG5 was improved by a factor of 2–30, with K_d in the lower range (3–32 nM), and the enhanced binding ability reflected the importance of Gln30 to Glu33 in ATG16L1. The half-life of the staple peptide 10 ($t_{1/2} = 110$ min) was extended by a factor of 10, compared to that of ATG16L1₁₃₋₃₃ ($t_{1/2} = 11$ min). Peptide 10 exhibited the longest half-life as the Arg15 position was excluded as a major cleavage site. This result

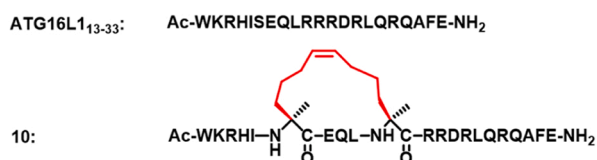
suggests that the use of all-hydrocarbon stapling reduces the exposure of Arg15 to proteases, thereby enhancing proteolytic stability. Stapled peptide 10 (Fig. 9a) showed the greatest inhibition of autophagosome formation.

LC3 and GABARAP, as Atg8 subfamily proteins, are involved in PPIs in several critical stages of autophagy [159]. Therefore, similar to the ATG protein, the blocking of LC3/GABARAP-protein interaction is also a promising strategy to inhibit autophagy [160,161]. Kritzer's group [112] screened out the natural GABARAP ligand peptide K1 having an affinity of 10 ± 1 nM for GABARAP by using phage display technology. Although K1 has high affinity for GABARAP, its biological stability and cellular permeability are poor. Therefore, K1 was optimised using a peptide stapling strategy in which the 3/4/5 positions were mutated to Cys and stapled with fixed Cys8 through adjacent/intermediate/para-xylene linkers. The results showed that the peptides stapled at the Cys3 site had an affinity similar to that of wild-type K1. Subsequently, they attempted to introduce β -branches into Cys to regulate the affinity and selectivity of the stapled peptides by replacing Cys3 or Cys8 with penicillamine (Pen), a Cys analogue containing β -branches. The results showed that pen3-Ortho had a high GABARAP affinity, whereas Pen8-ortho showed nanomolar affinity for both GABARAP and LC3B (Fig. 9b). Due to the similarity between Pen3-ortho and Pen8-ortho, despite their differing selectivity, the authors investigated their binding modes by determining their crystal structures when bound to GABARAP (Fig. 9b). The study revealed that Pen3-ortho and Pen8-ortho employ distinct side chains to interact with the two hydrophobic pockets of GABARAP. Specifically, Pen8-ortho occupies one pocket with Trp6 and the other with Leu9, whereas Pen3-ortho occupies the first pocket with Trp11 and both Trp6 and Leu9 in the second pocket. In addition, the chloroalkane penetration assay illustrated that the stapled peptides exhibited a 2–3-fold increase in cell permeability, compared with linear peptide K1. These highly potent stapled peptides are promising compounds capable of regulating autophagy and may serve as novel PPI inhibitors for cancer treatment.

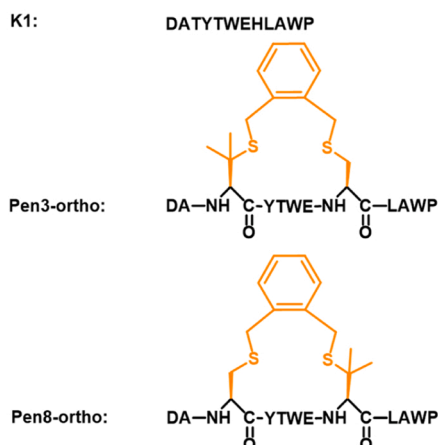
In this section, we comprehensively summarize functionalized

Anti-tumor stapled peptide based on ATG protein

a. Anti-tumor stapled peptide based on ATG5-ATG16L1 complex

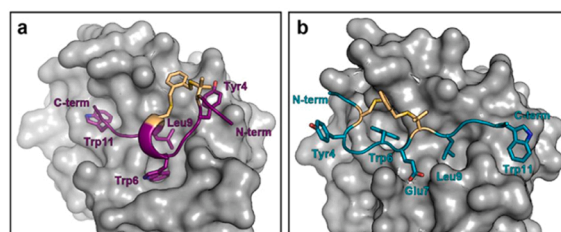


b. Anti-tumor stapled peptide based on LC3/GABARAP protein



Name	K_d (μ M)	Helicity	$t_{1/2}$ (min)-chymotrypsin
ATG16L1 ₁₃₋₃₃	0.072 \pm 0.059	5%	11
10	0.012 \pm 0.008	22%	110

Name	K_d (nM)-GABARAP	K_d (nM)-LC3	CP ₅₀ (μ M)
K1	10 \pm 1	1200 \pm 30	4.8 \pm 0.3
Pen3-ortho	14 \pm 2	1590 \pm 80	2.1 \pm 0.2
Pen8-ortho	12 \pm 2	33 \pm 4	1.3 \pm 0.1



The crystal structures of Pen3-ortho(a) and Pen8-ortho(b) bound to GABARAP¹¹²

Fig. 9. Anti-tumour stapled peptide based on ATG protein. Reproduced with permission from Ref. [112].

stapled peptides for anti-tumor purposes. These peptides are classified based on their targets, which include p53-MDM2, NOTCH ternary complex, Bcl-2 family proteins, β -catenin, WASF1, Beclin 1, ATG5-ATG16L1 complex, LC3/GABARAP, and others. Researchers have employed various strategies, such as all hydrocarbon, lactamization, Diels-Alder cyclization reaction, Ugi-MCR, and cysteine stapling, to design and develop these stapled peptides. Among these strategies, all hydrocarbon approach is the most widely used.

3.2. Stapled peptides in the treatment of bacterial infection

Antimicrobial peptides (AMPs) with lower drug resistance can kill pathogenic bacteria, such as gram-negative bacteria, gram-positive bacteria, and fungi [37,162]. With the abuse of antibiotics, which has resulted in a severe problem of drug resistance, AMPs have attracted interest as new therapeutic drugs [38,163]. The inherent structural properties of peptides result in their susceptibility to protein degradation and have hindered their clinical application. Stapling strategies that increase the structural stability of peptides have been widely used to develop peptide-based drugs for the treatment of bacterial infections (Table 2).

3.2.1. Antibacterial stapled peptides based on the bacterial cell membrane

Cationic AMPs can utilize their positively charged amino acids to insert themselves into the lipid bilayer located in the bacterial cell membrane. This leads to the induction of pore formation and membrane cleavage, thereby exerting antibacterial activity. This feature makes AMPs promising new drugs for treating antibiotic resistance [37,164,169].

Magain 2 (Mag2) [170] is a cationic AMP isolated from African clawed frog skin that utilises its hydrophobic and cationic amino acids to form holes in the lipid bilayer, ultimately leading to bacterial death [164]. Demizu et al. [163] designed a series of staple peptides by incorporating α , α -disubstituted amino acids (dAAs) and side chain stapling into the template peptides. This approach aims to stabilize the helical structure of the template peptides, enhance their biological function, and confer resistance to digestive enzymes, including proteases. In the present study, eight stapled peptides were synthesised using RCM at positions $i/i+4$ or $i/i+7$ and their antibacterial activity and haemolytic toxicity against erythrocytes were compared. It was found that the peptide Mag2-6 (Fig. 10a) showed 2–16-fold higher antibacterial activity than the linear peptide. Meanwhile, Walensky et al. [38] prepared Mag2 stapled peptide library by using RCM reaction and developed a two-dimensional method of α -helical-hydrophobic interaction and clarified the structural-functional-toxicity relationship of stapled peptides. The optimal double-ring staple peptide Mag($i+4$)₁, 15 (Fig. 10a) was obtained through a series of structural optimisations. Mag($i+4$)₁, 15 is structurally stable and resistant to protease and multi-drug resistant bacteria. This study accelerates the use of StAMPs as a novel class of antibiotics to combat MDR infections.

Bac2A [171–174] is a cationic uncyclised counterpart of the cyclic peptide bactenecin, which is one of the smallest natural AMPs, but generally fails to exhibit high antimicrobial efficacy against gram-positive bacteria. Chen and his team [164] found that Bac2A and its linear counterparts cannot spontaneously fold to form helical

structures in solution, resulting in reduced amphipathy and antimicrobial activity. Chen et al. designed four stapled Bac2A peptides using the RCM reaction by inserting a stapling side chain at position i , $i+4$ (Fig. 10b). The results showed that the stapling strategy promoted the folding of Bac2A into an amphiphilic α -helix and maintained a stable helical structure in solution. Moreover, the MIC of the stapled peptides was lower than that of the corresponding linear peptides.

Aurein1.2 [175] is an AMP composed of 13 amino acid residues secreted by *Litoria aurea*, an Australian tree frog, that can inhibit the growth of *Candida albicans* and other fungi. To improve the activity of Aurein1.2, our team [166] designed several stapled peptides (Sau) at positions i , $i+4$ using the RCM-based stapling strategy, which proved that most of the stapled peptides contained higher helicity and greater enzymatic stability than the linear peptide Aurein1.2. Antifungal experiments showed that Sau-1 (Fig. 10c) inhibited fluconazole-resistant *Candida albicans* 901. The inhibitory effects of Sau-2, Sau-5, and Sau-9 on *Candida tropicalis* isolate 895 were more potent than that of fluconazole, whereas the unmodified linear peptide had lower inhibitory activity against all the tested strains. These results indicated that the stapling strategy can be used to optimise antifungal peptides. OH-CM6 [176] is a highly effective cationic AMP derived from OH-CATH30, a naturally occurring peptide isolated from king cobra. To improve the proteolytic stability of OH-CM6 and retain the ϵ -amino group positive charge of Lys after stapling, Zhang et al. [80] synthesised an alkyl diamine bridge through N-alkylation reaction by cross-linking two lysine residues. The required stapled peptide (2–11) was obtained using (*E*)-but-2-ene-1, 4-diol and (*E*)-1, 4-dibromo-but-2-ene as linkers for N-alkylation under mildly alkaline conditions. The staple peptide OH-CM6-10 (Fig. 10d) displayed strong resistance to enzymatic hydrolysis, with MIC values $< 8 \mu\text{g/mL}$, which were markedly higher than those of linear peptides. To obtain peptide OH-CM6-10 analogues with a more rigid linker, stapled peptides OH-CM6-12,13,14 were subsequently synthesised using 1, 2-bis (bromomethyl), 1, 3-bis (bromomethyl), or 1,4-bis (bromomethyl) benzene as crosslinkers. Among them, peptide 12 containing a 1,2-bismethylenebenzene linker was the best candidate due to its excellent antibacterial activity and proteolytic stability. Therefore, a novel stapling strategy was successfully developed using the ϵ -amino N-alkylation reaction of lysine, and this strategy was applied to cationic stapled AMPs, demonstrating its promising potential to the development of new cationic antimicrobial peptides.

Three ultrashort linear AMPs each composed of only 7 amino acids were designed by Shan's group [165] through utilizing the hydrolysis site of chymotrypsin/antitrypsin and the folding principle of α -helical proteins as the basis for their design. However, the presence of conformational instability, low resistance to proteolysis, and poor antimicrobial activity prompted further investigation. Then, they incorporated the unnatural amino acid S_5 at the i , $i+4$ positions through an RCM reaction, resulting in the creation of the stapled peptides stLRL, stRLL, and stRRL. *In vitro* antimicrobial experiments revealed that the stapled peptide exhibited significantly greater activity, ranging from 8 to 32 times than that of the corresponding linear peptides. Among these, stRRL (as shown in Fig. 10e) demonstrated the most pronounced antimicrobial activity.

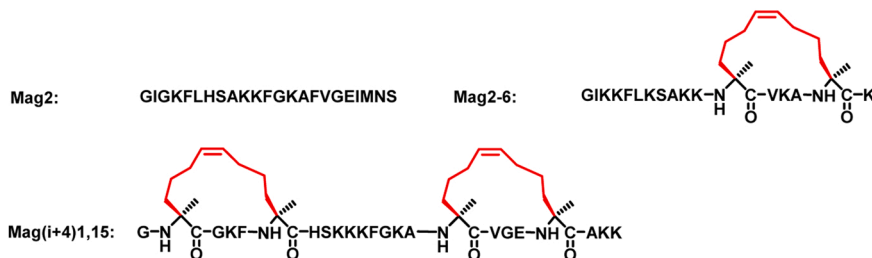
Furthermore, stRRL maintain high water solubility as linear peptides improved resistance to protease hydrolysis and showed typical α -helical conformation features. *In vivo* experiments further confirmed the

Table 2
Application of stapled peptides in the treatment of bacterial infection.

Template peptide	The target	Location	Strategy	Ref.
Magainin 2: GIKKFLKSXKKFVKXFK	Bacterial membrane	Extracellular	All hydrocarbon	[163,38]
Bac2A: RLARIVVIRVAR	Bacterial membrane	Extracellular	All hydrocarbon	[164]
OH-CM6: KFFKLLKAVKKGFKKFAV	Bacterial membrane	Extracellular	Lys-Lys N-alkylation	[80]
RRL: LARRLAR	Bacterial membrane	Extracellular	All hydrocarbon	[165]
Aurein1.2: GLFDIHKKIAESF	Bacterial membrane	Extracellular	All hydrocarbon	[166]
VapB30-VapC30: ELAAIRHR	Bacterial toxin proteins	Extracellular	All hydrocarbon	[167]
WT σ^{54} : FKVARRTVAKYREML	Transcription factors	Intracellular	All hydrocarbon	[168]

Antimicrobial stapled peptides based on bacterial cell membranes

a. Peptide sequences and antibacterial activity of Mag2 and stapled peptides Mag2-6 and Mag(i+4)1, 15



Name	MIC($\mu\text{g/mL}$)
Mag2	29.73
Mag2-6	0.78
Mag(i+4)1,15	1.56

b. Peptide sequences and antibacterial activity of Bac2A and stapled peptide Bac2A(s3-7)



Name	MIC($\mu\text{g/mL}$)
Bac2A	54-80
Bac2A(s3-7)	7.6-16

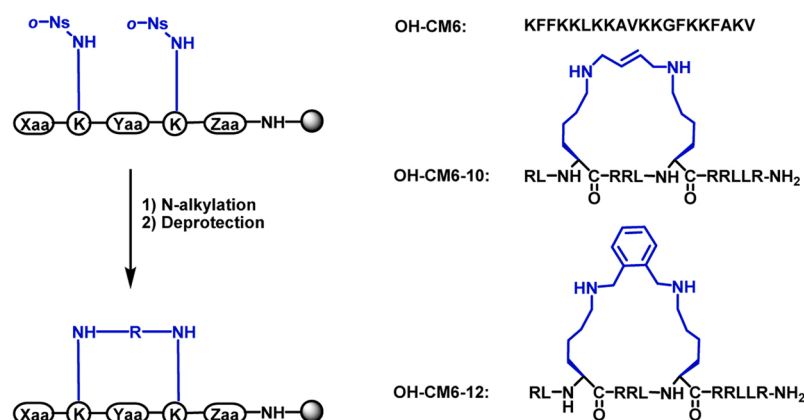
Stabilized α -helix

c. Peptide sequences and antibacterial activity of Aurein1.2 and stapled peptide Sau-1



Name	Helicity	MIC($\mu\text{g/mL}$)
Aurein1.2	56.6%	>128
Sau-1	60.2%	32

d. Peptide sequences and antibacterial activity of OH-CM6 and stapled peptides OH-CM6-10 and OH-CM6-12



Name	$t_{1/2}$ (h)	MIC($\mu\text{g/mL}$)
OH-CM6	2	4-128
OH-CM6-10	6	2-32
OH-CM6-12	10	2-8

e. Peptide sequences and antibacterial activity of RRL and stapled peptide stRRL



Name	Secondary structure	MIC _{GM} (μM)
RRL	random coil	>128
stRRL	α -helicity	14.11

Fig. 10. Anti-microbial stapled peptides based on bacterial cell membranes.

exceptional performance of stRRL in combating bacteria, though in high-protease and high-salt environments. These results indicate that the ultrashort all-hydrocarbon stapled antimicrobial amphiphiles, with their high solubility and strong *in vitro* and *in vivo* performance, represent an innovative avenue for advancing highly stapled peptide compounds.

3.2.2. Antimicrobial stapled peptides based on bacterial toxin proteins

The bacterial toxin-antitoxin (TA) system plays various roles in physiological processes, including multidrug resistance and cell growth inhibition [177]. Different studies have suggested that TA systems are widely present in *Mycobacteria*. For example, the VapB30 antitoxin

protein (or RNA) can bind to the VapC30 toxin protein of homologous *Mycobacterium tuberculosis* and inhibit *Mycobacterium tuberculosis* cell growth [167].

Lee and his team [167] utilised the binding interface of the VapBC30 complex crystal structure to design three helical peptide segments that could exert inhibitory activity against the TA system *in vitro*. However, helical peptides exhibited high conformational flexibility, resulting in low affinity and poor antibacterial activity. Lee et al. [167] identified key residues through alanine scanning and performed a stapled peptide design based on an all-hydrocarbon stapling strategy. Subsequently, the most active peptide, V30-SP-8/9, was screened using an *in vitro* ribonuclease assay. CD results and confocal laser scanning microscopy

displayed excellent α -helicity as well as cell penetration of V30-SP-8/9 in aqueous media, thus confirming the validity of the method. In the antibacterial activity test, the MIC of stapled peptide V30-SP-8 (Fig. 11A) against 50% of isolates of *Mycobacterium smegmatis* mc2155 ($MIC_{50} = 12.5\text{--}25.0\ \mu\text{M}$) was comparable to that of vancomycin ($MIC_{50} = 20\ \mu\text{M}$). Similarly, the bactericidal effect of stapled peptide V30-SP-9 at $6.25\ \mu\text{M}$ was higher than that of the linear peptide at $50\ \mu\text{M}$, indicating that V30-SP-9 had stronger antibacterial effect than the linear peptide.

3.2.3. Antimicrobial stapled peptides based on transcription factors

Transcription factors are essential for maintaining cellular homeostasis, and the initiation of transcription in bacteria requires complexation of a sigma factor with the core enzyme RNA polymerase (RNAP). The transcription factor σ^{54} subunit of bacterial RNAP controls the expression of several genes related to pathogen virulence. The σ^{54} C-terminal binding domain binds to specific promoter regions to regulate the transcription of these genes. Therefore, the interactions between endogenous σ^{54} and its promoter elements can be blocked to down-regulate the expression of virulence genes [168].

Federico and his team [168] developed an NMR model of the interaction between the σ^{54} C-terminal helix-loop-helix domain with the DNA major groove region. They synthesized stapled peptides $S\sigma^{54}$ -1 to $S\sigma^{54}$ -4 (Fig. 11B) maintaining the integrity of the binding site residues by changing the size and the position of the hydrocarbon cross-links. The stapled peptide $S\sigma^{54}$ can form a stable helical structure in solution, with hydrophobic and hydrophilic surfaces which enable it to destroy the lipopolysaccharide matrix. In addition, all stapled peptides can penetrate Gram-negative bacteria and bind to σ^{54} promoters to block the interaction between endogenous σ^{54} and the target DNA sequence. This causes the reduction of transcription and activation regulated by the σ^{54} gene, while the process of nitrogen fixation by Gram-negative bacteria for their growth and development is also effectively prevented. This opens new avenues for the development of therapies targeting gram-negative pathogens.

This section provides a comprehensive summary of functionalized stapled peptides for antimicrobial applications. These peptides are categorized based on their targets, which include bacterial membrane, bacterial toxin proteins, transcription factors, and others. Researchers have employed various strategies, such as all hydrocarbon and Lys-Lys N-alkylation, to design and develop these stapled peptides. Among these strategies, all hydrocarbon approach is the most prevalent.

3.3. Stapled peptides in the treatment of viral infection

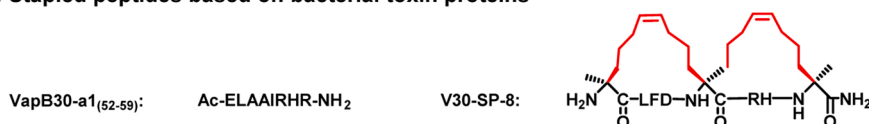
Viral infections are a diverse group of diseases that can affect humans' health in various ways. The continued use of antiviral drugs in recent years has resulted in the emergence of resistant strains of the virus [178]. Compared with traditional antiviral drugs, peptides have the advantages of high activity and less susceptibility to drug resistance, especially the stapled peptides which developed in recent years, have been widely explored and applied in antiviral infections [27,89]. In the following sections, we summarize the advancements of stapling technology in antiviral drug development, offering insights for future research on antiviral drugs (Table 3).

3.3.1. Antiviral stapled peptides based on the SARS-CoV-2 spiny (S) protein

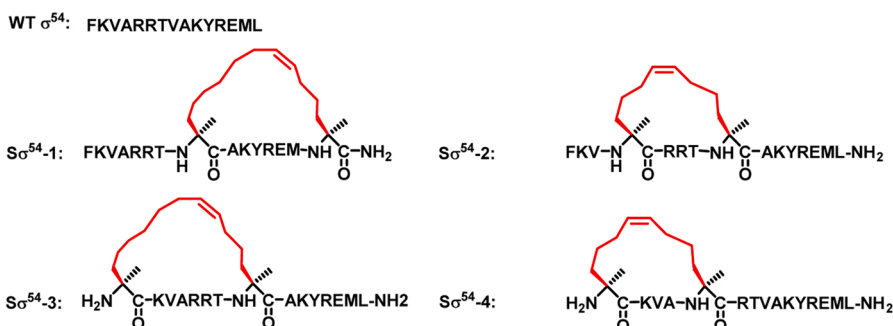
The spike protein of SARS-CoV-2 is a type I transmembrane glycoprotein made up of S1 and S2 subunits, and the C-terminal heptapeptide repeats HR1 and HR2 of the S2 subunit can interact with each other to form a stable 6-helix (6-HB). This triggers the fusion of the host and viral membranes, creating a direct passage for the viral genetic material to enter the host cell. Once inside, the viral genes replicate inside the cell [195,196]. The formation of 6-HB is highly conserved and occurs in all coronaviruses; thus, the HR1-HR2 complex can be an effective and attractive target for fusion inhibitor design.

Xia et al. [179] found that the peptide 2019-nCoV-HR2P, which is derived from the HR1-HR2 complex in SARS-CoV-2, binds the structural domains of the interfacial HR2 structure and has inhibitory activity against viral infection. To improve the stability and activity of 2019-nCoV-HR2P, our group [180] used it as a template peptide to design and synthesize 32 stapled peptides (SCH2-1-x) using the RCM-based stapling strategy and introduced the unnatural amino acid S_5 at the $i, i+4$ site. Peptides SCH2-1-20 and SCH2-1-27 (Figure 12Aa) displayed a 2-3-fold increase in helicity and an increased inhibitory effect by approximately 2 folds, compared with the template peptide. To explore the detailed binding mode of the optimized stapled peptide to the spike protein HR1 domain of SARS-CoV-2 virus, we performed a docking study of the SCH2-1-20-HR1 complex to generate structural models of the protein-protein complexes (Figure 12Aa). The structural modeling results showed that SCH2-1-20 adopted a helical conformation similar to that of the CoVHR2-0 peptide, with the introduced stapling group exposed to the solvent. Stapled peptides synthesized using an all-hydrocarbon strategy can be used as potent fusion inhibitors to treat and prevent SARS-CoV-2 infection. In addition, the peptide EK1 [197], derived from OC43-HR2, is designed to target the HR1 domain

(A) Stapled peptides based on bacterial toxin proteins



(B) Design and Structure of $S\sigma^{54}$ Peptides



Name	Helicity	MIC(μM)
VapB30-a1 ₍₅₂₋₅₉₎	random coil	/
V30-SP-8	26.1%	12.5-25.0

Name	K_d (μM)
WT σ^{54}	>40
$S\sigma^{54}$ -1	0.86±0.08
$S\sigma^{54}$ -2	1.14±0.09
$S\sigma^{54}$ -3	1.24±0.05
$S\sigma^{54}$ -4	5.98 ±0.25

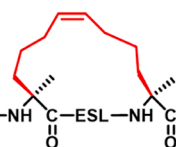
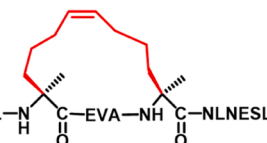
Fig. 11. Anti-microbial stapled peptides based on bacterial toxin proteins (A) and transcription factors (B).

(A) Antiviral stapled peptides targeting the SARS-CoV-2 spike (S) protein**a. Sequence alignment of linear peptide CoVHR2-0 and stapled peptide SCH2-1-20 and SCH2-1-27**

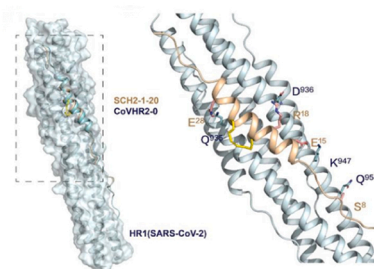
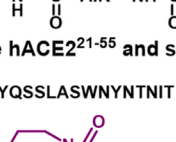
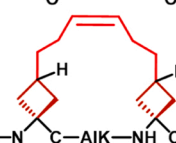
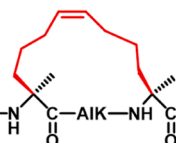
CoVHR2-0: DISGINASVVNIQKEIDRLNEVAKNLSLIDLQEL

SCH2-1-20: DISGINASVVNIQKEIDRL-NH-C(=O)-EVA-NH-C(=O)-NLNESLIDLQEL

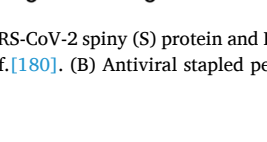
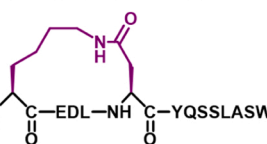
SCH2-1-27: DISGNASVVNIQKEIDRLNEVAKNL-NH-C(=O)-ESL-NH-C(=O)-DLQEL



Name	Helicity	Inhibition rate
CoVHR2-0	16.8%	32%
SCH2-1-20	47.2%	55%
SCH2-1-27	67.5%	51%

Structural modeling analysis of the spiking peptide SCH2-1-20 that binds to the HR1 domain of the SARS-CoV-2 spike protein¹⁸⁰**b. Sequence alignment of linear peptide EK1 and stapled peptide SEK1-12 and SEK1-12-1**EK1: Ac-SLDQINVTFLDLEYEMKKLEEAIAKKLEESYIDLKEL-NH₂SEK1-12: SLDQINVTFLDLEYEMKKLE-NH-C(=O)-AIK-NH-C(=O)-LEESYIDLKEL-NH₂SEK1-12-1: SLDQINVTFLDLEYEMKKLE-NH-C(=O)-AIK-NH-C(=O)-LEESYIDLKEL-NH₂

Name	Helicity	t _{1/2} (h)	IC ₅₀ (μM)
EK1	13.6%	3.2	91.8
SEK1-12	41.5%	9.4	6.3
SEK1-12-1	59.2%	>12	3.5

c. Sequence alignment of linear peptide hACE2²¹⁻⁵⁵ and stapled peptide hACE2²¹⁻⁵⁵-5hACE2²¹⁻⁵⁵: IEEQAKTFLDKFNHEAEDLFYQSSLASWNYNTNIThACE2²¹⁻⁵⁵-5: IEEQAKTFLDKFNHE-NH-C(=O)-EDL-NH-C(=O)-YQSSLASWNYNTNIT

Name	Helicity	K _d (μM)
hACE2 ²¹⁻⁵⁵	38%	/
hACE2 ²¹⁻⁵⁵ -5	52%	2.1±0.2

Fig. 12. Antiviral stapled peptide based on SARS-CoV-2 spiny (S) protein and HIV-1 capsid protein. (A) Antiviral stapled peptides targeting the SARS-CoV-2 spike (S) protein. Reproduced with permission from Ref. [180]. (B) Antiviral stapled peptides based on the HIV-1 capsid protein.

within the SARS-CoV-2 S protein, inhibiting virus-cell fusion. To enhance stability of the secondary structure and improve biological activity, our group [181] efficiently synthesized cyclobutane-based conformationally constrained amino acids, termed (*E*)-1-amino-3-(*n*-but-3-en-1-yl)cyclobutane-1-carboxylic acid (*E*₇) and (*Z*)-1-amino-3-(*n*-but-3-en-1-yl)cyclobutane-1-carboxylic acid (*Z*₇). In the following, these amino acids were employed in RCM-mediated peptide stapling, resulting in geometry-specific stapled peptides denoted as SEK-12-1 to SEK-12-4, with the combinations E7-E7, E7-Z7, Z7-Z7 and Z7-E7, respectively. Among these, the geometry-specific stapled peptide SEK-12-1 (Figure 12Ab), with E7-E7 anchoring, displayed higher α -helicity and consequently greater biological activity compared to conventional hydrocarbon stapled peptides. These cyclobutane-based restricted anchoring residues efficiently complement the existing olefin-terminated unnatural amino acids, and the resulting geometry-specific hydrocarbon peptide stapling offers promising potential for peptide therapeutics.

SARS-CoV-2 infection acts by the binding of the receptor-binding

domain (RBD) in the SARS-CoV-2 S protein to the host's cellular angiotensin-converting enzyme 2 receptor (hACE2) [198,199]. Cryo-electron microscopy structures of RBD and the full-length human ACE2 receptor showed that the critical binding of the complex is predominantly mediated by the α 1 region of ACE2 PD helix region. Moreover, the inhibition of the interaction between RBD and hACE2 may prevent coronaviruses from entering human cells by binding to hACE2, consequently this binding inhibits subsequent viral replication. Maas et al. [182] designed and synthesized three stapled peptides endo-amidated to improve structural stability and enhance binding activity of the linear peptide by using the N-terminal α 1-helix inhibitor 1 of hACE2 as a template peptide. CD revealed that the helicity of stapled peptides increased by 2–5 folds, compared with that of linear peptides. Moreover, when tested for their ability to inhibit the formation of the RBD-hACE2 complex, stapled peptides demonstrated a significant increase in inhibitory activity compared to the original peptides, exceeding the original activity by more than 3-fold. The stapled peptide 5 (Figure 12Ac) showed the highest activity. In conclusion, the stapled

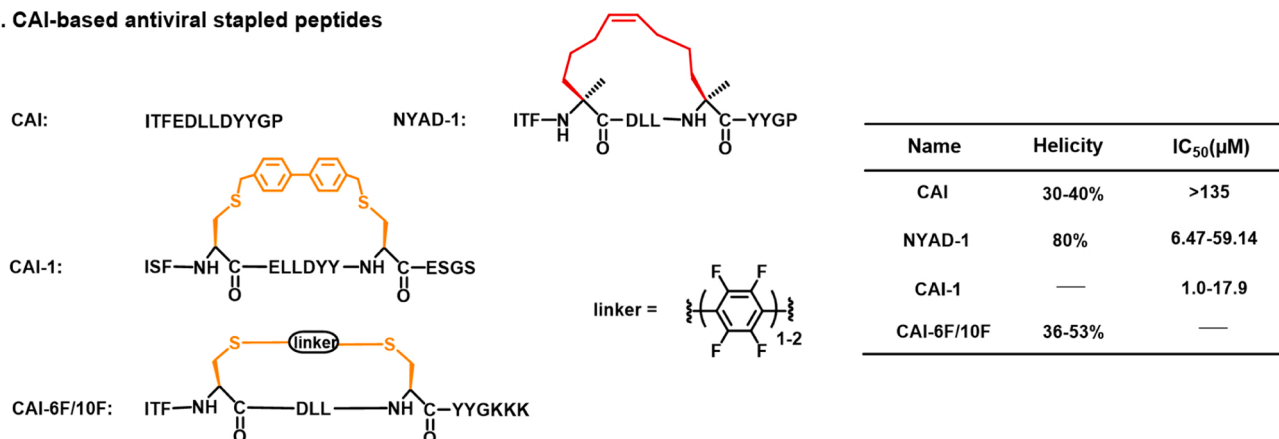
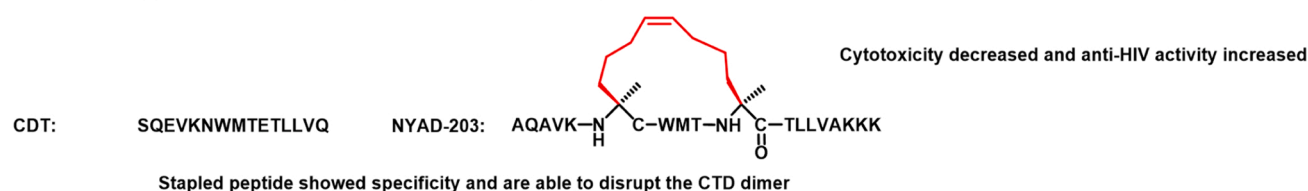
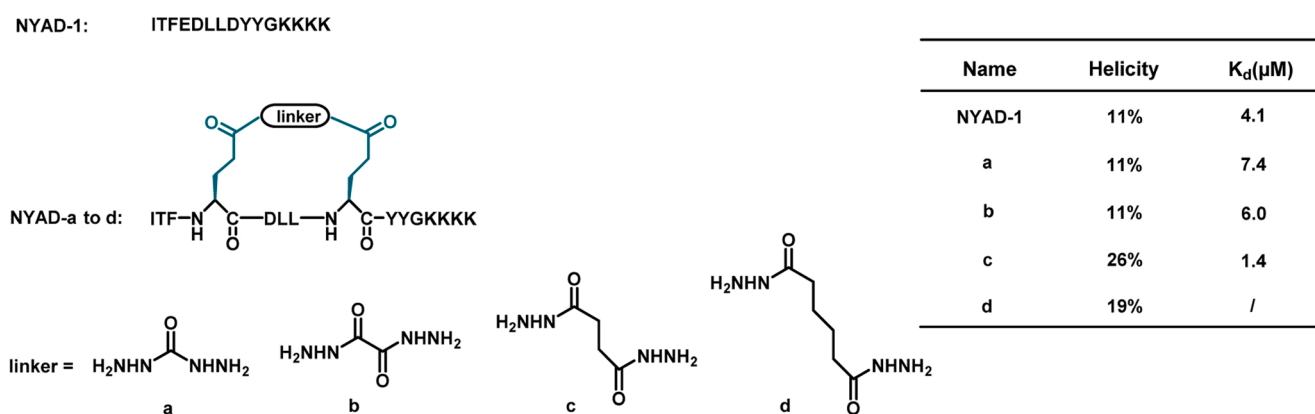
(B) Antiviral stapled peptides based on the HIV-1 capsid protein**a. CAI-based antiviral stapled peptides****b. Sequence alignment of linear peptide CDT and stapled peptide NYAD-203****c. Sequence alignment of linear peptide NYAD-1 and stapled peptide NYAD-a to d**

Fig. 12. (continued).

Table 3

Application of stapled peptides in the treatment of viral infection.

Template peptide	The target	Location	Strategy	Ref.
CoVHR2-0: DISGINASVVNIQKIDRLNEVAKNLNESLIDLQEL	SARS-CoV-2 spike (S) protein	Extracellular	All hydrocarbon	[179,180]
EK1: SLDQINVTFLDLEYEMKKLEEAIKKLEESYIDLKEL	SARS-CoV-2 spike (S) protein	Extracellular	Cyclobutane stapling	[181]
hACE2 ₂₁₋₅₅ : EEQAKTFLDKFNHEAEDLFYOSSLASWNYNTNIT	SARS-CoV-2 spike (S) protein	Extracellular	Lactamization	[182]
CAI: ITFEDLLDYYQP	HIV-1 Capsid protein (CA)	Intracellular	All hydrocarbon; Cys-alkylation	[71, 183-185]
CDT: SQEVKNWMTETLLVQ	HIV-1 Capsid protein (CA)	Intracellular	Cysteine stapled; All hydrocarbon	[186]
NYAD-1: ITFXDLLXYGKKKK	HIV-1 Capsid protein (CA)	Intracellular	Glu-Glu bisamidation	[59]
Enfuvirtide ₆₃₈₋₆₇₃ : YTSLIHSLIEESQNQEQEKNEQELLELDKWASLWNWF	HIV-1 surface envelope glycoprotein gp41	Extracellular	All hydrocarbon	[22]
T649v: BTWBWDREINNYTSLIHSLEEQNQEQEKNEQELLE	HIV-1 surface envelope glycoprotein gp41	Extracellular	All hydrocarbon	[187]
SC34EK: WXEWDRKIEEYTKKIEELIKKSOEQEQEKNEKELK	HIV-1 surface envelope glycoprotein gp41	Extracellular	All hydrocarbon	[188]
CP22: IEALIRAAEQEQEKNEAALREL	HIV-1 surface envelope glycoprotein gp41	Extracellular	Dithiol dialkylation	[188]
Vpr: EAIIRLQQLLFIFHRIG	HIV-1 Integrase (IN)	Intracellular	All hydrocarbon	[189,190]
T188: FDISISQVNEKINQSLAFIRKSDLELHNVNAGKST	RSV-F protein	Extracellular	All hydrocarbon	[191]
hCD81-L-EL: PSGSNIHSNLFKED	Human cell surface protein CD81	Extracellular	All hydrocarbon	[192]
EBOV GP2 (610-633): IEPHDWTKNITDKIDQIHDFVDK	EBOV-GP2	Extracellular	Lactamization	[193,194]

peptides synthesized by forming a lactam bridge at the i, i+4 site showed increased cellular uptake, reduced enzymatic degradation, and improved pharmacokinetic properties, resulting in a stronger inhibitory effect against the virus.

3.3.2. Antiviral stapled peptide based on HIV-1 capsid protein

HIV-1 viral capsid proteins have two structural domains, the C-terminal structural domain (CTD) and the N-terminal structural domain (NTD), which are essential for assembling infectious viral particles, encapsulating the genetic material and key enzymes associated with viral replication [200–202]. HIV-1 capsid proteins are involved in different phases of the viral replication cycle and are powerful targets for HIV therapy, since antiviral activity can be induced by inhibiting capsid assembly.

Kräusslich's group [183] identified the first peptide inhibitor, CAI, of immature HIV-1 assembly, which disrupts immature and mature capsid particle assembly *in vitro* but does not inhibit HIV-1 activity in cell culture because it cannot penetrate cells. Therefore, Debnath et al. [184] synthesised the stapled peptide NYAD-1 by retaining the key residues and employing an RCM-based stapling strategy to enhance the α -helical stability and cell penetration of CAI (Figure 12Ba). CD showed that the stapled peptide NYAD-1 exhibited > 4-fold increase in helicity, compared with the template peptide CAI. The cell penetration assay increased more than 2 times compared to the linear template peptide. Anti-HIV-1 viral activity assay showed that the linear peptide CAI did not display any activity up to at 200 μ M dose, whereas NYAD-1 showed a broad-spectrum HIV-1 inhibitory activity in cell cultures (IC_{50} = 4–15 μ M), indicating the potential of NYAD-1 as a novel class of drugs for treating AIDS. Furthermore, based on CAI inhibition [183], Muppidi et al. [185] designed and synthesised several stapled peptides with distance-matched biphenyl crosslinkers using a Cys-arylation stapling approach. They synthesised six stapled peptides by replacing the solvent-exposed residues in CAI with two cysteines and added a Ser-Gly-Ser tail at the C-terminus to improve water solubility. The evaluation of the anti-HIV-1 viral activity revealed a 10-fold increase in activity over the linear peptide CAI, with CAI-1 (Figure 12Ba) being the most effective. This cysteine-based biphenyl-stapled peptide exhibited significantly improved cell permeability and antiviral activity. In addition, Spokoynny et al. [71] also reported a facile transformation between perfluoroaromatic molecules and cysteine thiolate for an antiviral stapled peptide design based on the peptide CAI. Perfluoroaromatic substrates were co-incubated with unprotected peptides in DMF containing a TRIS base to prepare the stapled peptides. The linear peptide exhibited 16% α -helicity, while stapling with hexafluorobenzene and decafluorobiphenyl (Figure 12Ba) significantly enhanced the helicity of the linear peptide up to 53% and 36%, respectively. Moreover, this stapling strategy, which was performed on the HIV-1 virus capsid-associated peptide and designed to bind the HIV-1 CTD, displayed enhanced proteolytic stability, binding, and cell permeability, compared with that exhibited by the unstapled peptide. This expands the toolbox of techniques available for designing and creating stapled peptides for the improvement of thiol-containing biomolecules.

Different studies have shown that the host cells can be protected from HIV-1 infection by inhibiting the formation of the capsid protein CTD dimer [203,204]. Debnath's group [186] found that a peptide CDT from the α -helix region in the dimer interface prevents the formation of the CTD dimer, thereby inhibiting the activity of HIV-1. The linear peptide CDT has a flexible conformation and poor cellular penetration; hence, the group constructed stapled peptides using an RCM-based stapling strategy. Fluorescent labelling indicated that the stapled peptides penetrated the cells. Compared to the template peptide, the stapled peptide NYAD-203 (Figure 12Bb) showed a 9–10-fold decrease in cytotoxicity and an approximately 2-fold increase in anti-HIV activity. This study provides a basis for designing small and stable helical peptide inhibitors that target the CTD dimer interfaces.

NYAD-1 is a short peptide capable of binding to the HIV-1 capsid

(CA) to inhibit capsid assembly and thus exert antiviral activity. To study the impact of stapling on bioactivity and conformation of NYAD-1, Pentelute's group [59] modified the binding peptide NYAD-1 of CA. The peptide was stapled using different linker groups including carbazide (a), oxalyl dihydrazide (b), succinyl dihydrazide (c), and hexanedihydrazide (d) (Figure 12Bc). CD spectra showed that the stapled NYAD-1 exhibited α -helicity.

The stapled peptides with c and d linkers have raised helicity, suggesting that the length and the rigidity of the linking group can increase the degree of α -helicity of the linear peptide. Binding kinetics experiments revealed that the K_d value of the peptide stapled with c was approximately 3-fold higher, compared with that of the linear peptide. The results show that it is feasible to fine-tune biologically active stapled peptides using linkers with different properties.

3.3.3. Antiviral stapled peptides based on the HIV-1 surface envelope glycoprotein gp41

Gp41 mediates the fusion of HIV-1 and host cell membranes. Enfuvirtide can disrupt the formation of the 6-helix structure by mimicking the heptapeptide repeat 2 structural region in gp41, and thus to inhibit HIV infection [205]. However, its susceptibility to enzyme hydrolysis *in vivo*, lack of oral bioavailability, and the development of drug resistance have limited its widespread use [206,207]. Walensky et al. [22] synthesised monocyclic and bicyclic stapled peptides (SAH-gp41 C, D, and CD) using all hydrocarbon stapling strategies with enfuvirtide 638–673 as a template peptide. They also synthesised the monocyclic and bicyclic stapled peptides, SAH-gp41 (A, B, and AB), using T649v as a template. CD showed that the stapled peptides had a 2–6-fold enhancement in helicity, compared to the unstapled peptides. Trypsin resistance assays showed a 6–8-fold enhancement of the monocyclic peptide and a 3–4-fold enhancement of the bicyclic peptide over the corresponding template peptide. Furthermore, the antiviral activity assay showed that the activity of the bicyclic peptide SAH-gp41 (AB) (Fig. 13a) was approximately 4-fold higher than that of enfuvirtide, and the order of activity magnitude was SAH-gp41 (AB) > SAH-gp41 (A) > SAH-gp41 (B) > T649v > Enfuvirtide.

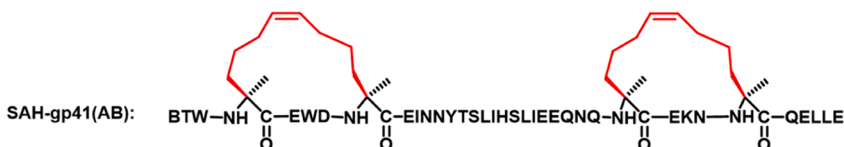
SC34EK is a peptide derived from the C-terminal heptapeptide repeat region of gp41, which binds to the N-terminal heptapeptide repeat region of gp41, thus inhibits the 6-helix bundle formation and blocks the key fusion of HIV-1 with the host cell [208]. To stabilize the helical conformation of SC34EK, our group [187] synthesised stapled peptides retaining natural side chains based on our previous studies. We chose SC34EK [208] as a template to obtain Leu¹, Serⁱ⁺⁴, Lys¹, and Leuⁱ⁺⁴ stapled peptides (SC34EK-1a,2a, Fig. 13b) retaining double side chains using an all-hydrocarbon stapling strategy. The results showed that this stapling strategy not only enhanced α -helicity and proteolytic stability of SC34EK, but also retained the structural characteristics of the linear peptide, including key peripheral residues, solubility, and charge, which are crucial for inhibiting the activity of anti-HIV-1. To understand the enhanced potency of SC34EK-1a compared to the parent peptide, we conducted an analysis of the crystal structure of the complex formed between HIV-1 gp41 fragment N36 and SC34EK. As anticipated, the side chains of Leu-645 and Ser-649 in SC34EK are positioned closer to the core of the helix bundle structure (Fig. 13b), specifically interacting with Asn-554 and Arg-557 of N36 (Fig. 13b). This suggests that the strong interaction between SC34EK-1a and N36 relies on the key residues Leu-645 and Ser-649 in SC34EK-1a. These findings provide clear evidence for the inherent superiority of double side-chain-retention stapled peptides over regular stapled peptides.

T20 is a 36-residue peptide originating from the CHR structural domain of gp41 and is a synthetic peptide approved for the treatment of HIV [209]. To address the problem of short half-life *in vivo* [210], Liu et al. [188] synthesised several m-xylene-sulfide-related stapled peptides using a dithiol bis-alkylation reaction which, can be used as fusion inhibitors targeting gp41 of HIV-1. The peptide T2635 was obtained by alanine scanning of T20. T2635 was truncated into the 22-residue

Stapled peptides based on HIV-1 surface envelope glycoprotein gp41

a. Sequence alignment of linear peptide T649v and stapled peptide SAH-gp41(AB)

T649v: BTWBEWDREINNYTSLIHSLIEEQNQKQEKNEQELLE

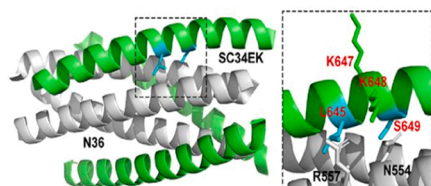


Name	Helicity	IC ₅₀ (nM)
T649v	13%	>3000
SAH-gp41(AB)	36%	2.5

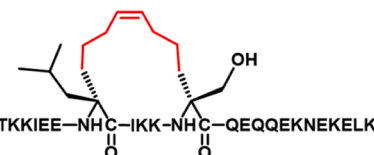
b. Sequence alignment of linear peptide SC34EK and stapled peptide SC34EK-1a

SC34EK: WXEWDKRKIEEYTKKIEELIKKSQEQQEKNEKELK

SC34EK-1a: WZEWDKKIEEYTKKIEE-NH-C(=O)-IKK-NH-C(=O)-QEQQEKNEKELK



The crystal structure of the complex between HIV-1 gp41 fragment N36 and SC34EK¹⁸⁷

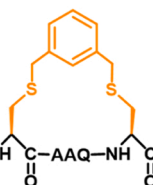


Name	Helicity	IC ₅₀ (nM)
SC34EK	6.6%	1.0
SC34EK-1a	11.9%	0.6

c. Sequence alignment of linear peptide CP22 and stapled peptide CS6

CP22: IEALIRAAQEQQEKNEAALREL

CS6: IEALI-NH-C(=O)-AAQ-NH-C(=O)-QEQQEKNEAALREL



Name	Helicity	EC ₅₀ (nM)
CP22	27%	127.3±28.7
CS6	35%	95.7±11.0

Fig. 13. Peptides with stapled structures derived from the surface envelope glycoprotein gp41 of HIV-1. Reproduced with permission from Ref. [187].

peptide, CP22. Subsequently, cysteine was introduced at the *i*, *i*+4 site and stapled through the cysteine-alkylating group to form *m*-xylene sulfide-stapled peptides (CS1-CS8). Peptide inhibitory activity was tested using the HIV-1 Env-mediated cell-cell fusion assay, which revealed moderate inhibitory activity for the linear peptide CP22 in contrast to the stapled peptide CS6, which exhibited maximum inhibitory activity (Fig. 13c). Subsequently, hCS6 was obtained by replacing Cys-6 and Cys-10 of CS6 with homocysteine (hC), which showed 3.8-fold increase in inhibitory activity, compared with CP22. Therefore, the *m*-xylene sulfide stapling strategy can compensate for the shortcomings of linear peptides, and this study provides a new direction for the design of anti-HIV peptides.

3.3.4. Antiviral stapled peptides based on HIV-1 integrase

HIV-1 integrase (IN) is an enzyme indispensable for the stable viral infection of host cells; it catalyses the insertion of viral DNA from the pre-integration complex (PIC) into the host cell genome. The gene insertion process is a critical step for HIV proliferation in host cells [211]. Therefore, the inhibition of IN activity would be effective in providing an anti-HIV-1 effect. Vpr can inhibit IN activity through its C-terminal structural domains [212–215]. Suzuki et al. [189] used the second helical domain fragment of Vpr as a template peptide to design an octa-arginine conjugate with improved cellular membrane permeability. The addition of octa-arginine leads to significant inhibition of HIV replication but is accompanied by a relatively high level of cytotoxicity. To reduce the cytotoxicity of the octa-arginine peptide, Tamamura's group [190] synthesised 14 stapled peptides using RCM at the *i*, *i*+4 site. The stapled peptide (Fig. 14A) exhibited the strongest inhibitory activity against HIV, which was approximately 3-fold stronger than that of the linear peptide. In addition, the stapling strategy employed for

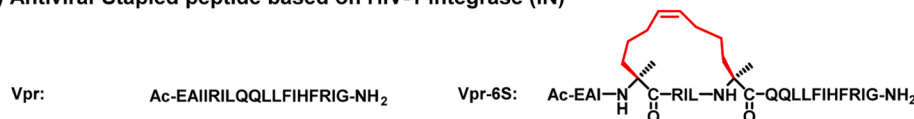
the Vpr-derived peptides led to an obvious reduction in cytotoxicity.

3.3.5. Antiviral stapled peptides based on RSV-F protein

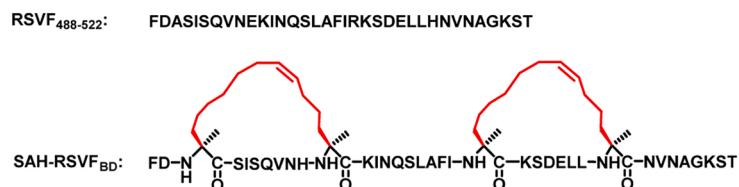
The fusion protein (F) of respiratory syncytial virus (RSV) mediates the fusion between RSV envelope and host cell membrane, enabling the virus to cross the host cell membrane and play an important role in the process of viral invasion [216]. Peptide T118 derived from the CHR of RSV-F demonstrated excellent nanomolar inhibitory activity in both RSV infectivity and syncytium formation assays [217]. However, the linear peptide T118 have low α -helicity and exist in solution as random coils, which influences their inhibitory activity. Bird et al. [191] applied an all-hydrocarbon stapling strategy to improve the secondary conformation of linear peptides. The stapled peptide SAH-RSVF (A-F) was synthesised by stapling T188 as a template at sites *i*/*i*+4 or *i*/*i*+7. CD showed that monocyclic stapled peptides resulted in a 2–3-fold enhancement of α -helicity, compared to linear peptides. Most monocyclic stapled peptides with *i*, *i*+7 spacing were associated with a significant increase in competitive binding activity to RSV 5-HB, compared to the stapled peptides with *i*, *i*+4 spacing. Therefore, stapling position of *i*, *i*+7 was chosen for bicyclic stapled peptide synthesis. Compared to the linear peptide T188, the bicyclic stapled peptides exhibited 2–5-fold and 4-fold increases in α -helicity and half-life, respectively. The proteolytic hydrolysis resistance of bicyclic stapled peptides was improved by 3–33 folds, compared to that of the unmodified peptides, and SAH-RSVF_{BD} (Fig. 14B) demonstrated the highest level of activity. This study provides a strategy to inhibit RSV infection through the mucosal and intratracheal delivery of bicyclic stapled RSV fusion peptides.

3.3.6. Antiviral stapled peptides based on human cell surface protein CD81

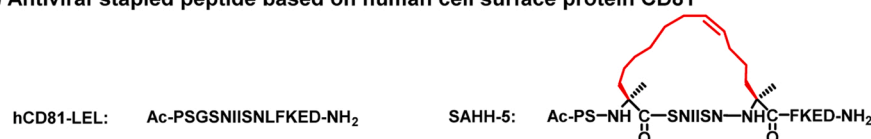
The interaction between HCV envelope glycoprotein and human cell

(A) Antiviral Stapled peptide based on HIV-1 integrase (IN)

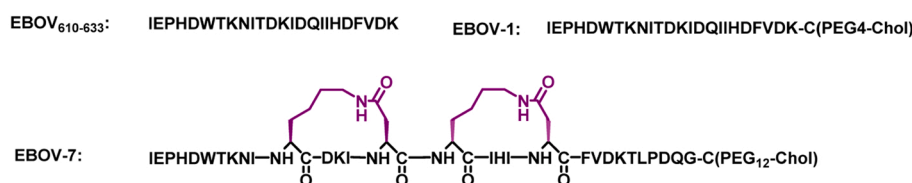
Name	EC ₅₀ (μ M)
Vpr	>10
Vpr-6S	3.55

(B) Antiviral Stapled peptide based on RSV-F protein

Name	Helicity	K _i (nM)	t _{1/2}
RSVF ₄₈₈₋₅₂₂	23%	99	21min
SAH-RSVF _{BD}	61%	59	>860min

(C) Antiviral stapled peptide based on human cell surface protein CD81

Name	Helicity
hCD81-LEL	6%
SAHH-5	57%

(D) Antiviral stapled based on Class I fusion protein GP2

Name	EC ₅₀ (μ M)
EBOV ₆₁₀₋₆₃₃	/
EBOV-1	>30
EBOV-7	3.88

Fig. 14. Antiviral stapled peptides based on HIV-1 integrase, RSV-F protein, Human cell surface protein CD81, and Class I fusion protein GP2. (A) Antiviral Stapled peptide based on HIV-1 integrase. (B) Antiviral Stapled peptide based on RSV-F protein. (C) Antiviral stapled peptide based on human cell surface protein CD81. (D) Antiviral stapled based on Class I fusion protein GP2.

surface protein CD81 plays a key role in viral entry, and CD81 can act as a receptor for HCV to mediate the entry of viral particles into the host cell [218,219]. The peptide hCD81-LEL, designed based on a large extracellular loop fragment of CD81, disrupts the binding of HCV envelope glycoprotein E2 to CD81 [192,220]. To solve the poor hydrolytic stability of hCD81-LEL, Liu's group [192] employed all-hydrocarbon stapling strategy to develop inhibitors of HCV membrane fusion by using hCD81-LEL as a template and introducing the unnatural amino acids S₅ and R₈ into the i/i+4 or i/i+7 sites. They synthesised several stapled peptides, including SAHH-1–5. Compared with that of the parent peptide hCD81-LEL, the α -helicity of the stapled peptides was increased by 2–10 folds; moreover, the activity of the stapled peptide SAHH-5 (Fig. 14C) increased by > 10 folds. This stapling strategy could provide new routes for the development of novel molecules against viral infections.

3.3.7. Antiviral stapled peptides based on Class I fusion protein GP2

Ebola virus transmembrane glycoprotein 2 (EBOV-GP2), a class I fusion protein based on two heptapeptide repeat (HR) regions, facilitates viral attachment to host cells, catalyses membrane fusion, and serves as an attractive target for the development of fusion inhibitors [221,222]. Higgins et al. [193] identified an HR2-derived inhibitor composed of the peptide EBOV-GP2₆₁₀₋₆₃₃ sequence and cholesterol bound to the C-terminus. To stabilize the peptide helical structure and increase the inhibitory potency, Pessi et al. [194] used polyethylene glycol spacers of different lengths between Cys and cholesterol moieties to synthesise several stapled peptides (EBOV-x) through a stapling strategy with the introduction of a lactam ring, as proposed by Fairlie [223] and Higgins [193]. The evaluation of the antiviral activity of the stapled peptides *in vitro* revealed that EBOV-7 (Fig. 14D) with a 15-fold enhancement over

the template peptide exhibited the strongest activity.

In this section, we summarize functionalized stapled peptides developed for antiviral purposes. These peptides are classified based on their targets, including the SARS-CoV-2 spike (S) protein, HIV-1 Capsid protein (CA), HIV-1 surface envelope glycoprotein gp41, HIV-1 Integrase (IN), RSV-F protein, Human cell surface protein CD81, EBOV-GP2, and others. Researchers have employed various strategies, such as all hydrocarbon, lactamization, cyclobutane stapling, Cys-alkylation, cysteine stapling, Glu-Glu bisamidation, and dithiol dialkylation, to design and develop these stapled peptides. Among these strategies, all hydrocarbon approach is the most prevalent.

3.4. Stapled peptides in the treatment of diabetes

Currently, diabetes mellitus, one of the most common chronic diseases, has become a severe public health problem, second only to malignant tumours and cardiovascular diseases [224,225]. Currently, nine GLP-1R peptide agonists have been approved for the treatment of diabetes, including liraglutide, semaglutide, and exenatide [226]. However, peptide-based anti-diabetic drugs are usually subjected to short plasma half-life, which involves higher doses and frequent injections which affects negatively patients' compliance. Stapling strategies have been broadly adopted for the development of peptide-based anti-diabetic drugs with positive results (Table 4). In the following sections, we summarise the research progress on the applications of stapling strategy in the development of anti-diabetic drugs and provide insights for the future development of anti-diabetic peptide drugs.

3.4.1. Antidiabetic stapled peptides based on GLP-1/GCGR receptor

Exendin-4 is an agonist of the glucagon-like peptide-1 receptor (GLP-

Table 4

Application of stapled peptides in the treatment of diabetes.

Template peptide	The target	Location	Strategy	Ref.
Exendin-4: HEGGTFSTDSLKQMEEEEAVRLFIEWLKNGGPSSGAPPPS	Glucagon-like peptide-1 receptor (GLP-1R)	Extracellular	Cys-alkylation	[227]
xGLP/GCG-13: HSQGTYTNDVKYLDSSRAQDFIEWLKNGGPSSGAPPPS	Glucagon-like peptide-1 receptor (GLP-1R)	Extracellular	Cys-alkylation	[228,229]
VIP ₍₁₅₋₂₂₎ : HSDAVFTDNYTRLRQKQIAVKKYLNLSILNGK	Vasoactive intestinal peptide receptor 2 (VPAC2)	Extracellular	Triazole click reaction Lactamization; All hydrocarbon	[230,231]
A helical peptide fragment derived from the LXXLL motif region	Peroxisome proliferator-activated receptor gamma (PPAR γ)	Intracellular	All hydrocarbon	[232]
BAD BH3 : NLWAAQRYGRELRRMSDEFVDSEKK	Glucokinase	Intracellular	All hydrocarbon	[233]
α -helices fragment in the human PKC α kinase domain : VECTMVEKRVLALLDKPPFLTQLHS	Endogenous ALMS1-PKC α protein in adipocytes	Intracellular	All hydrocarbon	[234]

1R), which is administered twice a day through subcutaneous injection to control glycaemic levels [235]. To enhance the pharmacological properties and therapeutic effect of exendin-4, Shen et al. developed a new peptide engineering strategy by incorporating a binding motif from serum protein onto peptide side-chain staples [227]. This strategy is an advancement over the previous strategy, and it involves the stapling of two turns of oxyntomodulin at the *i* and *i*+7 positions with a biaryl cross-linker to increase its circulatory half-life. Based on the complex crystal structure of N-terminal domain of peptide Ex-4 (9–39)-NH₂ and the GLP-1R, the paired residues Glu17 and Glu24, Gln13 and Glu24, and Leu10 and Glu24, which were exposed to solvents and located at the same side of the α -helix, were replaced by the double Cys to synthesize SEQ-1, SEQ-2, and SEQ-3 at positions *i*/*i*+7, *i*/*i*+11, and *i*/*i*+14, respectively. The crosslinker N, N'-butane-1, 4-diyl bis (bromoacetamide) was used to cross link two cysteine residues (L2) of the SEQ-1.

Using this strategy, a group of crosslinkers with ethylene glycol or aliphatic spacers (L1-L12) were employed to staple peptides with cysteine residues at positions *i*/*i*+7, *i*/*i*+11, or *i*/*i*+14. Compared with the corresponding unstapled peptides, these stapled peptides displayed an obvious enhancement in activity. To further enhance the pharmacokinetic properties of the peptide, a binding moiety from natural albumin was attached to the peptide through a “depot” effect to obtain stapled peptide E6, which contained the fatty acid side chain and retained sufficient agonist activity (EC₅₀ = 16 pM), as that of Ex-4. Moreover, the stapled peptide E6 (Fig. 15a) showed a *t*_{1/2} almost 15 folds higher than that of Ex-4 *in vivo*. Despite its excellent pharmacokinetic properties, the stapling strategy used for synthesizing E6 generated mixtures of isomers in the stapling reaction. This poses challenges for the preparation, as well as the pharmacological and toxicological studies on the isomers. To circumvent these problems, the symmetric staple S2 was

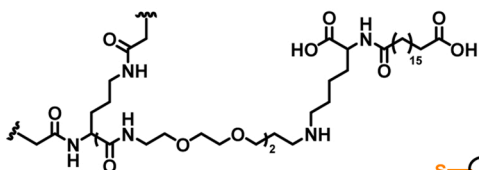
Antidiabetic stapled peptide based on GLP-1/GCGR receptor

a. Sequence alignment of linear peptide Ex-4 and stapled peptide E6

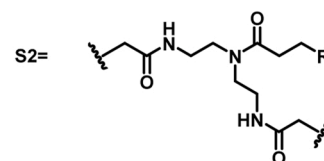
Ex-4: HEGGTFSTDSLKQMEEEEAVRLFIEWLKNGGPSSGAPPPS

E6: HGE GTFSTDSLKQMER-NH-C(=O)-AVRLF I-NH-C(=O)-WLKNGGPSSGAPPPS

linker=



Ex-4[M14L, E17C, E24C] - S2: HGE GTFSTDSLKQLER-NH-C(=O)-AVRLF I-NH-C(=O)-WLKNGGPSSGAPPPS



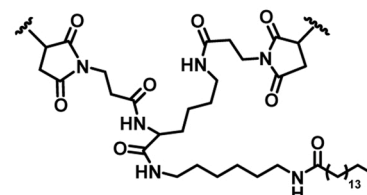
Name	EC ₅₀ (pM)	<i>t</i> _{1/2} (h)
Ex-4	16	0.5
E6	16	13.8
Ex-4[M14L, E17C, E24C] - S2	43±2	8±0.3

b. Sequence alignment of linear peptide xGLP/GCG-13 and stapled peptide 2c

xGLP/GCG-13: HSQGTYTNDVKYLDSSRAQDFIEWLKNGGPSSGAPPPS-NH₂

2c: HSQGTYTNDVSKYLDSS-NH-C(=O)-RAQDFI-NH-C(=O)-WLKNGGPSSGAPPPS-NH₂

linker=



Name	EC ₅₀ (nM)
xGLP / GCG-13	0.053
2c	0.035

Fig. 15. Antidiabetic stapled peptide based on GLP-1/GCGR receptor.

adopted to synthesise the first-generation long-acting S2-stapled peptide exenatide. The newly developed symmetric staple extending-4 analogue exhibited excellent efficacy *in vivo* in animal models of diabetes and obesity.

Han et al. discovered a new xGLP-1-based dual agonist (xGLP/GCG-13) of GLP-1R/GCGR based on a structure-activity study and rational design of peptides [228]. However, the clinical development of xGLP/GCG-13 is impeded by its short half-life *in vivo*. To overcome this problem, xGLP/GCG-13 was stapled using symmetrical BisMAL (SYM-BisMAL) [229]. The dual Cys residues were scanned to determine the appropriate stapling positions in xGLP/GCG-13. The results showed that the Cys-mutated peptides 1a, 1 f, 1 g, and 1k were appropriate linear peptides for subsequent side-chain cyclisation. The two Cys residues were then cross-linked using an sSYM-BisMAL cross-linker, based on the solid-phase addition reaction between maleimide and thiol at the i and i+7 positions. A lithocholic acid or long-chain fatty acid containing a C₁₂ alkyl chain as a serum albumin-binding motif was added to the SYM-BisMAL terminal amine to further optimise the pharmacokinetic properties of the peptides, and this yielded peptides 2a-h. Stapled peptide 2c showed stronger activity and a longer half-life in rodents than the linear peptide xGLP/GCG-13. Furthermore, 2c (Fig. 15b) displayed excellent activity in the control of glucose control in mice and in the restoration of glycaemic control and pancreatic function in db/db mice.

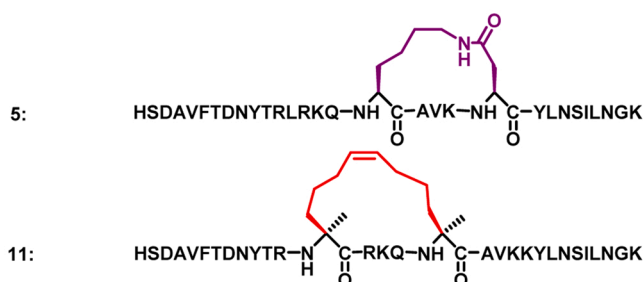
These enhancements in biological activity and pharmacodynamics suggest the excellent therapeutic potential of 2c as an antidiabetic drug. Furthermore, this approach may be applicable for the development of other therapeutic peptides.

3.4.2. Antidiabetic stapled peptides based on VPAC2 receptor

Vasoactive intestinal peptide (VIP), with 28 amino acid residues, is a linear endogenous peptide hormone that potently agonises vasoactive intestinal peptide receptor 2 (VPAC2), and research has demonstrated its ability to secrete insulin [236]. However, as a linear peptide, VIP has a poor half-life of < 1 min and *in vivo* poor pharmacokinetics, which severely limit its development as a therapeutic agent. To overcome these challenges, Adrian Gill and co-workers investigated the effects of two cyclisation strategies, including RCM-based stapling and lactamization using an i, i+4 pattern on VPAC2 agonism, proteolytic stability, secondary structure of peptide, and cell membrane permeability [230]. The design principle was based on the assumption that the peptide VIP with an α -helical conformation binds to the VPAC2 receptor, similar to the way that glucose-dependent insulin stimulating peptide (GIP) binds to the extracellular region of its receptor. Sequence alignments of VIP and GIP revealed that certain residues (L13, M17, K21, N24, S25, and N28) could be stapled without disturbing these interactions. The VIP-stapled peptides showed significantly enhanced VPAC2 agonist potency, with

(A) Antidiabetic stapled peptide based on VPAC2 receptor

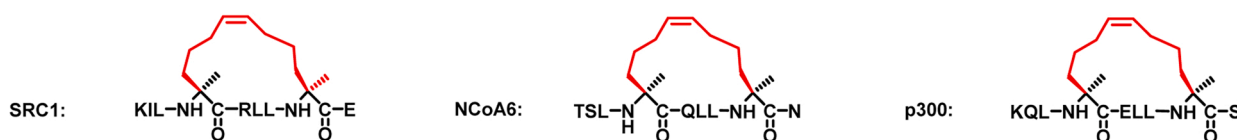
I17-VIP-GK: HSDAVFTDNYTRLRQKQIAVKKYLNSILNGK



Name	EC ₅₀ (nM)	Helicity
I17-VIP-GK	0.14	5.1%
5	0.10	37.0%
11	0.049	9.6%

Name	K _d (μ M)-linear	K _d (μ M)-stapled
SRC1	82.6	11.4
NCoA6	196	46.2
p300	374	65.4

(B) Antidiabetic stapled peptide based on PPAR γ receptor



(C) Antidiabetic stapled peptide based on glucokinase

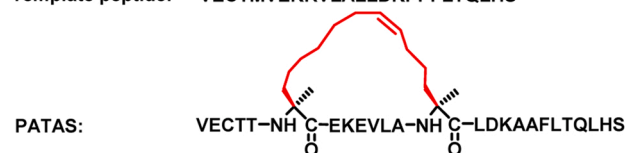
BAD BH3: NLWAAQRYGRELRRMSDFVDSEKK

BAD SAHB_{A(S-ps)}: NLWAAQRYGRELR-NH-C(=O)-N_L-pS-DNH-C(=O)-FVDSEKK

Helical enhancement ; The proapoptotic function of BAD is inactivated ; Activated glucokinase

(D) Antidiabetic stapled peptide based on ALMS1-PKC α protein

Template peptide: VECTMVEKRVLALLDKPPFLTQLHS



Name	Dose required to activate PKC(ng)
Template peptide	12.5
PATAS	2.5

Fig. 16. Antidiabetic stapled peptides based on VPAC2 receptor, PPAR γ receptor, glucokinase, and ALMS1-PKC α protein. (A) Antidiabetic stapled peptide based on VPAC2 receptor. (B) Antidiabetic stapled peptide based on PPAR-g receptor. (C) Antidiabetic stapled peptide based on glucokinase. (D) Antidiabetic stapled peptide based on ALMS1-PKC α protein.

EC₅₀ values as low as 0.049 nM for 11 (Fig. 16A), which was approximately four folds stronger than native VIP. They also showed improved helical stability and enhanced secretion activity of glucose-dependent insulin; 11 showed a plateau effect from 10 nM, indicating that it was approximately ten folds more potent than native VIP. However, the proteolytic stability of the stapled peptides did not improve, possibly because inserting a single staple within lengthy peptide sequences failed to maintain the helical structure of the peptide to some extent and multiple staples may be required to prevent the degradation of proteases. Steven Ballet and co-workers investigated the effect of three cyclisation methods on the α -helical conformation in an octapeptide segment of VIP [231]. The results showed that the peptide secondary structure varies when different chemical cyclisation strategies are employed within a 'helical' fragment. Notably, the tetrazole-based cyclisation strategy demonstrated superior α -helical stability, compared to other stapling methods.

3.4.3. Antidiabetic stapled peptides based on peroxisome proliferator-activated receptor γ receptor

Peroxisome proliferator-activated receptor γ (PPAR γ) is a potent insulin sensitiser and glucose metaboliser involved in adipogenesis and glucose metabolism [237,238]. Zhang et al. [232] employed 15 co-activated proteins as the study object and helical peptides containing the LXXLL motif region with low structural stability (which can recognise the interaction of co-activated proteins with PPAR γ) as the template. They used an RCM-based stapling strategy to constrain the helical peptide conformation and improve its stability. The non-natural amino acid S₅ was introduced at sites i, i+4, and the corresponding stapled peptides were synthesized through olefin metathesis. Combined with subsequent fluorescence analysis, three effective stapled peptides with strong binding affinity to PPAR γ were selected, including SRC1, NCoA6, and p300 (Fig. 16B). The binding affinities increased by 7.2, 4.2, and 5.7 folds, respectively, compared with the corresponding linear peptides. The designed stapled peptides may provide a reference for the development of relevant therapeutics against diabetes.

3.4.4. Antidiabetic stapled peptides based on glucokinase

Glucokinase GK is the first key enzyme in intracellular glucose metabolism; it maintains glucose homeostasis by regulating the release of glucose-controlling hormones and glycogen synthesis [239]. BAD, a pro-apoptotic BCL-2 family member, is present in a complex containing glucokinase (GK) and has been found to activate GK by phosphorylating specific residues in the BH3 region of BAD, which in turn promotes glucose response and insulin secretion in pancreatic β -cells [240,241]. The peptide BAD BH3 from BH3 (the BAD death domain) is a linear peptide with impaired structural stability. Danial et al. [233] encountered some challenges in maintaining the helical structure of the peptide, and multiple staple may be required to prevent the degradation of proteases (Fig. 16C). This approach yielded significant improvement effect, with glucokinase activity in rat islet tumour cells measuring 1.0–1.2 μ mol/mg, compared with 0.6–0.8 μ mol/mg observed with the linear peptide. This study identified glucokinase as a new direct physiological target of the BAD BH3 domain, suggesting potential therapeutic applications of BAD BH3 stapled peptides in the restoration of insulin secretion.

3.4.5. Antidiabetic stapled peptides based on ALMS1-PKC α protein

The PPI between ALMS1 and protein kinase C- α (PKC α) hinders PKC α -mediated glucose uptake in adipocytes [242,243]. Screening of the α -helix in the PKC α kinase structural domain allows the identification of the peptide sequence of the ALMS1-PKC α protein interaction. Recently, Schreyer et al. [234]. screened α -helical sequences within the structural domain of human PKC α kinase and found that the peptide ECTMVEKKVLALL effectively blocked the binding of ALMS1 to PKC α and stimulated PKC α kinase activity. Subsequently, the linear peptide was stapled and modified by a full hydrocarbon linkage, and the

synthesized stapled peptide was named PATAS (Fig. 16D). The dose required for PKC activation by PATAS was reduced by five folds, compared to the original sequence, and its activity was significantly enhanced. PATAS can target endogenous ALMS1-PKC α protein-protein interactions in adipocytes in the absence of insulin to alleviate insulin resistance and its associated comorbidities for the effective reverse of type 2 diabetes. It is expected to be a "first-in-class" adipocyte-specific therapeutic agent.

In this section, we comprehensively summarize functionalized stapled peptides for the treatment of diabetes. They were classified by various targets, including glucagon-like peptide-1 receptor (GLP-1R), peroxisome proliferator-activated receptor gamma (PPAR γ), vasoactive intestinal peptide receptor 2 (VIPAC2), glucokinase, endogenous ALMS1-PKC α protein in adipocytes. Researchers employed various strategies, including all hydrocarbon, Cys-alkylation, triazole click reaction, and lactamization, to design and develop different stapled peptides. All hydrocarbon strategy represents the most prevalent approach among them.

3.5. Stapled peptides in the treatment of inflammation

Inflammation is a defence-oriented reaction that occurs when tissues are damaged or are invaded by foreign substances [90], whereas severe inflammations may lead to death. Currently, the drugs used to treat inflammation include small molecules and peptide drugs. The peptides include pentagastrin and somatostatin for treating gastroenteritis and pancreatitis, respectively. GLP-2 G has been assessed against inflammation in clinical trials. However, the short half-life of peptides and the need for subsequent repeated treatments are some of the most notable limitations in their clinical use; therefore, chemical modification of linear peptides is required to overcome these shortcomings. Stapling is a promising modification technology that has gained wide attention in recent years and resulted in the development of peptide mimetics with high stability and good cell permeability [27]. The following sections will briefly introduce the advancements in the application of stapled strategy in anti-inflammatory drug studies in order to provide insights for subsequent research on anti-inflammatory peptide drugs (Table 5).

3.5.1. Anti-inflammatory stapled peptides based on GLP-2 receptor

The binding of the GLP-2 receptor to the peptide GLP-2 can stimulate the growth of intestinal epithelial cells, which can reduce intestinal permeability and motility, epithelial apoptosis, and inflammation [249, 250]. The first approved GLP-2 analogue, teduglutide (GLP2-2 G) (Fig. 17A), is undergoing clinical trials for inflammatory bowel disease; however, teduglutide has a short half-life in humans. Moreover, frequent injections of high doses are required, which can negatively affect patient compliance [251–253]. The development of long-acting GLP-2 analogues to lower dose frequency and offer a lasting therapeutic effect is necessary. Stapling strategies to stabilise the secondary structure of peptides are effective in improving their biological activity, metabolic stability, and cell permeability.

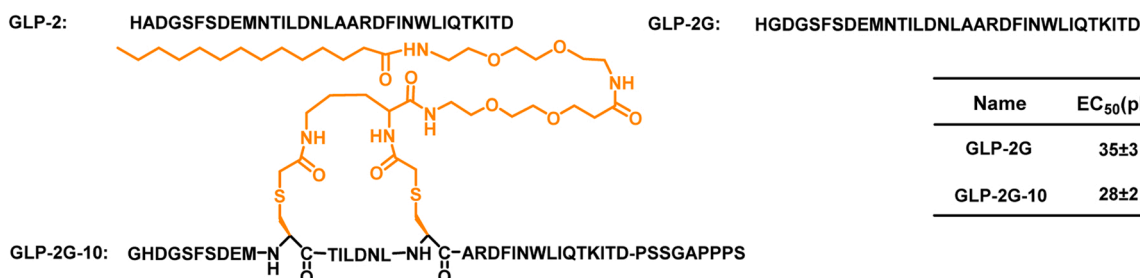
Yang et al. [244] used GLP2-2 G as a template peptide to synthesise the double-stapled peptides SEQ-1, SEQ-3, and SEQ-5 by substituting Leu17 and Asn24, Glu9 and Asn16, and Asn11 and Ala18 with Cys, respectively. To improve the solubility of the stapled peptides, an Ex-4 peptide was introduced at the C-terminus resulting in the three stapled peptides: SEQ2, SEQ-4, and SEQ-6. *In vitro* activity tests of different stapled peptides showed that stapled peptide 10 (Fig. 17A), cross-linked by linker 3, showed the best efficacy, and the t_{1/2} of stapled peptide 10 was approximately 7.2 folds longer than that of the template peptide GLP2-2 G. In summary, long-acting GLP-2 analogues can be synthesized using this method through the formation of double cysteine mutants. The stapling peptide synthesized by this method has higher efficacy and a better therapeutic effect against enteritis than teduglutide (GLP2-2 G).

Table 5

Application of stapled peptides in the treatment of inflammation.

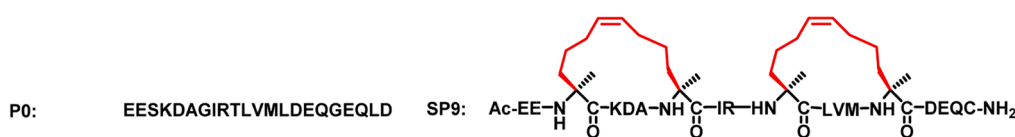
Template peptide	The target	Location	Strategy	Ref.
GLP2-2 G : HGDGFSDEMNTILDNLAARDFINWLIQTKITD	GLP-2	Extracellular	Dithiol dialkylation	[244]
SNAP-25A : EESKDAGIRTLVMLDEQGEQLD	Synaptotagmin-2	Extracellular	All hydrocarbon	[245,246]
PYD helix 2 sequence of ASC : TAEELKKFKLKLLSV	ASC protein	Intracellular	All hydrocarbon	[247]
HAP: IHVTIPADLWDWINK	IL-17A	Extracellular	Lactamization	[248]

(A) GLP-2-based stapled peptide against intestinal inflammation

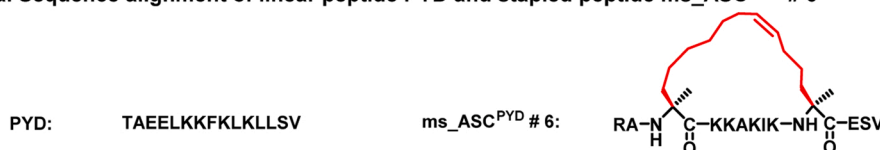


Name	EC ₅₀ (pM)	t _{1/2} (h)
GLP-2G	35±3	0.5
GLP-2G-10	28±2	3

(B) Sequence alignment of linear peptide P0 and double-stapled peptide SP9

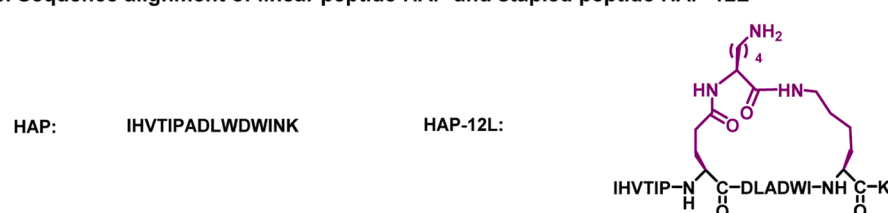


Name	Helicity
P0	5%
SP9	86%

a. Sequence alignment of linear peptide PYD and stapled peptide ms_ASC^{PYD} # 6

Name	Helicity
PYD	No helicity
ms_ASC ^{PYD} # 6	48%

b. Sequence alignment of linear peptide HAP and stapled peptide HAP-12L



Name	IC ₅₀ (nM)
HAP	30
HAP-12L	24

Fig. 17. Anti-inflammatory staple peptide based on GLP-2, calcium ion-sensing protein, and interleukin. (A) GLP-2-based stapled peptide against intestinal inflammation. (B) Sequence alignment of linear peptide P0 and double-stapled peptide SP9. (C) Sequence alignment of linear peptide HAP and stapled peptide HAP-12 L.

3.5.2. Anti-inflammation stapled peptides based on calcium ion-sensing protein

Excessive mucin release may lead to various chronic airway inflammatory diseases, such as chronic obstructive pulmonary disease, asthma, and cystic fibrosis; therefore, it is important to develop drugs that inhibit the hypersecretion of myxins [254]. Lai's team [255] found that the calcium-sensing protein synaptotagmin-2 is the target protein that mediates the excessive release of myxins. The neuronal SNARE complex, composed of synaptobrevin-2/VAMP-2, SNAP-25A, and syntaxin-1A (Stx1), forms the preferred interface with the Ca²⁺-binding region of synaptotagmin-2. The interaction between these two proteins induces Ca²⁺-triggered membrane fusion to moderate myxin release. Targeting the interaction site of the SNARE/synaptotagmin-2 protein, Lai's team [245,246] designed a stapled peptide, SP9 (Fig. 17B), that can compete with SNARE to bind synaptotagmin-2. Many key residues at the

interface formed by the interaction between synaptotagmin-2 and the neuronal SNARE complex are mainly located in SNAP-25A. Therefore, the SNAP-25A fragment can be used as a template to selectively interfere with the interaction between Synaptotagmin-2 and SNARE, thereby disrupting Ca²⁺-triggered membrane fusion. Because of the structural instability defect of the SNAP-25A fragment, they utilised an RCM-based stapling strategy to replace the key residues at sites i/i+4 or i/i+7 and synthesised a series of monocyclic and bicyclic stapled peptides through olefin metathesis, namely SP1-SP12. Circular dichroism spectroscopy showed that the template peptide P0 displayed only 5% α -helicity in solution, while stapled peptides had improved α -helicity, and several dicyclic peptides had α -helicity as high as 86%. The inhibition of Ca²⁺-triggered membrane fusion experiments showed that the stapled peptide SP9 improved the inhibitory effect of the template peptide by approximately 70%. The SNSNARE/synaptotagmin-2 mediated myxin

secretion process was recombined *in vitro* using a single-vesicle content fusion experimental system, and the results confirmed that the stapled peptide SP9 effectively inhibited the Ca²⁺-triggered airway SNARE and synaptotagmin-2-mediated vesicle fusion process. Therefore, the bicyclic stapled peptide SP9, based on an all-hydrocarbon stapling strategy, can inhibit myxins hypersecretion and is a promising drug candidate for the treatment of airway inflammation.

3.5.3. Anti-chronic inflammation stapled peptides based on interleukin

Interleukin-1 β (IL-1 β) is a main cytokine capable of initiating and enhancing the inflammatory response, while the excessive production of IL-1 β is a factor in most chronic inflammatory diseases, such as cardiovascular diseases and metabolic diseases [256]. Apoptosis-associated spot-like protein ASC, which can activate caspase-1 and then transform IL-1 β from inactive precursor to mature active form, plays an important role in activating intracellular cysteine protease caspase-1 [257–259]. Therefore, ASC may be a potential target for the ASC-dependent inflammatory pathway to block excessive IL-1 β production and suppress inflammation. Pal et al. [247] used an all-hydrocarbon stapling strategy to design a series of stapled peptides to disrupt ASC-dependent inflammatory pathways and improve the pharmacological properties of peptides by enhancing their target affinity and proteolytic stability. The ASC PYD domain was selected as the target, and PYD helix region 2 was used as the template peptide. The two corresponding Leu residues at position i, i+7, were replaced, and cyclisation was accomplished by RCM using Grubbs' catalyst. CD showed that the template peptide PYD did not show significant helicity, whereas the stapled peptide showed increased helicity by > 48% (Figure 17Ca). The study also found that the stapled peptide reduced the production of IL-1 β by almost 50%, compared to the template peptide. The stapled peptides reduced caspase-1 activation and IL-1 β production, which in turn reduced inflammation.

IL-17A can induce the production of other pro-inflammatory mediators, such as TNF- α , IL-1, and IL-6, which play an important role in tissue damage [260]. Therefore, reducing IL-17A production is a promising direction for the control of inflammation and related diseases. Dong's group [248] used the inhibitory helical peptide HAP of IL-17A as a model peptide and mutated the residues Ala7/Asn14 into Glu and Lys, respectively, in order to introduce carboxyl and amino side chains and achieve lactamidation. Dong et al. successfully introduced nine α -amino acids with different configurations and side chains into HAP. The CD results showed that the helicity of the L-type stapled peptides was stronger than that of the D-type stapled peptides (Figure 17Cb). The results of proteinase K and anti-inflammatory activity assays using normal dermal fibroblast also showed that L-type stapled peptides had a higher potency than D-type stapled peptides. Based on the results of molecular dynamics simulations, the non-hot, large-sized Trp residue was mutated into a smaller, more helical Ala residue. The simulation results of modelling and dynamic simulation showed that the mutant stapled peptide could maintain the α -helix conformation, without producing geometric conflicts. Among them, the substitution of Trp10 with an Ala residue and the inclusion of a L-Lys linker bridge in 12 L demonstrated improved enzyme stability, IL-17A binding ability, and *in vitro* bioactivity. These results provide an important reference for the design of stapled peptides and the modification of amino acids.

In this section, we summarize functionalized stapled peptides designed for the treatment of inflammation. These peptides are classified based on their targets, including GLP-2, Synaptotagmin-2, ASC protein, IL-17A, and others. Researchers have employed various strategies, such

as all hydrocarbon, dithiol dialkylation, lactamization, and others, to design and develop these stapled peptides. Among these strategies, all hydrocarbon approach represents the largest proportion.

3.6. Stapled peptides in the treatment of osteoporosis

Table 6.

3.6.1. Anti-osteoporosis stapled peptides based on phosphorylated GSK-3 β

FRATtide [264] derived from GSK-3 binding protein GBP could reduce the phosphorylation level of GSK-3 β to negatively regulate osteoclasts. As a linear peptide, FRATtide exhibits poor proteolytic stability and cellular membrane permeability. To overcome this problem, our group [261] used an all-hydrocarbon stapling strategy to prepare a series of stapled peptides. CD showed that most of the stapled peptides showed a stronger tendency to form α -helix conformation (3–4 folds), compared with the linear peptides. Protease stability analysis showed that the stapled peptide was > 10 folds more stable than the FRATtide. Biological evaluation showed that most of the stapled peptides inhibited the differentiation of osteoclasts, among them FRC-2 and FRN-2 peptides displayed the best inhibitory effect (Figure 18Aa).

Our team [262] used a linear peptide, FRT-0, as the template peptide, and a double-bound peptide, FRNC-1 (Figure 18Ab), was designed by introducing S₅ at the i, i+4 sites. Compared to the linear peptide, FRNC-1 showed significantly improved helical content; FRT-0 was quickly cleared within 2 h, and no significant changes were observed in FRNC-1 peptides after 48 h. The results showed that FRNC-1 had a lower inhibitory concentration than FRT-0 in BMM and MSC. By analysing the changes in serum drug concentrations after different administration routes, we found that the concentration of FRNC-1 in the blood increased significantly after gavage, indicating that the peptide could enter the plasma and exert anti-osteoporotic effects. Subsequently, we investigated the binding mode of FRNC-1 with phosphorylated GSK-3 β through structural modeling analysis. FRNC-1 exhibited a binding pattern to the target protein that closely resembled its linear counterpart, owing to the high sequence similarity between them (Figure 18Ab). Notably, an additional hydrophobic interaction was observed between the staple at the C-terminus of FRNC-1 and Val267 and Ile270 of the target protein. This observed phenomenon likely contributes to the potential for enhanced affinity of stapled peptides to their target proteins. Our bicyclic peptide, FRNC-1, which was designed based on a bistapling modification technique, is the first orally effective peptide drug candidate for the treatment of the osteoporosis.

3.6.2. Anti-osteoporosis stapled peptides based on PTH/ PTHrP

PTH_{1–34} is used in the clinical treatment of glucocorticoid-induced osteoporosis and bone destruction [265,266]; however, as a linear peptide, it is structurally unstable. The earliest structural study of PTHrP by Chorev et al. [267] reported that the introduction of Lactam Bridge led to enhanced biological efficacy. Based on this finding, Bisello et al. [263] concluded that replacing the potential salt bridge formed by the opposite charges on Lys₁₃ and Asp₁₇ side chains with a stable covalently lactam bond is conducive to peptide conformational stability, which will improve α -helicity and biological activity. Using PTH (1–34) as a template peptide, a lactam ring was synthesized between the amino acid residues Lys and Asp at positions i and i+4 and a bi-lactam ring between the residues. The obtained monocyclic and bicyclic stapled peptides (Fig. 18B) were subjected to conformational analysis and evaluated for their biological activity, which was approximately 10 folds higher in the

Table 6

Application of stapled peptides in the treatment of osteoporosis.

Template peptide	The target	Location	Strategy	Ref.
FRATtide : DPHRLQLVLSGNLIKEAVRRRLHSR	GSK-3 β	Intracellular	All hydrocarbon	[261,262]
PTH (1–34): AVSEHQLLHDKGSIQDLRRRFFLHKLIADIHTA	PTH/ PTHrP receptor	Intracellular	Lactamization	[263]

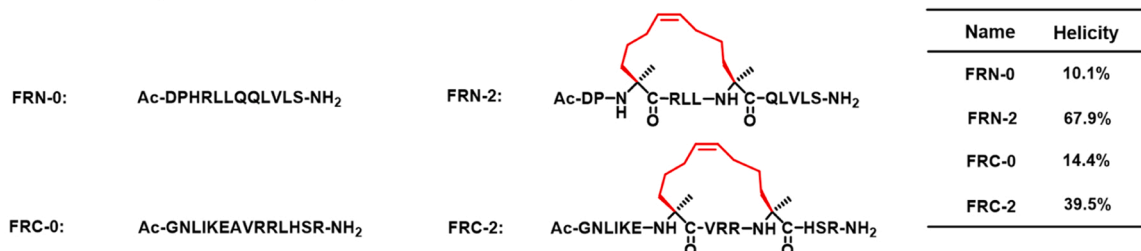
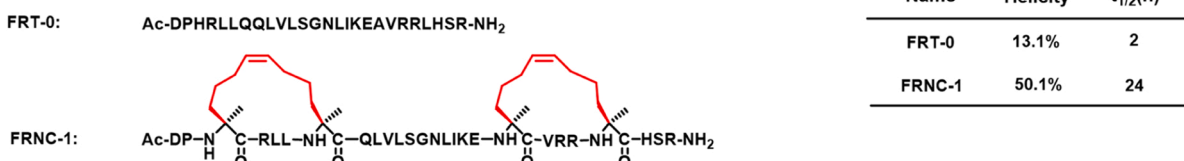
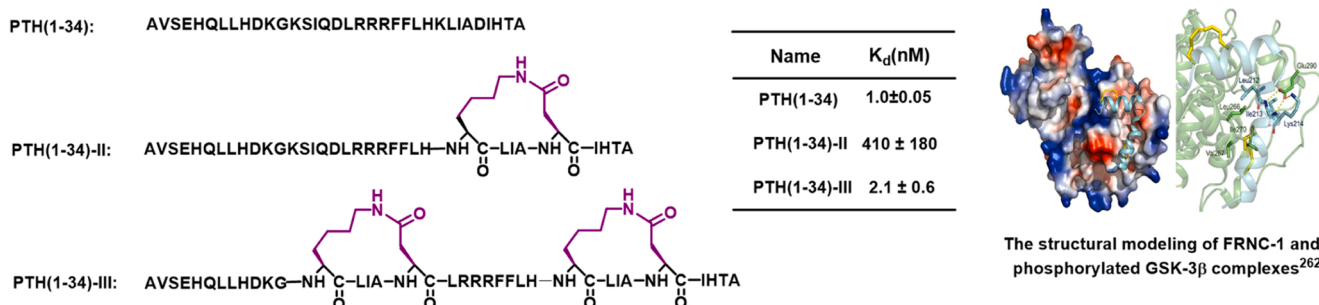
(A) Anti-osteoporosis stapled peptide based on phosphorylated glycogen synthase kinase-3 β (GSK-3 β)**a. Sequence alignment of linear peptides FRN-0 and FRC-0, and stapled peptides FRN-2 and FRC-2****b. Sequence alignment of linear peptide FRT-0 and stapled peptide FRN-2****(B) Sequence alignment of linear peptide PTH(1-34), and stapled peptides PTH(1-34)-II and PTH(1-34)-III**

Fig. 18. Stapled peptides for the treatment of osteoporosis. (A) Anti-osteoporosis stapled peptide based on phosphorylated glycogen synthase kinase-3 β (GSK-3 β). Reproduced with permission from Ref. [262]. (B) Sequence alignment of linear peptide PTH (1–34), and stapled peptides PTH (1–34)-II and PTH (1–34)-III.

sub-nanomolar range than that of the linear peptide. Monocyclic and bicyclic stapled peptides synthesized using the lactam ring formation method were the first cyclic PTH/PTHrP receptor agonists.

In this section, we summarize functionalized stapled peptides developed for the treatment of osteoporosis. These peptides are classified based on their targets, including GSK-3 β , PTH/PTHrP receptor, and others. Researchers have employed various strategies, such as all hydrocarbon and lactamization, to design and develop these stapled peptides. Among these strategies, the all hydrocarbon approach represents the largest proportion.

3.7. Stapled peptides in the treatment of neuropathic disease

Table 7.

Autophagy is an important process of material turnover in eukaryotic cells. Impaired autophagy can cause the aggregation of neurotoxic proteins, which in turn results in the emergence of neurodegenerative diseases, including Alzheimer's disease and Parkinson's disease [271, 272]. One of the most effective autophagy inducers is the protein TAT-Beclin 1. However, it is too large and cannot enter cells in the absence of multi-cationic Tat sequences [273,274]. Leila et al. [268] determined the minimum active part of Tat-Beclin 1 by conducting a

HeLa autophagy experiment and used cysteine for stapled peptide synthesis at positions $i, i + 3$. Stapled peptides DD6-m and DD5-o (Fig. 19A) of beclin 1 were generated using a disulfide bond as a stapling bridge. It has been reported that stapled peptide DD6-m can significantly induce autophagy and remove protein aggregates, while stapled peptide DD5-o, although slightly less potent, can form a stable α -helical conformation in methanol and does not need to rely on Tat sequence to penetrate the cell. The staple within DD5-o is formed by the $(i, i+3)$ linkage between two D-cysteines and the o -xylene group, resulting in enhanced cell permeability. The smaller size and inherent cell penetration of DD5-o make it a promising foundation for the development of peptide and small-molecule therapeutics. Relaxin-3 binds to the receptor RXFP3 through the B chain and plays a role in regulating appetite, mental stress, and metabolism [275–279]. To address the fact that the RXFP3 B chain is easily degraded by enzymes and cannot cross the blood-brain barrier, Jayakody et al. [269] synthesised stapled peptides 14s18 and 18s22 (Fig. 19B), in which Cys residues were replaced with Ser to prevent peptide oxidation and oligomerisation. CD analysis revealed that the stapled peptide 14s18 displayed a 10-fold enhancement in helicity, compared with the unstapled peptide. The 14s18 sequence remained unchanged after incubation with the protease, indicating good resistance to degradation. Subsequently, Jayakody et al. [280] performed a

Table 7

Application of stapled peptides in the treatment of neuropathic disease.

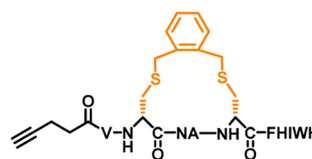
Template peptide	The target	Location	Strategy	Ref.
Tat-Beclin 1 : YGRKKRRORRRGGTNVENATFEIWHDGFEFGT	Beclin 1	Intracellular	Thiols are dialkylated	[268]
Relaxin-3 B chain : RAAPYGVRLCGREFIRAVIFTCCGSRW	RXFP3	Extracellular	All hydrocarbon	[269]
dynA ₁₋₁₃ : YGGFLRRIRPKLK	KOR	Extracellular	Cysteine stapled	[270]

(A) Sequences of autophagy-inducing peptides

Tat-Beclin 1: YGRKKRRORRRGG-TNVENATFEIWHDGEFGT

Tat-11mer: YGRKKRRORRRGG-VENATFHIWHD

DD5-o:

A stable α -helical conformation is formed in methanol without the need for Tat sequences to penetrate cells**(B) Sequences of the wild type B chain of relaxin-3 (H3 B chain) and stapled B chain of relaxin-3 (14s18 and 14s21)**

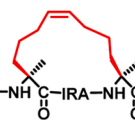
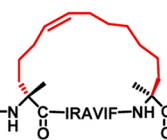
H3 B chain: RAAPYGVRLCGREFIRAVIFTCGGSRW

14s21:

RAAPYGVRLSGRE-NH-C-IRAVIF-NH-C-CGGSRW

14s18:

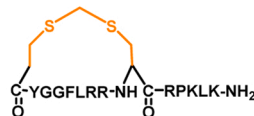
RAAPYGVRLSGRE-NH-C-IRA-NH-C-IFTSGGSRW



Name	Helicity
H3 B chain	1.8%
14s18	18.5%
14s21	23.5%

(C) Sequences of dynA₁₋₁₃ and stapled peptide CSD-CH_{2(1,8)}-NH₂dynA₁₋₁₃:

YGGFLRRIRPKLK

CSD-CH_{2(1,8)}-NH₂:

Name	t _{1/2} (min)	K _i ± SD (nM)
dynA ₁₋₁₃	4	0.29 ± 0.4
CSD-CH _{2(1,8)} -NH ₂	95	6.8 ± 1.8

Fig. 19. Stapled peptides for the treatment of neurological disorders. (A) Sequences of autophagy-inducing peptides. (B) Sequences of the wild type relaxin-3 B chain (H3 B chain) and stapled relaxin-3 B chain (14s18 and 14s21). (C) Sequences of dynA₁₋₁₃ and stapled peptide CSD-CH_{2(1,8)}-NH₂.

conformational analysis of peptide 14s18 and found that the N-terminal residues may be related to the optimal α -helicity of the peptide. Therefore, they designed stapled relaxin 3 mimics (14s21 and 11s18) by using all hydrocarbon stapling strategy in the i, i+7 position. CD results showed that the stapled peptide 14s21 effectively retained the helicity of the relaxin-3 B chain. Intranasal administration of the stapled peptide 14s21 in rat anxiety and depression models showed superior anti-anxiety effects to those of relaxin-3 in behavioural paradigms. Stapled peptide 14s21 is expected to be an important tool for further exploration of the relaxin-3 receptor system and a potential new strategy for treating severe depression and anxiety disorders.

The K opioid receptor (KOR) is involved in emotional and cognitive physiological processes and is broadly expressed in the peripheral and central nervous systems [281,282]. KOR antagonists can relieve symptoms of anxiety, depression, or substance abuse by binding to KOR receptors. DynA₁₋₁₃ is a KOR antagonist with a short half-life and flexible conformation, which limits its application as a druggable target. Gruber's group [270] used dynA₁₋₁₃ as a template peptide and cyclised it using a cysteine stapling strategy to synthesise a stable KOR-specific competitive antagonist CD-CH_{2(1,8)}-NH₂ (Fig. 19C) to overcome the aforementioned challenges. The plasma stability test showed that the stability of CD-CH_{2(1,8)}-NH₂ was significantly improved, compared to that of the linear peptide. Radioligand-binding studies showed that the affinity of CSD-CH_{2(1,8)}-NH₂ was approximately 12 times higher than that of the linear peptide dynA₁₋₁₃. The experimental results of the mouse model of acute heat injury showed that CD-CH_{2(1,8)}-NH₂ significantly reduced the injury. These results indicate that the cysteine stapling strategy can improve the poor protease resistance and low activity of linear peptides, providing a promising approach for the development of therapeutics against KOR-related diseases.

In this section, we summarize functionalized stapled peptides developed for the treatment of neuropathic disease. These peptides are classified based on their targets, including Beclin 1, RXFP3, KOR, and others. Researchers have employed various strategies, such as all hydrocarbon, thiol dialkylation, and cysteine stapling, to design and develop these stapled peptides.

4. Summary and outlook

Inspired by the all-hydrocarbon peptide stapling technique

developed by Verdine et al., numerous peptide stapling strategies have been discovered and developed to address the poor proteolytic stability and weak membrane permeability of the linear peptides (Fig. 20). As a result, numerous linear peptides derived from PPI-interacting interfaces, natural peptide products and phage-displayed or in silico-designed peptides have undergone modifications by introducing various staples at the side chains. (Fig. 21). Stapled peptides target different signalling pathways or exhibit different biological activities against specific diseases. Herein, we comprehensively summarise the functionalised stapled peptides against various diseases, including cancer, bacterial and viral infections, inflammation, osteoporosis, and diabetes. Among the investigated peptides, all-hydrocarbon-hydrocarbon-stapled peptides emerged as the most prevalent approach, focusing predominantly on cancer and viral diseases.

Although these stapled peptides showed significantly improved proteolytic resistance and/or enhanced membrane penetration, most of them displayed moderate and poor biological activities *in vitro* and *in vivo*, respectively. Notably, these activities were associated with the intravenous injection of the peptides. Stapled peptides hardly exhibit biological activities when administered through other routes, especially oral route, except in extremely rare cases. Therefore, these two major weaknesses of peptides severely limit their applications in drug design,

S Strengths <ul style="list-style-type: none"> • Good efficacy and proteolytic stability • High helicity and cell permeability • Strong binding affinity • Orally available • Convenient synthesis protocols 	W Weaknesses <ul style="list-style-type: none"> • Tendency for aggregation • High hydrophobicity • Low cell selectivity • Poor biological activity <i>in vivo</i>
O Opportunities <ul style="list-style-type: none"> • New hydrophilic stapling strategy • Combined with other peptide modifying strategies • Nano-particle based delivering technique • Prodrug strategy 	T Threats <ul style="list-style-type: none"> • Immunogenicity • Small in the clinical phase • Price and reimbursement environment • Increasing safety requirements for novel drugs

Fig. 20. Analysis of the strengths, weaknesses, opportunities, and threats (SWOT) of stapled peptides in their use as therapeutics.

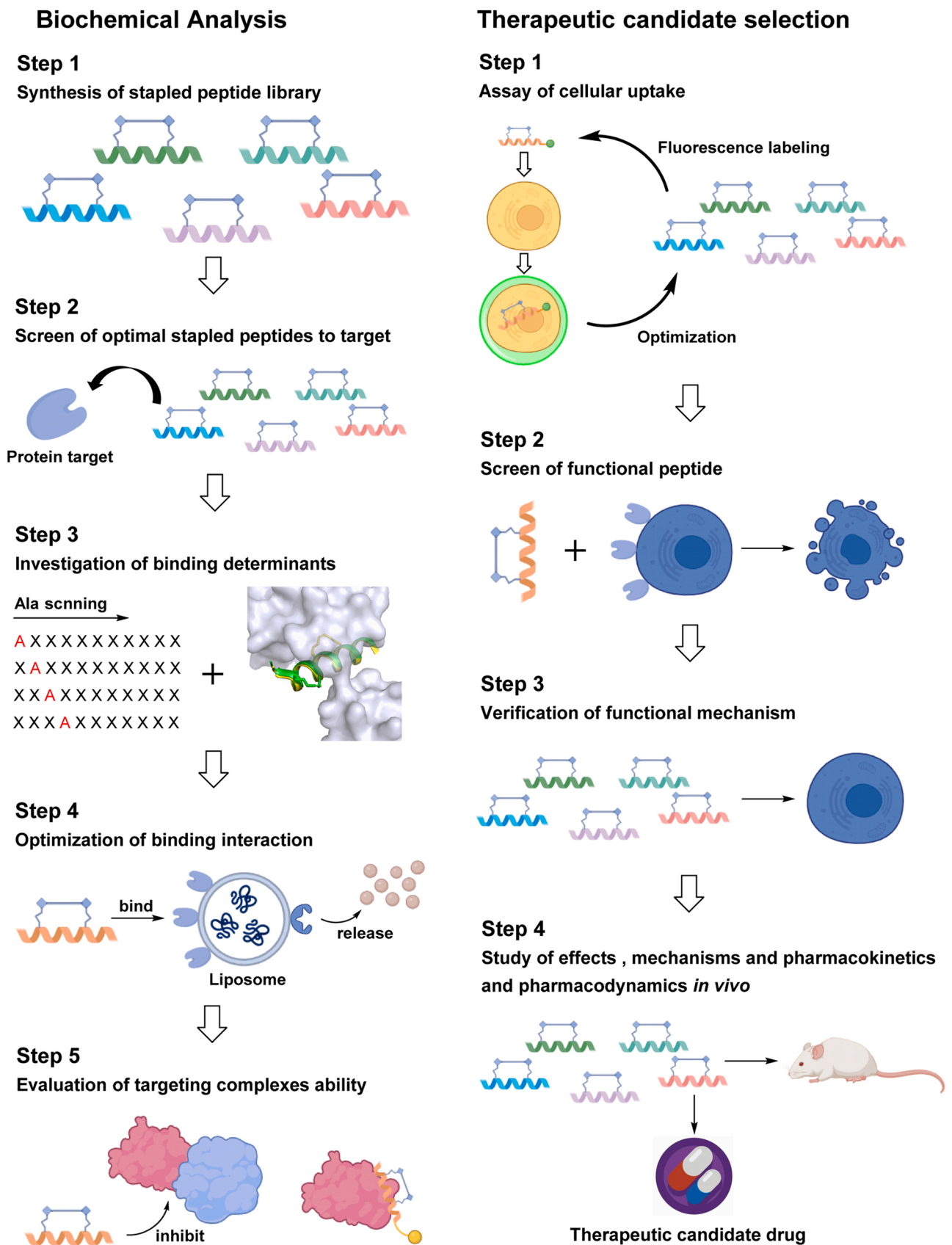


Fig. 21. Comprehensive overview of the application of stapled peptides in biological research [22].

and more advanced and powerful stapling strategies are urgently required. Another alternative method is to combine peptide stapling with other peptide-modifying strategies, such as PEG modification and glycosylation. Our team has previously shown that glycosylated stapled peptides exhibit improved activity and reduced cytotoxicity. Another important aspect is the delivery of stapled peptides into a specific zone to exhibit the corresponding efficacy. Nanoparticle-based delivery techniques are a vital solution, and peptide/nanoparticle co-assembly and controlled release have attracted increasing attention in the peptide research field. Stapled peptide-based nanoparticle co-assembly into a specific target environment and the consequent enzyme- or pH-triggered release is in progress in our laboratory.

Funding

This work was supported by Taishan Scholars Program (No. tsqn202306268, to Yulei Li), the National Nature Science Foundation of China No. 21807112 (to Xiang Li), No. 91849129 (to Honggang Hu), No. 22077078 (to Honggang Hu) and No. 22207065 (to Yulei Li), academic promotion program of Shandong First Medical University (No 2019LJ003, China, to Yulei Li), Shanghai Rising-Star Program (to Xiang Li).

Author statement

Yulei Li, Minghao Wu and Yinxue Fu contributed equally to this work; Yulei Li, Honggang Hu and Xiang Li conceived and revised the manuscript. The manuscript was wrote by Yulei Li, Minghao Wu, Yinxue Fu, Jingwen Xue, Fei Yuan. Xiang Li, Minghao Wu and Yinxue Fu designed and prepared the figures. All authors edited the manuscript and figures and approved the final version for submission.

CRedit authorship contribution statement

Fei Yuan: Writing – original draft. **Xiang Li:** Writing – review & editing, Writing – original draft. **Honggang Hu:** Writing – review & editing, Writing – original draft. **Yulei Li:** Writing – review & editing, Writing – original draft, Investigation, Funding acquisition. **Minghao Wu:** Writing – original draft. **Yinxue Fu:** Writing – original draft. **Jingwen Xue:** Writing – original draft.

Declaration of Competing Interest

None.

Data availability

The data that has been used is confidential.

References

- [1] A. Henninot, J.C. Collins, J.M. Nuss, The current state of peptide drug discovery: back to the future? *J. Med. Chem.* 61 (2018) 1382–1414, <https://doi.org/10.1021/acs.jmedchem.7b00318>.
- [2] K. Fosgerau, T. Hoffmann, Peptide therapeutics: current status and future directions, *Drug Discov. Today* 20 (2015) 122–128, <https://doi.org/10.1038/s41573-019-0053-0>.
- [3] J.L. Lau, M.K. Dunn, Therapeutic peptides: historical perspectives, current development trends, and future directions, *Bioorg. Med. Chem.* 26 (2018) 2700–2707, <https://doi.org/10.2174/138161210793292555>.
- [4] M. Muttenthaler, G.F. King, D.J. Adams, et al., Trends in peptide drug discovery, *Nat. Rev. Drug Discov.* 20 (2021) 309–325, <https://doi.org/10.1038/s41573-020-00135-8>.
- [5] F.J. Chen, N. Pinnette, F. Yang, et al., A cysteine-directed proximity-driven crosslinking method for native peptide bicyclization, *Angew. Chem. Int. Ed. Engl.* 62 (2023) e202306813, <https://doi.org/10.1002/anie.202306813>.
- [6] D.J. Drucker, Advances in oral peptide therapeutics, *Nat. Rev. Drug Discov.* 19 (2020) 277–289, <https://doi.org/10.1038/s41573-019-0053-0>.
- [7] R. Jwad, D. Weissberger, L. Hunter, Strategies for fine-tuning the conformations of cyclic peptides, *Chem. Rev.* 120 (2020) 9743–9789, <https://doi.org/10.1021/acs.chemrev.0c00013>.
- [8] L. Liu, X. Fan, B. Wang, et al., P(III)-Directed Late-Stage Ligation and Macrocyclization of Peptides with Olefins by Rhodium Catalysis, *Angew. Chem. Int. Ed. Engl.* 61 (2022) e202206177, <https://doi.org/10.1002/anie.202206177>.
- [9] A.S. Mackay, J.W.C. Maxwell, M.J. Bedding, et al., Electrochemical modification of polypeptides at selenocysteine, *Angew. Chem. Int. Ed. Engl.* 62 (2023) e202313037, <https://doi.org/10.1002/anie.202313037>.
- [10] K.M. Sicinski, V. Montanari, V.S. Raman, et al., A non-perturbative molecular grafting strategy for stable and potent therapeutic peptide ligands, *ACS Cent. Sci.* 7 (2021) 454–466, <https://doi.org/10.1021/acscentsci.0c01237>.
- [11] X.J. Zheng, L. Zhu, T.L. Li, et al., Improve stability of bioactive peptides by enzymatic modular synthesis of peptides with O-linked sialyl lewis x, *ACS Catal.* 11 (2021) 8042–8048, <https://doi.org/10.1021/acscatal.1c00955>.
- [12] M. Erak, K. Bellmann-Sickert, S. Els-Heindl, et al., Peptide chemistry toolbox – Transforming natural peptides into peptide therapeutics, *Bioorg. Med. Chem.* 26 (2018) 2759–2765, <https://doi.org/10.1016/j.bmc.2018.01.012>.
- [13] M. Muttenthaler, A. Andersson, A.D. de Araujo, et al., Modulating oxytocin activity and plasma stability by disulfide bond engineering, *J. Med. Chem.* 53 (2010) 8585–8596, <https://doi.org/10.1021/jm100989w>.
- [14] D.S. Nielsen, N.E. Shepherd, W. Xu, et al., Orally absorbed cyclic peptides, *Chem. Rev.* 117 (2017) 8094–8128, <https://doi.org/10.1021/acs.chemrev.6b00838>.
- [15] D. Garcia Jimenez, V. Poongavanam, J. Kihlberg, Macrocycles in drug discovery—learning from the past for the future, *J. Med. Chem.* 66 (2023) 5377–5396, <https://doi.org/10.1021/acs.jmedchem.3c00134>.
- [16] D. Sethio, V. Poongavanam, R. Xiong, et al., Simulation reveals the chameleonic behavior of macrocycles, *J. Chem. Inf. Model* 63 (2023) 138–146, <https://doi.org/10.1021/acs.jcim.2c01093>.
- [17] H.Y. Chow, Y. Zhang, E. Matheson, et al., Ligation technologies for the synthesis of cyclic peptides, *Chem. Rev.* 119 (2019) 9971–10001, <https://doi.org/10.1021/acs.chemrev.8b00657>.
- [18] V. Azzarito, K. Long, N.S. Murphy, et al., Inhibition of α -helix-mediated protein–protein interactions using designed molecules, *Nat. Chem.* 5 (2013) 161–173, <https://doi.org/10.1038/nchem.1568>.
- [19] P.M. Cromm, J. Spiegel, T.N. Grossmann, Hydrocarbon Stapled Peptides as Modulators of Biological Function, *ACS Chem. Biol.* 10 (2015) 1362–1375, <https://doi.org/10.1021/cb501020r>.
- [20] J. Iegre, J.S. Gaynord, N.S. Robertson, et al., Two-component stapling of biologically active and conformationally constrained peptides: past, present, and future, *Adv. Ther.* 1 (2018) 1800052, <https://doi.org/10.1002/adtp.201800052>.
- [21] Y.H. Lau, P. de Andrade, Y. Wu, et al., Peptide stapling techniques based on different macrocyclisation chemistries, *Chem. Soc. Rev.* 44 (2015) 91–102, <https://doi.org/10.1039/C4CS00246F>.
- [22] L.D. Walensky, G.H. Bird, Hydrocarbon-stapled peptides: principles, practice, and progress, *J. Med. Chem.* 57 (2014) 6275–6288, <https://doi.org/10.1021/jm4011675>.
- [23] X. Li, Y. Zou, H.G. Hu, Different stapling-based peptide drug design: mimicking α -helix as inhibitors of protein–protein interaction, *Chin. Chem. Lett.* 29 (2018) 1088–1092, <https://doi.org/10.1016/j.ccllet.2018.01.018>.
- [24] K.J. Skowron, T.E. Speltz, T.W. Moore, Recent structural advances in constrained helical peptides, *Med Res Rev.* 39 (2019) 749–770, <https://doi.org/10.1002/med.21540>.
- [25] Y.S. Tan, D.P. Lane, C.S. Verma, Stapled peptide design: principles and roles of computation, *Drug Discov. Today* 21 (2016) 1642–1653, <https://doi.org/10.1016/j.drudis.2016.06.012>.
- [26] Y.W. Zhang, J.B. Guo, J.J. Cheng, et al., High-throughput screening of stapled helical peptides in drug discovery, *J. Med. Chem.* (2022), <https://doi.org/10.1021/acs.jmedchem.2c01541>.
- [27] X. Li, S. Chen, W.D. Zhang, et al., Stapled helical peptides bearing different anchoring residues, *Chem. Rev.* 120 (2020) 10079–10144, <https://doi.org/10.1021/acs.chemrev.0c00532>.
- [28] C.E. Schafmeister, J. Po, G.L. Verdine, An all-hydrocarbon cross-linking system for enhancing the helicity and metabolic stability of peptides, *J. Am. Chem. Soc.* 122 (2000) 5891–5892, <https://doi.org/10.1021/ja000563a>.
- [29] H.E. Blackwell, R.H. Grubbs, Highly efficient synthesis of covalently cross-linked peptide helices by ring-closing metathesis, *Angew. Chem. Int. Ed. Engl.* 37 (1998) 3281–3284, [https://doi.org/10.1002/\(SICI\)1521-3773\(19981217\)37:23<3281::AID-ANIE3281>3.3.CO;2-M](https://doi.org/10.1002/(SICI)1521-3773(19981217)37:23<3281::AID-ANIE3281>3.3.CO;2-M).
- [30] M. Buyanova, D. Pei, Targeting intracellular protein–protein interactions with macrocyclic peptides, *Trends Pharm. Sci.* 43 (2022) 234–248, <https://doi.org/10.1016/j.tips.2021.11.008>.
- [31] Y.S. Chang, B. Graves, V. Guerlavais, et al., Stapled α -helical peptide drug development: a potent dual inhibitor of MDM2 and MDMX for p53-dependent cancer therapy, *Proc. Natl. Acad. Sci. USA* 110 (2013) E3445–E3454, <https://doi.org/10.1073/pnas.1303002110>.
- [32] M.G. Ricardo, A.M. Ali, J. Plewka, et al., Multicomponent peptide stapling as a diversity-driven tool for the development of inhibitors of protein–protein interactions, *Angew. Chem. Int. Ed. Engl.* 59 (2020) 5235–5241, <https://doi.org/10.1002/anie.201916257>.
- [33] N.S. Robertson, S.J. Walsh, E. Fowler, et al., Macrocyclisation and functionalisation of unprotected peptides via divinyltriazine cysteine stapling, *Chem. Comm.* 55 (2019) 9499–9502, <https://doi.org/10.1039/c9cc05042f>.
- [34] A.M. Ali, J. Atmaj, N. Van Oosterwijk, et al., Stapled peptides inhibitors: a new window for target drug discovery, *Comput. Struct. Biotechnol. J.* 17 (2019) 263–281, <https://doi.org/10.1016/j.csbj.2019.01.012>.

- [35] M.E. Pachon-Ibanez, Y. Smani, J. Pachon, et al., Perspectives for clinical use of engineered human host defense antimicrobial peptides, *FEMS Microbiol. Rev.* 41 (2017) 323–342, <https://doi.org/10.1093/femsre/fux012>.
- [36] D.J. Holthausen, S.H. Lee, V.T.V. Kumar, et al., An amphibian host defense peptide is virucidal for human H1 hemagglutinin-bearing influenza viruses, *Immunity* 46 (2017) 587–595, <https://doi.org/10.1016/j.immuni.2017.03.018>.
- [37] W. Li, F. Separovic, N.M. O'Brien-Simpson, et al., Chemically modified and conjugated antimicrobial peptides against superbugs, *Chem. Soc. Rev.* 50 (2021) 4932–4973, <https://doi.org/10.1039/d0cs01026j>.
- [38] R. Mourtada, H.D. Herce, D.J. Yin, et al., Design of stapled antimicrobial peptides that are stable, nontoxic and kill antibiotic-resistant bacteria in mice, *Nat. Biotechnol.* 37 (2019) 1186–1197, <https://doi.org/10.1038/s41587-019-0222-z>.
- [39] Y. Li, M. Wu, Q. Chang, et al., Stapling strategy enables improvement of antitumor activity and proteolytic stability of host-defense peptide hymenochirin-1B, *RSC Adv.* 8 (2018) 22268–22275, <https://doi.org/10.1039/c8ra03446j>.
- [40] M.H. Wu, Q. Chen, Y.D. Wang, et al., Structural modification and antifungal activity of antimicrobial peptide HYL, *Chin. Chem. Lett.* 31 (2020) 1288–1292, <https://doi.org/10.1016/j.ccl.2019.10.013>.
- [41] D.C. Brice, G. Diamond, Antiviral activities of human host defense peptides, *Curr. Med. Chem.* 27 (2020) 1420–1443, <https://doi.org/10.2174/0929867326666190805151654>.
- [42] K.A. Brogden, Antimicrobial peptides: pore formers or metabolic inhibitors in bacteria? *Nat. Rev. Microbiol.* 3 (2005) 238–250, <https://doi.org/10.1038/nrmicro1098>.
- [43] M.N. Melo, R. Ferre, M.A. Castanho, Antimicrobial peptides: linking partition, activity and high membrane-bound concentrations, *Nat. Rev. Microbiol.* 7 (2009) 245–250, <https://doi.org/10.1038/nrmicro2095>.
- [44] W.C. Wimley, K. Hristova, Antimicrobial peptides: successes, challenges and unanswered questions, *J. Membr. Biol.* 239 (2011) 27–34, <https://doi.org/10.1007/s00232-011-9343-0>.
- [45] A.M. Felix, E.P. Heimer, C.T. Wang, et al., Synthesis, biological activity and conformational analysis of cyclic GRF analogs, *Int. J. Pept. Protein Res.* 32 (1988) 441–454, <https://doi.org/10.1111/j.1399-3011.1988.tb01375.x>.
- [46] L.D. Walensky, A.L. Kung, I. Escher, et al., Activation of apoptosis in vivo by a hydrocarbon-stapled BH3 helix, *Science* 305 (2004) 1466–1470, <https://doi.org/10.1126/science.1099191>.
- [47] M. Moiola, M.G. Memeo, P. Quadrelli, stapled peptides—a useful improvement for peptide-based drugs, *Molecules* 24 (2019), <https://doi.org/10.3390/molecules24203654>.
- [48] J.W. Taylor, The synthesis and study of side-chain lactam-bridged peptides, *Biopolymers* 66 (2002) 49–75, <https://doi.org/10.1002/bip.10203>.
- [49] N.E. Shepherd, H.N. Hoang, G. Abbenante, et al., Single turn peptide alpha helices with exceptional stability in water, *J. Am. Chem. Soc.* 127 (2005) 2974–2983, <https://doi.org/10.1021/ja0456003>.
- [50] T.E. Speltz, C.G. Mayne, S.W. Fanning, et al., A “cross-stitched” peptide with improved helicity and proteolytic stability, *Org. Biomol. Chem.* 16 (2018) 3702–3706, <https://doi.org/10.1039/c8ob00790j>.
- [51] H.J. Li, X.Y. Chen, M.H. Wu, et al., Bicyclic stapled peptides based on p53 as dual inhibitors for the interactions of p53 with MDM2 and MDMX, *Chin. Chem. Lett.* 33 (2022) 1254–1258, <https://doi.org/10.1016/j.ccl.2021.08.130>.
- [52] Y. Tian, Y. Jiang, J. Li, et al., Effect of stapling architecture on physicochemical properties and cell permeability of stapled alpha-helical peptides: a comparative study, *Chembiochem* 18 (2017) 2087–2093, <https://doi.org/10.1002/cbic.201700352>.
- [53] K. Fujimoto, N. Oimoto, K. Katsuno, et al., Effective stabilisation of alpha-helical structures in short peptides with acetylenic cross-linking agents, *Chem. Comm.* (2004) 1280–1281, <https://doi.org/10.1039/b403615h>.
- [54] K. Fujimoto, M. Amano, Y. Horibe, et al., Reversible photoregulation of helical structures in short peptides under indoor lighting/dark conditions, *Org. Lett.* 8 (2006) 285–287, <https://doi.org/10.1021/ol0526524>.
- [55] K. Fujimoto, M. Kajino, I. Sakaguchi, et al., Photoswitchable, DNA-binding helical peptides assembled with two independently designed sequences for photoregulation and DNA recognition, *Chem. Eur. J.* 18 (2012) 9834–9840, <https://doi.org/10.1002/chem.201201431>.
- [56] S. Mahesh, V. Adebomi, Z.P. Muneeswaran, et al., Bioinspired nitroalkylation for selective protein modification and peptide stapling, *Angew. Chem. Int. Ed. Engl.* 59 (2020) 2793–2801, <https://doi.org/10.1002/anie.201908593>.
- [57] A. Patgiri, A.L. Jochim, P.S. Arora, A hydrogen bond surrogate approach for stabilization of short peptide sequences in alpha-helical conformation, *Acc. Chem. Res.* 41 (2008) 1289–1300, <https://doi.org/10.1021/ar700264k>.
- [58] M.G. Ricardo, F.E. Morales, H. Garay, et al., Bidirectional macrocyclization of peptides by double multicomponent reactions, *Org. Biomol. Chem.* 13 (2015) 438–446, <https://doi.org/10.1039/c4ob01915f>.
- [59] A.A. Vinogradov, Z.N. Choo, K.A. Totaro, et al., Macrocyclization of unprotected peptide isocyanates, *Org. Lett.* 18 (2016) 1226–1229, <https://doi.org/10.1021/acs.orglett.5b03626>.
- [60] A.A. Vinogradov, M.D. Simon, B.L. Pentelute, C-Terminal modification of fully unprotected peptide hydrazides via in situ generation of isocyanates, *Org. Lett.* 18 (2016) 1222–1225, <https://doi.org/10.1021/acs.orglett.5b03625>.
- [61] K. Sakagami, T. Masuda, K. Kawano, et al., Importance of net hydrophobicity in the cellular uptake of all-hydrocarbon stapled peptides, *Mol. Pharm.* 15 (2018) 1332–1340, <https://doi.org/10.1021/acs.molpharmaceut.7b01130>.
- [62] G.L. Verdine, G.J. Hilinski, Stapled peptides for intracellular drug targets, *Method Enzym.* 503 (2012) 3–33, <https://doi.org/10.1016/B978-0-12-396962-0.00001-X>.
- [63] M. Scrima, A. Le Chevalier-Isaad, P. Rovero, et al., Cu-I-Catalyzed azide-alkyne intramolecular i-to-(i+4) side-chain-to-side-chain cyclization promotes the formation of helix-like secondary structures, *Eur. J. Org. Chem.* 2010 (2010) 446–457, <https://doi.org/10.1002/ejoc.200901157>.
- [64] S.A. Kawamoto, A. Coleska, X. Ran, et al., Design of Triazole-Stapled BCL9 alpha-helical peptides to target the beta-catenin/B-Cell CLL/lymphoma 9 (BCL9) protein-protein interaction, *J. Med. Chem.* 55 (2012) 1137–1146, <https://doi.org/10.1021/jm201125d>.
- [65] A.S. Barrow, C.J. Smedley, Q. Zheng, et al., The growing applications of SuFEx click chemistry, *Chem. Soc. Rev.* 48 (2019) 4731–4758, <https://doi.org/10.1039/c8cs00960k>.
- [66] N. Kaplaneris, T. Rogge, R. Yin, et al., Late-stage diversification through manganese-catalyzed C-H activation: access to acyclic, hybrid, and stapled peptides, *Angew. Chem. Int. Ed. Engl.* 58 (2019) 3476–3480, <https://doi.org/10.1002/anie.201812705>.
- [67] J. Liu, P. Wang, Z. Yan, et al., Recent advances in late-stage construction of stapled peptides via C-H activation, *Chembiochem* 22 (2021) 2762–2771, <https://doi.org/10.1002/cbic.202100044>.
- [68] B.B. Zhan, M.X. Jiang, B.F. Shi, Late-stage functionalization of peptides via a palladium-catalyzed C(sp³)-H activation strategy, *Chem. Comm.* 56 (2020) 13950–13958, <https://doi.org/10.1039/d0cc06133f>.
- [69] J. Tang, Y. He, H. Chen, et al., Synthesis of bioactive and stabilized cyclic peptides by macrocyclization using C(sp³)-H activation, *Chem. Sci.* 8 (2017) 4565–4570, <https://doi.org/10.1039/c6sc05530c>.
- [70] P. Timmerman, J. Beld, W.C. Puijk, et al., Rapid and quantitative cyclization of multiple peptide loops onto synthetic scaffolds for structural mimicry of protein surfaces, *Chembiochem: a Eur. J. Chem. Biol.* 6 (2005) 821–824, <https://doi.org/10.1002/cbic.200400374>.
- [71] A.M. Spokoiny, Y. Zou, J.J. Ling, et al., A perfluoroaryl-cysteine S(N)Ar chemistry approach to unprotected peptide stapling, *J. Am. Chem. Soc.* 135 (2013) 5946–5949, <https://doi.org/10.1021/ja400119t>.
- [72] J.E. Swedberg, C.I. Schroeder, J.M. Mitchell, et al., Cyclic alpha-conotoxin peptidomimetic chimeras as potent GLP-1R agonists, *Eur. J. Med. Chem.* 103 (2015) 175–184, <https://doi.org/10.1016/j.ejmech.2015.08.046>.
- [73] X. Li, W.D. Tolbert, H.G. Hu, et al., Dithiocarbamate-inspired side chain stapling chemistry for peptide drug design, *Chem. Sci.* 10 (2019) 1522–1530, <https://doi.org/10.1039/c8sc03275k>.
- [74] F.M. Brunel, P.E. Dawson, Synthesis of constrained helical peptides by thioether ligation: application to analogs of gp41, *Chem. Comm.* (2005) 2552–2554, <https://doi.org/10.1039/b419015g>.
- [75] K. Hu, H. Geng, Q. Zhang, et al., An in-tether chiral center modulates the helicity, cell permeability, and target binding affinity of a peptide, *Angew. Chem. Int. Ed. Engl.* 55 (2016) 8013–8017, <https://doi.org/10.1002/anie.201602806>.
- [76] Y. Tian, J. Li, H. Zhao, et al., Stapling of unprotected helical peptides via photo-induced intramolecular thiol-yne hydrothiolation, *Chem. Sci.* 7 (2016) 3325–3330, <https://doi.org/10.1039/c6sc00106h>.
- [77] X. Shi, Y. Liu, R. Zhao, et al., Constructing Thioether/Vinyl Sulfide-tethered Helical Peptides Via Photo-induced Thiol-yne Hydrothiolation, *J. Vis. Exp.* (2018), <https://doi.org/10.3791/57356>.
- [78] G. Lautrette, F. Touti, H.G. Lee, et al., Nitrogen arylation for macrocyclization of unprotected peptides, *J. Am. Chem. Soc.* 138 (2016) 8340–8343, <https://doi.org/10.1021/jacs.6b03757>.
- [79] H.G. Lee, G. Lautrette, B.L. Pentelute, et al., Palladium-mediated arylation of lysine in unprotected peptides, *Angew. Chem. Int. Ed. Engl.* 56 (2017) 3177–3181, <https://doi.org/10.1002/anie.201611202>.
- [80] H. Li, Y. Hu, Q. Pu, et al., Novel stapling by lysine tethering provides stable and low hemolytic cationic antimicrobial peptides, *J. Med. Chem.* 63 (2020) 4081–4089, <https://doi.org/10.1021/acs.jmedchem.9b02025>.
- [81] X.D. Shi, R.T. Zhao, Y.X. Jiang, et al., Reversible stapling of unprotected peptides via chemoselective methionine bis-alkylation/dealkylation, *Chem. Sci.* 9 (2018) 3227–3232, <https://doi.org/10.1039/c7sc05109c>.
- [82] X.D. Cai, W.H. Zheng, X.D. Shi, et al., HBx-Derived constrained peptides inhibit the secretion of hepatitis B virus antigens, *Mol. Pharm.* 15 (2018) 5646–5652, <https://doi.org/10.1021/acs.molpharmaceut.8b00807>.
- [83] D.Y. Wang, M.Y. Yu, N. Liu, et al., A sulfonium tethered peptide ligand rapidly and selectively modifies protein cysteine in vicinity, *Chem. Sci.* 10 (2019) 4966–4972, <https://doi.org/10.1039/c9sc00034h>.
- [84] A. Afonso, L. Feliu, M. Planas, Solid-phase synthesis of biaryl cyclic peptides by borylation and microwave-assisted intramolecular Suzuki-Miyaura reaction, *Tetrahedron* 67 (2011) 2238–2245, <https://doi.org/10.1016/j.tet.2011.01.084>.
- [85] H.X. Luong, H.T.P. Bui, T.T. Tung, Application of the all-hydrocarbon stapling technique in the design of membrane-active peptides, *J. Med. Chem.* 65 (2022) 3026–3045, <https://doi.org/10.1021/acs.jmedchem.1c01744>.
- [86] H. Sung, J. Ferlay, R.L. Siegel, et al., Global Cancer Statistics 2020: Globocan estimates of incidence and mortality worldwide for 36 cancers in 185 Countries, *CA Cancer J. Clin.* 71 (2021) 209–249, <https://doi.org/10.3322/caac.21660>.
- [87] L. Miao, S. Guo, C.M. Lin, et al., Nanoformulations for combination or cascade anticancer therapy, *Adv. Drug Deliv. Rev.* 115 (2017) 3–22, <https://doi.org/10.1016/j.addr.2017.06.003>.
- [88] L. Wang, N. Wang, W. Zhang, et al., Therapeutic peptides: current applications and future directions, *Signal Transduct. Target Ther.* 7 (2022) 48, <https://doi.org/10.1038/s41392-022-00904-4>.
- [89] P. Vlieghe, V. Lisowski, J. Martinez, et al., Synthetic therapeutic peptides: science and market, *Drug Discov. Today* 15 (2010) 40–56, <https://doi.org/10.1016/j.drudis.2009.10.009>.

- [90] D.J. Craik, D.P. Fairlie, S. Liras, et al., The future of peptide-based drugs, *Chem. Biol. Drug Des.* 81 (2013) 136–147, <https://doi.org/10.1111/cbdd.12055>.
- [91] Y.H. Liu, S. Zeng, M.H. Wu, Novel insights into noncanonical open reading frames in cancer, *Bba-Rev. Cancer* 1877 (2022) 188755, <https://doi.org/10.1016/j.bbcan.2022.188755>.
- [92] S. Mitra, J.E. Montgomery, M.J. Kolar, et al., Stapled peptide inhibitors of RAB25 target context-specific phenotypes in cancer, *Nat. Commun.* 8 (2017) 660, <https://doi.org/10.1038/s41467-017-00888-8>.
- [93] S. Chen, X. Li, Y. Li, et al., Design of stapled peptide-based PROTACs for MDM2/MDMX atypical degradation and tumor suppression, *Theranostics* 12 (2022) 6665–6681, <https://doi.org/10.7150/thno.75444>.
- [94] L. Lu, H. Zhang, Y. Zhou, et al., Polymer chimera of stapled oncolytic peptide coupled with anti-PD-L1 peptide boosts immunotherapy of colorectal cancer, *Theranostics* 12 (2022) 3456–3473, <https://doi.org/10.7150/thno.71129>.
- [95] K.M. Hawley, R.J. Eclow, M.R. Schnorenberg, et al., Inhibition of FOXP3 by stapled alpha-helical peptides dampens regulatory T cell function, *Proc. Natl. Acad. Sci. USA* 119 (2022) e2209044119, <https://doi.org/10.1073/pnas.2209044119>.
- [96] J.E. Montgomery, J.A. Donnelly, S.W. Fanning, et al., Versatile peptide macrocyclization with diels-alder cycloadditions, *J. Am. Chem. Soc.* 141 (2019) 16374–16381, <https://doi.org/10.1021/jacs.9b07578>.
- [97] F. Bernal, A.F. Tyler, S.J. Korsmeyer, et al., Reactivation of the p53 tumor suppressor pathway by a stapled p53 peptide, *J. Am. Chem. Soc.* 129 (2007) 2456–2457, <https://doi.org/10.1021/ja0693587>.
- [98] F. Bernal, M. Wade, M. Godes, et al., A stapled p53 helix overcomes HDMX-mediated suppression of p53, *Cancer Cell* 18 (2010) 411–422, <https://doi.org/10.1016/j.ccr.2010.10.024>.
- [99] Y. Méndez, A.V. Vasco, G. Ivey, et al., Merging the Isonitrile-Tetrazine (4+1) Cycloaddition and the Ugi Four-Component Reaction into a Single Multicomponent Process, *Angew. Chem. Int. Ed. Engl.* 62 (2023) e202311186, <https://doi.org/10.1002/anie.202311186>.
- [100] Y. Wang, D.H. Chou, A thiol-ene coupling approach to native peptide stapling and macrocyclization, *Angew. Chem. Int. Ed. Engl.* 54 (2015) 10931–10934, <https://doi.org/10.1002/anie.201503975>.
- [101] C.J. Brown, S.T. Quah, J. Jong, et al., Stapled peptides with improved potency and specificity that activate p53, *ACS Chem. Biol.* 8 (2013) 506–512, <https://doi.org/10.1021/cb3005148>.
- [102] R.E. Moellering, M. Cornejo, T.N. Davis, et al., Direct inhibition of the NOTCH transcription factor complex, *Nature* 462 (2009) 182–188, <https://doi.org/10.1038/nature08543>.
- [103] M.L. Stewart, E. Fire, A.E. Keating, et al., The MCL-1 BH3 helix is an exclusive MCL-1 inhibitor and apoptosis sensitizer, *Nat. Chem. Biol.* 6 (2010) 595–601, <https://doi.org/10.1038/Nchembio.391>.
- [104] S. Kneissl, E.J. Loveridge, C. Williams, et al., Photocontrollable peptide-based switches target the anti-apoptotic protein Bcl-X-L, *Chem. -Eur. J.* 9 (2008) 3046–3054, <https://doi.org/10.1002/anie.200800502>.
- [105] T.N. Grossmann, J.T. Yeh, B.R. Bowman, et al., Inhibition of oncogenic Wnt signaling through direct targeting of β -catenin, *Proc. Natl. Acad. Sci.* 109 (2012) 17942–17947, <https://doi.org/10.1073/pnas.1208396109>.
- [106] H.W. Liao, X. Li, L.Z. Zhao, et al., A PROTAC peptide induces durable β -catenin degradation and suppresses Wnt-dependent intestinal cancer, *Cell Discov.* 6 (2020) 35, <https://doi.org/10.1038/s41421-020-0171-1>.
- [107] K. Takada, D. Zhu, G.H. Bird, et al., Targeted disruption of the BCL9/ β -catenin complex inhibits oncogenic Wnt signaling, *Sci. Transl. Med.* 4 (2012) 148ra117, <https://doi.org/10.1126/scitranslmed.3003808>.
- [108] Y. Teng, A. Bahassan, D. Dong, et al., Targeting the WASF3-CYFIP1 Complex using stapled peptides suppresses cancer cell invasion, *Cancer Res* 76 (2016) 965–973, <https://doi.org/10.1158/0008-5472.CAN-15-1680>.
- [109] S. Wu, Y. He, X. Qiu, et al., Targeting the potent Beclin 1-UVRAG coiled-coil interaction with designed peptides enhances autophagy and endolysosomal trafficking, *Proc. Natl. Acad. Sci. USA* 115 (2018) E5669–E5678, <https://doi.org/10.1073/pnas.1721173115>.
- [110] Q.F. Yang, X.X. Qiu, X.Z. Zhang, et al., Y Optimization of Beclin 1-Targeting Stapled Peptides by Staple Scanning Leads to Enhanced Antiproliferative Potency in Cancer Cells, *J. Med. Chem.* 64 (2021) 13475–13486, <https://doi.org/10.1021/acs.jmedchem.1c00870>.
- [111] J. Cui, Y. Ogasawara, I. Kurata, et al., Targeting the ATG5-ATG16L1 Protein-Protein Interaction with a Hydrocarbon-Stapled Peptide Derived from ATG16L1 for Autophagy Inhibition, *J. Am. Chem. Soc.* 144 (2022) 17671–17679, <https://doi.org/10.1021/jacs.2c07648>.
- [112] H. Brown, M. Chung, A. Üffing, et al., Structure-based design of stapled peptides that bind GABARAP and inhibit autophagy, *J. Am. Chem. Soc.* 144 (2022) 14687–14697, <https://doi.org/10.1021/jacs.2c04699>.
- [113] E.R. Kastenhuber, S.W. Lowe, Putting p53 in Context, *Cell* 170 (2017) 1062–1078, <https://doi.org/10.1016/j.cell.2017.08.028>.
- [114] H. Wang, M. Guo, H. Wei, et al., Targeting p53 pathways: mechanisms, structures, and advances in therapy, *Signal Transduct. Target Ther.* 8 (2023) 92, <https://doi.org/10.1038/s41392-023-01347-1>.
- [115] A. Hock, K.H. Vousden, Regulation of the p53 pathway by ubiquitin and related proteins, *Int. J. Biochem. Cell B* 42 (2010) 1618–1621, <https://doi.org/10.1016/j.biocel.2010.06.011>.
- [116] L. Huang, Z. Yan, X.D. Liao, et al., The p53 inhibitors MDM2/MDMX complex is required for control of p53 activity in vivo, *Proc. Natl. Acad. Sci. USA* 108 (2011) 12001–12006, <https://doi.org/10.1073/pnas.1102309108>.
- [117] L.T. Vassilev, B.T. Vu, B. Graves, et al., In vivo activation of the p53 pathway by small-molecule antagonists of MDM2, *Science* 303 (2004) 844–848, <https://doi.org/10.1126/science.1092472>.
- [118] K. Sakurai, H.S. Chung, D. Kahne, Use of a retroinverso p53 peptide as an inhibitor of MDM2, *J. Am. Chem. Soc.* 126 (2004) 16288–16289, <https://doi.org/10.1021/ja044883w>.
- [119] J. Phan, Z. Li, A. Kasprzak, et al., Structure-based design of high affinity peptides inhibiting the interaction of p53 with MDM2 and MDMX, *J. Biol. Chem.* 285 (2010) 2174–2183, <https://doi.org/10.1074/jbc.M109.073056>.
- [120] V. Guerlavais, T.K. Sawyer, L. Carvajal, et al., Discovery of Sulanemadlin (ALRN-6924), the first cell-permeating, stabilized alpha-helical peptide in clinical development, *J. Med. Chem.* (2023) 9401–9417, <https://doi.org/10.1021/acs.jmedchem.3c00623>.
- [121] M.N. Saleh, M.R. Patel, T.M. Bauer, et al., Phase 1 Trial of ALRN-6924, a Dual Inhibitor of MDMX and MDM2, in Patients with Solid Tumors and Lymphomas Bearing Wild-type TP53, *Clin. Cancer Res.: Off. J. Am. Assoc. Cancer Res.* 27 (2021) 5236–5247, <https://doi.org/10.1158/1078-0432.CCR-21-0715>.
- [122] M.N. Saleh, M.R. Patel, T.M. Bauer, et al., Correction: Phase I Trial of ALRN-6924, a Dual Inhibitor of MDMX and MDM2, in Patients with Solid Tumors and Lymphomas bearing wild-type TP53, *Clin. Cancer Res.: Off. J. Am. Assoc. Cancer Res.* 28 (2022) 429, <https://doi.org/10.1158/1078-0432.CCR-21-4241>.
- [123] A.R. Shustov, A. Mehta, L. Sokol, et al., Pseudoprogression (PsP) in Patients with Peripheral T-Cell Lymphoma (PTCL) Treated with the Novel Stapled Peptide ALRN-6924, a Dual Inhibitor of MDMX and MDM2, *Blood* 132 (2018) 5348, <https://doi.org/10.1182/blood-2018-99-119489>.
- [124] F. Meric-Bernstam, M.N. Saleh, J.R. Infante, et al., Phase I trial of a novel stapled peptide ALRN-6924 disrupting MDMX- and MDM2-mediated inhibition of WT p53 in patients with solid tumors and lymphomas, *J. Clin. Oncol.* 35 (2017) 15, <https://doi.org/10.1200/JCO.2017.35.15.suppl.2505>.
- [125] C. Li, M. Paggier, C. Li, et al., Systematic mutational analysis of peptide inhibition of the p53-MDM2/MDMX interactions, *J. Mol. Biol.* 398 (2010) 200–213, <https://doi.org/10.1016/j.jmb.2010.03.005>.
- [126] M. Paggiera, M. Liu, G.Z. Zou, et al., Structural basis for high-affinity peptide inhibition of p53 interactions with MDM2 and MDMX, *Proc. Natl. Acad. Sci. USA* 106 (2009) 4665–4670, <https://doi.org/10.1073/pnas.0900947106>.
- [127] E.M. Stocking, R.M. Williams, Chemistry and biology of biosynthetic Diels-Alder reactions, *Angew. Chem. Int. Ed.* 42 (2003) 3078–3115, <https://doi.org/10.1002/anie.200200534>.
- [128] H. Oikawa, Nature's strategy for catalyzing diels-alder reaction, *Cell Chem. Biol.* 23 (2016) 429–430, <https://doi.org/10.1016/j.chembiol.2016.04.002>.
- [129] D.G. Rivera, O.E. Vercillo, L.A. Wessjohann, Rapid generation of macrocycles with natural-product-like side chains by multiple multicomponent macrocyclizations (MiBs), *Org. Biomol. Chem.* 6 (2008) 1787–1795, <https://doi.org/10.1039/b715393g>.
- [130] L. Reguera, D.G. Rivera, Multicomponent reaction toolbox for peptide macrocyclization and stapling, *Chem. Rev.* 119 (2019) 9836–9860, <https://doi.org/10.1021/acs.chemrev.8b00744>.
- [131] A. Domling, I.I. Ugi, Multicomponent reactions with isocyanides, *Angew. Chem. Int. Ed. Engl.* 39 (2000) 3168–3210, [https://doi.org/10.1002/1521-3773\(20000915\)39:18<3168::aid-anie3168>3.0.co;2-u](https://doi.org/10.1002/1521-3773(20000915)39:18<3168::aid-anie3168>3.0.co;2-u).
- [132] M. Paggier, M. Liu, G. Zou, et al., Structural basis for high-affinity peptide inhibition of p53 interactions with MDM2 and MDMX, *Proc. Natl. Acad. Sci. USA* 106 (2009) 4665–4670, <https://doi.org/10.1073/pnas.0900947106>.
- [133] A.G. Petcherski, J. Kimble, Mastermind is a putative activator for Notch, *Curr. Biol.* 10 (2000) R471–R473, [https://doi.org/10.1016/s0960-9822\(00\)00577-7](https://doi.org/10.1016/s0960-9822(00)00577-7).
- [134] L.Z. Wu, J.C. Aster, S.C. Blacklow, et al., MAMLI1, a human homologue of drosophila mastermind, is a transcriptional co-activator for NOTCH receptors, *Nat. Genet.* 26 (2000) 484–489, <https://doi.org/10.1038/82644>.
- [135] A.A. Ahmed, T. Robinson, M. Palande, et al., Targeted Notch1 inhibition with a Notch1 antibody, OMP-A2G1, decreases tumor growth in two murine models of prostate cancer in association with differing patterns of DNA damage response gene expression, *J. Cell Biochem* 120 (2019) 16946–16955, <https://doi.org/10.1002/jcb.28954>.
- [136] A.P. Weng, Y. Nam, M.S. Wolfe, et al., Growth suppression of pre-T acute lymphoblastic leukemia cells by inhibition of notch signaling, *Mol. Cell Biol.* 23 (2003) 655–664, <https://doi.org/10.1128/MCB.23.2.655-664.2003>.
- [137] N.N. Danial, BCL-2 family proteins: critical checkpoints of apoptotic cell death, *Clin. Cancer Res.: Off. J. Am. Assoc. Cancer Res.* 13 (2007) 7254–7263, <https://doi.org/10.1158/1078-0432.CCR-07-1598>.
- [138] A.R.D. Delbridge, S. Grabow, A. Strasser, et al., Thirty years of BCL-2: translating cell death discoveries into novel cancer therapies, *Nat. Rev. Cancer* 16 (2016) 99–109, <https://doi.org/10.1038/nrc.2015.17>.
- [139] S.W. Muchmore, M. Sattler, H. Liang, et al., X-ray and NMR structure of human Bcl-xL, an inhibitor of programmed cell death, *Nature* 381 (1996) 335–341, <https://doi.org/10.1038/381335a0>.
- [140] M. Germain, A.P. Nguyen, J.N. Le Grand, et al., MCL-1 is a stress sensor that regulates autophagy in a developmentally regulated manner, *Embo J.* 30 (2011) 395–407, <https://doi.org/10.1038/emboj.2010.327>.
- [141] H.L. Wang, M. Guo, H.D. Wei, et al., Targeting MCL-1 in cancer: current status and perspectives, *J. Hematol. Oncol.* 14 (2021) 67, <https://doi.org/10.1186/s13045-021-01079-1>.
- [142] S. Yue, Y. Li, X. Chen, et al., FGFR-TKI resistance in cancer: current status and perspectives, *J. Hematol. Oncol.* 14 (2021) 23, <https://doi.org/10.1186/s13045-021-01040-2>.

- [143] M. Sattler, H. Liang, D. Nettesheim, et al., Structure of Bcl-x(L)-Bak peptide complex: recognition between regulators of apoptosis, *Science* 275 (1997) 983–986, <https://doi.org/10.1126/science.275.5302.983>.
- [144] B.T. MacDonald, K. Tamai, X. He, Wnt/ β -catenin signaling: components, mechanisms, and diseases, *Dev. Cell* 17 (2009) 9–26, <https://doi.org/10.1016/j.devcel.2009.06.016>.
- [145] R. Nusse, H. Clevers, Wnt/ β -Catenin signaling, disease, and emerging therapeutic modalities, *Cell* 169 (2017) 985–999, <https://doi.org/10.1016/j.cell.2017.05.016>.
- [146] J. Sampietro, C.L. Dahlberg, U.S. Cho, et al., Crystal structure of a β -catenin/BCL9/Tcf4 complex, *Mol. Cell* 24 (2006) 293–300, <https://doi.org/10.1016/j.molcel.2006.09.001>.
- [147] Y. Xing, W.K. Clements, D. Kimelman, et al., Crystal structure of a β -catenin/axin complex suggests a mechanism for the β -catenin destruction complex, *Genes Dev.* 17 (2003) 2753–2764, <https://doi.org/10.1101/gad.1142603>.
- [148] A.C. Lai, C.M. Crews, Induced protein degradation: an emerging drug discovery paradigm, *Nat. Rev. Drug Discov.* 16 (2017) 101–114, <https://doi.org/10.1038/nrd.2016.211>.
- [149] F.H. Brembeck, M. Wiese, N. Zatul, et al., BCL9-2 Promotes early stages of intestinal tumor progression, *Gastroenterology* 141 (2011) 1359–U1810, <https://doi.org/10.1053/j.gastro.2011.06.039>.
- [150] J. Deka, N. Wiedemann, P. Anderle, et al., Bcl9/Bcl9l are critical for Wnt-mediated regulation of stem cell traits in colon epithelium and adenocarcinomas, *Cancer Res.* 70 (2010) 6619–6628, <https://doi.org/10.1158/0008-5472.CAN-10-0148>.
- [151] J.D. Rotty, C.Y. Wu, J.E. Bear, New insights into the regulation and cellular functions of the ARP2/3 complex, *Nat. Rev. Mol. Cell Bio* 14 (2013) 7–12, <https://doi.org/10.1038/nrm3492>.
- [152] K. Sossey-Alaoui, A. Safina, X. Li, et al., Down-regulation of WAVE3, a metastasis promoter gene, inhibits invasion and metastasis of breast cancer cells, *Am. J. Pathol.* 170 (2007) 2112–2121, <https://doi.org/10.2353/ajpath.2007.060975>.
- [153] B. Chen, K. Brinkmann, Z. Chen, et al., The WAVE regulatory complex links diverse receptors to the actin cytoskeleton, *Cell* 156 (2014) 195–207, <https://doi.org/10.1016/j.cell.2013.11.048>.
- [154] S. Vega-Rubin-de-Celis, Z. Zou, A.F. Fernandez, et al., Increased autophagy blocks HER2-mediated breast tumorigenesis, *Proc. Natl. Acad. Sci. USA* 115 (2018) 4176–4181, <https://doi.org/10.1073/pnas.1717800115>.
- [155] B. Levine, G. Kroemer, Biological functions of autophagy genes: a disease perspective, *Cell* 176 (2019) 11–42, <https://doi.org/10.1016/j.cell.2018.09.048>.
- [156] H. Nakatogawa, Mechanisms governing autophagosome biogenesis, *Nat. Rev. Mol. Cell Biol.* 21 (2020) 439–458, <https://doi.org/10.1038/s41580-020-0241-0>.
- [157] T. Whitmarsh-Everiss, L. Lاراia, Small molecule probes for targeting autophagy, *Nat. Chem. Biol.* 17 (2021) 653–664, <https://doi.org/10.1038/s41589-021-00768-9>.
- [158] T. Saitoh, N. Fujita, M.H. Jang, et al., Loss of the autophagy protein Atg16L1 enhances endotoxin-induced IL-1 β production, *Nature* 456 (2008) 264–268, <https://doi.org/10.1038/nature07383>.
- [159] Y.K. Lee, J.A. Lee, Role of the mammalian ATG8/LC3 family in autophagy: differential and compensatory roles in the spatiotemporal regulation of autophagy, *BMB Rep.* 49 (2016) 424–430, <https://doi.org/10.5483/bmbrep.2016.49.8.081>.
- [160] T.N. Nguyen, B.S. Padman, J. Usher, et al., Atg8 family LC3/GABARAP proteins are crucial for autophagosome-lysosome fusion but not autophagosome formation during PINK1/Parkin mitophagy and starvation, *J. Cell Biol.* 215 (2016) 857–874, <https://doi.org/10.1083/jcb.201607039>.
- [161] M. Putyrski, O. Vakhrusheva, F. Bonn, et al., Disrupting the LC3 Interaction Region (LIR) binding of selective autophagy receptors sensitizes AML cell lines to cytarabine, *Front Cell Dev. Biol.* 8 (2020) 208, <https://doi.org/10.3389/fcell.2020.00208>.
- [162] S. Seena, R. Ferrao, M. Pala, et al., Acidic sophorolipid and antimicrobial peptide based formulation as antimicrobial and antibiofilm agents, *Biomater. Adv.* 146 (2023) 213299, <https://doi.org/10.1016/j.bioadv.2023.213299>.
- [163] M. Hirano, C. Saito, H. Yokoo, et al., Development of antimicrobial stapled peptides based on magainin 2 sequence, *Molecules* 26 (2021) 2, <https://doi.org/10.3390/molecules26020444>.
- [164] X. Bai, X. Chen, Rational design, conformational analysis and membrane-penetrating dynamics study of Bac2A-derived antimicrobial peptides against gram-positive clinical strains isolated from pyemia, *J. Theor. Biol.* 473 (2019) 44–51, <https://doi.org/10.1016/j.jtbi.2019.03.018>.
- [165] C. Shao, Q. Jian, B. Li, et al., Ultrashort all-hydrocarbon stapled α -Helix amphiphile as a potent and stable antimicrobial compound, *J. Med. Chem.* 66 (2023) 11414–11427, <https://doi.org/10.1021/acs.jmedchem.3c00856>.
- [166] M. Zheng, R. Wang, S. Chen, et al., Design, Synthesis and antifungal activity of stapled aurein1.2 peptides, *Antibiot. (Basel)* 10 (2021), <https://doi.org/10.3390/antibiotics10080956>.
- [167] S.M. Kang, H. Moon, S.W. Han, et al., Structure-based de novo design of Mycobacterium Tuberculosis VapC-Activating Stapled Peptides, *ACS Chem. Biol.* 15 (2020) 2493–2498, <https://doi.org/10.1021/acscchembio.0c00492>.
- [168] S.R. Payne, D.I. Pau, A.L. Whiting, et al., Inhibition of bacterial gene transcription with an RpoN-based stapled peptide, *e1054*, *Cell Chem. Biol.* 25 (2018) 1059–1066, <https://doi.org/10.1016/j.cchembiol.2018.05.007>.
- [169] A. Matejuk, Q. Leng, M.D. Begum, et al., Peptide-based antifungal therapies against emerging infections, *Drugs Future* 35 (2010) 197, <https://doi.org/10.1358/dof.2010.035.03.1452077>.
- [170] M. Hirano, H. Yokoo, C. Goto, et al., Magainin 2-derived stapled peptides derived with the ability to deliver pDNA, mRNA, and siRNA into cells, *Chem. Sci.* 14 (2023) 10403–10410, <https://doi.org/10.1039/d3sc04124g>.
- [171] W.R. Qiu, B.Q. Sun, X. Xiao, et al., iPhos-PseEvo: identifying human phosphorylated proteins by incorporating evolutionary information into general PseAAC via Grey System Theory, *Mol. Inf.* 36 (2017) 5–6, <https://doi.org/10.1002/minf.201600010>.
- [172] P.K. Meher, T.K. Sahu, V. Saini, et al., Predicting antimicrobial peptides with improved accuracy by incorporating the compositional, physico-chemical and structural features into Chou's general PseAAC, *Sci. Rep. Uk* 7 (2017) 42362, <https://doi.org/10.1038/srep42362>.
- [173] D. Migon, D. Neubauer, W. Kamysz, Hydrocarbon stapled antimicrobial peptides, *Protein J.* 37 (2018) 2–12, <https://doi.org/10.1007/s10930-018-9755-0>.
- [174] C.D. Fjell, H. Jensen, K. Hilpert, et al., Identification of Novel Antibacterial Peptides by Chemoinformatics and Machine Learning, *J. Med. Chem.* 52 (2009) 2006–2015, <https://doi.org/10.1021/jm8015365>.
- [175] M. Shahmiri, M. Enciso, A. Mechler, Controls and constrains of the membrane disrupting action of Aurein 1.2, *Sci. Rep.* 5 (2015) 16378, <https://doi.org/10.1038/srep16378>.
- [176] S.A. Li, W.H. Lee, Y. Zhang, Efficacy of OH-CATH30 and its analogs against drug-resistant bacteria in vitro and in mouse models, *Antimicrob. Agents Chemother.* 56 (2012) 3309–3317, <https://doi.org/10.1128/Aac.06304-11>.
- [177] E. Maisonneuve, K. Gerdes, Molecular mechanisms underlying bacterial persisters, *Cell* 157 (2014) 539–548, <https://doi.org/10.1016/j.cell.2014.02.050>.
- [178] A.M. Wensing, V. Calvez, H.F. Gunthard, et al., 2015 Update of the drug resistance mutations in HIV-1, *Top. Antivir. Med* 23 (2015) 132–141, (<https://www.ncbi.nlm.nih.gov/pmc/articles/PMC6148920/>).
- [179] S. Xia, Y. Zhu, M. Liu, et al., Fusion mechanism of 2019-nCoV and fusion inhibitors targeting HR1 domain in spike protein, *Cell Mol. Immunol.* 17 (2020) 765–767, <https://doi.org/10.1038/s41423-020-0374-2>.
- [180] M. Zheng, W. Cong, H. Peng, et al., Stapled peptides targeting SARS-CoV-2 Spike Protein HR1 inhibit the fusion of virus to its cell receptor, *J. Med. Chem.* 64 (2021) 17486–17495, <https://doi.org/10.1021/acs.jmedchem.1c01681>.
- [181] H.G. Hu, B.B. Chen, C. Liu, et al., Cyclobutane-bearing restricted anchoring residues enabled geometry-specific hydrocarbon peptide stapling, *Chem. Sci.* (2023) 11499–11506, <https://doi.org/10.1039/d3sc04279k>.
- [182] M.N. Maas, J.C.J. Hintzen, P.M.G. Loffler, et al., Targeting SARS-CoV-2 spike protein by stapled HACE2 peptides, *Chem. Comm.* 57 (2021) 3283–3286, <https://doi.org/10.1039/d0cc08387a>.
- [183] J. Sticht, M. Humbert, S. Findlow, et al., A peptide inhibitor of HIV-1 assembly in vitro, *Nat. Struct. Mol. Biol.* 12 (2005) 671–677, <https://doi.org/10.1038/nsmb964>.
- [184] H. Zhang, Q. Zhao, S. Bhattacharya, et al., A cell-penetrating helical peptide as a potential HIV-1 inhibitor, *J. Mol. Biol.* 378 (2008) 565–580, <https://doi.org/10.1016/j.jmb.2008.02.066>.
- [185] A. Muppidi, H.T. Zhang, F. Curreli, et al., Design of antiviral stapled peptides containing a biphenyl cross-linker, *Bioorg. Med. Chem. Lett.* 24 (2014) 1748–1751, <https://doi.org/10.1016/j.bmcl.2014.02.038>.
- [186] H.T. Zhang, F. Curreli, X.H. Zhang, et al., Antiviral activity of alpha-helical stapled peptides designed from the HIV-1 capsid dimerization domain, *Retrovirology* 8 (2011) 28, <https://doi.org/10.1186/1742-4690-8-28>.
- [187] Y. Wu, Y. Zou, L.L. Sun, et al., Peptide stapling with the retention of double native side-chains (vol 32, pg 4045, 2021), *Chin. Chem. Lett.* 33 (2022) 3296, <https://doi.org/10.1016/j.ccl.2022.03.066>.
- [188] G.P. Meng, J. Pu, Y. Li, et al., Design and biological evaluation of m-Xylene thioether-stapled short helical peptides targeting the HIV-1 gp41 hexameric coiled-coil fusion complex, *J. Med. Chem.* 62 (2019) 8773–8783, <https://doi.org/10.1021/acs.jmedchem.9b00882>.
- [189] S. Suzuki, E. Urano, C. Hashimoto, et al., Peptide HIV-1 Integrase Inhibitors from HIV-1 Gene Products, *J. Med. Chem.* 53 (2010) 5356–5360, <https://doi.org/10.1021/jm1003528>.
- [190] W. Nomura, H. Aikawa, N. Ohashi, et al., Cell-Permeable stapled peptides based on HIV-1 integrase inhibitors derived from HIV-1 gene products, *ACS Chem. Biol.* 8 (2013) 2235–2244, <https://doi.org/10.1021/cb400495h>.
- [191] G.H. Bird, S. Boyapalle, T. Wong, et al., Mucosal delivery of a double-stapled RSV peptide prevents nasopharyngeal infection, *J. Clin. Invest.* 124 (2014) 2113–2124, <https://doi.org/10.1172/Jci71856>.
- [192] H.K. Cui, J. Qing, Y. Guo, et al., Stapled peptide-based membrane fusion inhibitors of hepatitis C virus, *Bioorg. Med. Chem.* 21 (2013) 3547–3554, <https://doi.org/10.1016/j.bmc.2013.02.011>.
- [193] C.D. Higgins, J.F. Koellhoffer, K. Chandran, et al., C-peptide inhibitors of Ebola virus glycoprotein-mediated cell entry: effects of conjugation to cholesterol and side chain-side chain crosslinking, *Bioorg. Med. Chem. Lett.* 23 (2013) 5356–5360, <https://doi.org/10.1016/j.bmcl.2013.07.056>.
- [194] A. Pessi, S.L. Bixler, V. Soloveva, et al., Cholesterol-conjugated stapled peptides inhibit Ebola and Marburg viruses in vitro and in vivo, *Antivir. Res.* 171 (2019) 104592, <https://doi.org/10.1016/j.antiviral.2019.104592>.
- [195] Q.Q. Zhang, R. Xiang, S.S. Huo, et al., Molecular mechanism of interaction between SARS-CoV-2 and host cells and interventional therapy, *Signal Transduct. Tar.* 6 (2021) 233, <https://doi.org/10.1038/s41392-021-00653-w>.
- [196] R.D. de Vries, K.S. Schmitz, F.T. Bovier, et al., Intranasal fusion inhibitory lipopeptide prevents direct-contact SARS-CoV-2 transmission in ferrets, *Science* 371 (2021) 1379–1382, <https://doi.org/10.1126/science.abf4896>.
- [197] S. Xia, Q. Lan, Y. Zhu, et al., Structural and functional basis for pan-CoV fusion inhibitors against SARS-CoV-2 and its variants with preclinical evaluation, *Signal*

- Transduct. Target Ther. 6 (2021) 288, <https://doi.org/10.1038/s41392-021-00712-2>.
- [198] H.B. Zhang, J.M. Penninger, Y.M. Li, et al., Angiotensin-converting enzyme 2 (ACE2) as a SARS-CoV-2 receptor: molecular mechanisms and potential therapeutic target, *Intens. Care Med* 46 (2020) 586–590, <https://doi.org/10.1007/s00134-020-05985-9>.
- [199] Q. Wang, Y. Zhang, L. Wu, et al., Structural and functional basis of SARS-CoV-2 entry by using human ACE2, *e899, Cell* 181 (2020) 894–904, <https://doi.org/10.1016/j.cell.2020.03.045>.
- [200] J.O. Link, M.S. Rhee, W.C. Tse, et al., Clinical targeting of HIV capsid protein with a long-acting small molecule, *Nature* 584 (2020) 614–618, <https://doi.org/10.1038/s41586-020-2443-1>.
- [201] L. Sun, X.J. Zhang, S.J. Xu, et al., An insight on medicinal aspects of novel HIV-1 capsid protein inhibitors, *Eur. J. Med. Chem.* 217 (2021) 113380, <https://doi.org/10.1016/j.ejmech.2021.113380>.
- [202] M. Yamashita, M. Emerman, Capsid is a dominant determinant of retrovirus infectivity in nondividing cells, *J. Virol.* 78 (2004) 5670–5678, <https://doi.org/10.1128/Jvi.78.11.5670-5678.2004>.
- [203] D.K. Worthylake, H. Wang, S.H. Yoo, et al., Structures of the HIV-1 capsid protein dimerization domain at 2.6 angstrom resolution, *Acta Crystallogr D.* 55 (1999) 85–92, <https://doi.org/10.1107/S0907444998007689>.
- [204] I.J.L. Byeon, X. Meng, J.W. Jung, et al., Structural Convergence between Cryo-EM and NMR Reveals Intersubunit Interactions Critical for HIV-1 Capsid Function, *Cell* 139 (2009) 780–790, <https://doi.org/10.1016/j.cell.2009.10.010>.
- [205] Z.Y.J. Sun, K.J. Oh, M.Y. Kim, et al., HIV-1 broadly neutralizing antibody extracts its epitope from a kinked gp41 ectodomain region on the viral membrane, *Immunity* 28 (2008) 52–63, <https://doi.org/10.1016/j.immuni.2007.11.018>.
- [206] G.H. Bird, A. Irimia, G. Ofek, et al., Stapled HIV-1 peptides recapitulate antigenic structures and engage broadly neutralizing antibodies, *Nat. Struct. Mol. Biol.* 21 (2014) 1058–1067, <https://doi.org/10.1038/nsmb.2922>.
- [207] L.A. Carvajal, D. Ben Neriah, A. Senecal, et al., Dual inhibition of MDMX and MDM2 as a therapeutic strategy in leukemia, *Sci. Transl. Med.* 10 (2018) eaao3003, <https://doi.org/10.1126/scitranslmed.aao3003>.
- [208] W. Nomura, C. Hashimoto, T. Suzuki, et al., Multimerized CHR-derived peptides as HIV-1 fusion inhibitors, *Bioorg. Med. Chem.* 21 (2013) 4452–4458, <https://doi.org/10.1016/j.bmc.2013.05.060>.
- [209] Y.X. He, J.W. Cheng, H. Lu, et al., Potent HIV fusion inhibitors against Enfuvirtide-resistant HIV-1 strains, *Proc. Natl. Acad. Sci. USA* 105 (2008) 16332–16337, <https://doi.org/10.1073/pnas.0807335105>.
- [210] L. Peraro, T.R. Siegert, J.A. Kritzer, Conformational restriction of peptides using dithiol bis-alkylation, *Pept., Protein Eng. Des. Sel.* 580 (2016) 303–332, <https://doi.org/10.1016/bs.mie.2016.05.035>.
- [211] H.M. Chen, A. Engelman, The barrier-to-autointegration protein is a host factor for HIV type 1 integration, *Proc. Natl. Acad. Sci. USA* 95 (1998) 15270–15274, <https://doi.org/10.1073/pnas.95.26.15270>.
- [212] M.D. Miller, C.M. Farnet, F.D. Bushman, Human immunodeficiency virus type 1 preintegration complexes: studies of organization and composition, *J. Virol.* 71 (1997) 5382–5390, <https://doi.org/10.1128/JVI.71.7.5382-5390.1997>.
- [213] C.M. Farnet, F.D. Bushman, HIV-1 cDNA integration: requirement of HMGI(Y) protein for function of preintegration complexes in vitro, *Cell* 88 (1997) 483–492, [https://doi.org/10.1016/s0092-8674\(00\)81888-7](https://doi.org/10.1016/s0092-8674(00)81888-7).
- [214] I.O. Gleenberg, A. Herschhorn, A. Hizi, Inhibition of the activities of reverse transcriptase and integrase of human immunodeficiency virus type-1 by peptides derived from the homologous viral protein R (Vpr), *J. Mol. Biol.* 369 (2007) 1230–1243, <https://doi.org/10.1016/j.jmb.2007.03.073>.
- [215] J. Bischerour, P. Tauc, H. Leh, et al., The (52–96) C-terminal domain of Vpr stimulates HIV-1 IN-mediated homologous strand transfer of mini-viral DNA, *Nucleic Acids Res* 31 (2003) 2694–2702, <https://doi.org/10.1093/nar/gkg364>.
- [216] X. Zhao, M. Singh, V.N. Malashkevich, et al., Structural characterization of the human respiratory syncytial virus fusion protein core, *Proc. Natl. Acad. Sci. USA* 97 (2000) 14172–14177, <https://doi.org/10.1073/pnas.260499197>.
- [217] M.K. Lawless-Delmedico, P. Sista, R. Sen, et al., Heptad-repeat regions of respiratory syncytial virus F1 protein form a six-membered coiled-coil complex, *Biochem. -Us* 39 (2000) 11684–11695, <https://doi.org/10.1021/bi000471y>.
- [218] M.P. Manns, G.R. Foster, J.K. Rockstroh, et al., The way forward in HCV treatment - finding the right path (vol 6, pg 991, 2007), *Nat. Rev. Drug Discov.* 7 (2008), <https://doi.org/10.1038/nrd2411>.
- [219] M.E. Hemler, Targeting of tetraspanin proteins - potential benefits and strategies, *Nat. Rev. Drug Discov.* 7 (2008) 747–758, <https://doi.org/10.1038/nrd2659>.
- [220] M. Dhanasekaran, P.W. Baures, S. VanCompernelle, et al., Structural characterization of peptide fragments from hCD8(1)-LEL, *J. Pept. Res.* 61 (2003) 80–89, <https://doi.org/10.1034/j.1399-3011.2003.00038.x>.
- [221] W.R. Gallahe, Similar structural models of the transmembrane proteins of Ebola and avian sarcoma viruses, *Cell* 85 (1996) 477–478, [https://doi.org/10.1016/s0092-8674\(00\)81248-9](https://doi.org/10.1016/s0092-8674(00)81248-9).
- [222] N. Mulherkar, M. Raaben, J.C. de la Torre, et al., The Ebola virus glycoprotein mediates entry via a non-classical dynamin-dependent macropinocytotic pathway, *Virology* 419 (2011) 72–83, <https://doi.org/10.1016/j.virol.2011.08.009>.
- [223] D.P. Fairlie, A. Dantas de Araujo, Review stapling peptides using cysteine crosslinking, *Biopolymers* 106 (2016) 843–852, <https://doi.org/10.1002/bip.22877>.
- [224] R. Zhao, Z. Lu, J. Yang, et al., Drug delivery system in the treatment of diabetes mellitus, *Front Bioeng. Biotechnol.* 8 (2020) 880, <https://doi.org/10.3389/fbioe.2020.00880>.
- [225] P. Saeedi, I. Petersohn, P. Salpea, et al., Global and regional diabetes prevalence estimates for 2019 and projections for 2030 and 2045: results from the International Diabetes Federation Diabetes Atlas, 9th edition, *Diabetes Res Clin.* Pr. 157 (2019) 107843, <https://doi.org/10.1016/j.diabres.2019.107843>.
- [226] R. Gentilella, V. Pechtnar, A. Corcos, et al., Glucagon-like peptide-1 receptor agonists in type 2 diabetes treatment: are they all the same? *Diabetes Metab. Res Rev.* 35 (2019) e3070 <https://doi.org/10.1002/dmrr.3070>.
- [227] P.-Y. Yang, H. Zou, E. Chao, et al., Engineering a long-acting, potent GLP-1 analog for microstructure-based transdermal delivery, *Proc. Natl. Acad. Sci. USA* 113 (2016) 4140–4145, <https://doi.org/10.1073/pnas.1601653113>.
- [228] N. Jiang, L. Jing, Q. Li, et al., Design of novel Xenopus GLP-1-based dual glucagon-like peptide 1 (GLP-1)/glucagon receptor agonists, *Eur. J. Org. Chem.* 212 (2021) 113118, <https://doi.org/10.1016/j.ejmech.2020.113118>.
- [229] C. Han, Y. Sun, Q. Yang, et al., Stapled, long-acting xenopus GLP-1-based dual GLP-1/Glucagon receptor agonists with potent therapeutic efficacy for metabolic disease, *Mol. Pharm.* 18 (2021) 2906–2923, <https://doi.org/10.1021/acs.molpharmaceut.0c00995>.
- [230] F. Giordanetto, J.D. Revell, L. Knerr, et al., Stapled Vasoactive Intestinal Peptide (VIP) Derivatives Improve VPAC2 Agonism and Glucose-Dependent Insulin Secretion, *ACS Med Chem. Lett.* 4 (2013) 1163–1168, <https://doi.org/10.1021/ml400257h>.
- [231] L. Frankiewicz, C. Betti, K. Guillemyn, et al., Stabilisation of a short α -helical VIP fragment by side chain to side chain cyclisation: a comparison of common cyclisation motifs by circular dichroism, *J. Pept. Sci.* 19 (2013) 423–432, <https://doi.org/10.1002/psc.2515>.
- [232] Y. Zhang, J. Wang, W.C. Li, et al., Rational design of stapled helical peptides as anti-diabetic PPAR gamma antagonists to target coactivator site by decreasing unfavorable entropy penalty instead of increasing favorable enthalpy contribution, *Eur. Biophys. J.* 51 (2022) 535–543, <https://doi.org/10.1007/s00249-022-01616-x>.
- [233] N.N. Danial, L.D. Walensky, C.Y. Zhang, et al., Dual role of proapoptotic BAD in insulin secretion and beta cell survival, *Nat. Med.* 14 (2008) 144–153, <https://doi.org/10.1038/nm1717>.
- [234] E. Schreyer, C. Obringer, N. Messaddeq, et al., PATAS, a First-in-Class Therapeutic Peptide Biologic, Improves Whole-Body Insulin Resistance and Associated Comorbidities In Vivo, *Diabetes* 71 (2022) 2034–2047, <https://doi.org/10.2337/db22-0058>.
- [235] M.C. Lagerström, H.B. Schiöth, Structural diversity of G protein-coupled receptors and significance for drug discovery, *Nat. Rev. Drug Discov.* 7 (2008) 339–357, <https://doi.org/10.1038/nrd2518>.
- [236] M. Tsutsumi, T.H. Claus, Y. Liang, et al., A potent and highly selective VPAC2 agonist enhances glucose-induced insulin release and glucose disposal: a potential therapy for type 2 diabetes, *Diabetes* 51 (2002) 1453–1460, <https://doi.org/10.2337/diabetes.51.5.1453>.
- [237] B. Grygiel-Gorniak, Peroxisome proliferator-activated receptors and their ligands: nutritional and clinical implications - a review, *Nutr. J.* 13 (2014) 17, <https://doi.org/10.1186/1475-2891-13-17>.
- [238] T. Umemoto, Y. Fujiki, Ligand-dependent nucleo-cytoplasmic shuttling of peroxisome proliferator-activated receptors, PPAR alpha and PPAR gamma, *Genes Cells* 17 (2012) 576–596, <https://doi.org/10.1111/j.1365-2443.2012.01607.x>.
- [239] L. Massa, S. Baltrusch, D.A. Okar, et al., Interaction of 6-phosphofructo-2-kinase/fructose-296-bisphosphatase (PFK-2/FBPase-2) with glucokinase activates glucose phosphorylation and glucose metabolism in insulin-producing cells, *Diabetes* 53 (2004) 1020–1029, <https://doi.org/10.2337/diabetes.53.4.1020>.
- [240] H. Harada, B. Becknell, M. Wilm, et al., Phosphorylation and inactivation of BAD by mitochondria-anchored protein kinase A, *Mol. Cell* 3 (1999) 413–422, [https://doi.org/10.1016/s1097-2765\(00\)80469-4](https://doi.org/10.1016/s1097-2765(00)80469-4).
- [241] H. Harada, J.S. Andersen, M. Mann, et al., p70S6 kinase signals cell survival as well as growth, inactivating the pro-apoptotic molecule BAD, *Proc. Natl. Acad. Sci. USA* 98 (2001) 9666–9670, <https://doi.org/10.1073/pnas.171301998>.
- [242] K.I. Rother, R.J. Brown, Novel Forms of Lipodystrophy Why should we care? *Diabetes Care* 36 (2013) 2142–2145, <https://doi.org/10.2337/dc13-0561>.
- [243] L.R. Strickland, F.J. Guo, K. Lok, et al., Type 2 Diabetes With Partial Lipodystrophy of the Limbs A new lipodystrophy phenotype, *Diabetes care* 36 (2013) 2247–2253, <https://doi.org/10.2337/dc12-1529>.
- [244] P.Y. Yang, H.F. Zou, C. Lee, et al., Stapled, Long-Acting Glucagon-like Peptide 2 Analog with Efficacy in Dextran Sodium Sulfate Induced Mouse Colitis Models, *J. Med. Chem.* 61 (2018) 3218–3223, <https://doi.org/10.1021/acs.jmedchem.7b00768>.
- [245] Y. Lai, M.J. Tuvim, J. Leitz, et al., Screening of Hydrocarbon-Stapled Peptides for Inhibition of Calcium-Triggered Exocytosis, *Front Pharm.* 13 (2022) 891041, <https://doi.org/10.3389/fphar.2022.891041>.
- [246] Y. Lai, G. Pois, J.R. Flores, et al., Inhibition of calcium-triggered secretion by hydrocarbon-stapled peptides, *Nature* 603 (2022) 949–956, <https://doi.org/10.1038/s41586-022-04543-1>.
- [247] A. Pal, K. Neo, L. Rajamani, et al., Inhibition of NLRP3 inflammasome activation by cell-permeable stapled peptides, *Sci. Rep. -Uk* 9 (2019) 4913, <https://doi.org/10.1038/s41598-019-41211-3>.
- [248] Q. Wang, F.Z. Wang, R. Li, et al., Fine tuning the properties of stapled peptides by stereogenic alpha-amino acid bridges, *Chem. -Eur. J.* (2023) e202203624, <https://doi.org/10.1002/chem.202203624>.
- [249] J.J. Meier, M.A. Nauack, A. Pott, et al., Glucagon-like peptide 2 stimulates glucagon secretion, enhances lipid absorption, and inhibits gastric acid secretion in humans, *Gastroenterology* 130 (2006) 44–54, <https://doi.org/10.1053/j.gastro.2005.10.004>.

- [250] K. Austin, M.A. Markovic, P.L. Brubaker, Current and potential therapeutic targets of glucagon-like peptide-2, *Curr. Opin. Pharm.* 31 (2016) 13–18, <https://doi.org/10.1016/j.coph.2016.08.008>.
- [251] A.L. Buchman, S. Katz, J.C. Fang, et al., Teduglutide, a Novel Mucosally Active Analog of Glucagon-Like Peptide-2 (GLP-2) for the Treatment of Moderate to Severe Crohn's Disease, *Inflamm. Bowel Dis.* 16 (2010) 962–973, <https://doi.org/10.1002/ibd.21117>.
- [252] D.L. Seidner, F. Joly, N.N. Youssef, Effect of teduglutide, a glucagon-like peptide 2 analog, on citrulline levels in patients with short bowel syndrome in two phase iii randomized trials, *Clin. Transl. Gastroen* 6 (2015) e93, <https://doi.org/10.1038/ctg.2015.15>.
- [253] J. Iturrino, M. Camilleri, A. Acosta, et al., Acute effects of a glucagon-like peptide 2 analogue, teduglutide, on gastrointestinal motor function and permeability in adult patients with short bowel syndrome on home parenteral nutrition, *J. Parent. Enter. Nutr.* 40 (2016) 1089–1095, <https://doi.org/10.1177/0148607115597644>.
- [254] D.R. Curran, L. Cohn, Advances in mucous cell metaplasia a plug for mucus as a therapeutic focus in chronic airway disease, *Am. J. Respir.* 42 (2010) 268–275, <https://doi.org/10.1165/rcmb.2009-0151TR>.
- [255] Q.J. Zhou, Y. Lai, T. Bacaj, et al., Architecture of the synaptotagmin-SNARE machinery for neuronal exocytosis, *Nature* 525 (2015) 62–67, <https://doi.org/10.1038/nature14975>.
- [256] C.A. Dinarello, A. Simon, J.W.M. van der Meer, Treating inflammation by blocking interleukin-1 in a broad spectrum of diseases, *Nat. Rev. Drug Discov.* 11 (2012) 633–652, <https://doi.org/10.1038/nrd3800>.
- [257] C. Conforti-Andreoni, P. Ricciardi-Castagnoli, A. Mortellaro, The inflammasomes in health and disease: from genetics to molecular mechanisms of autoinflammation and beyond, *Cell Mol. Immunol.* 8 (2011) 135–145, <https://doi.org/10.1038/cmi.2010.81>.
- [258] A.V. Hauenstein, L.M. Zhang, H. Wu, The hierarchical structural architecture of inflammasomes, supramolecular inflammatory machines, *Curr. Opin. Struct. Biol.* 31 (2015) 75–83, <https://doi.org/10.1016/j.sbi.2015.03.014>.
- [259] C. de Torre-Minguela, P.M. del Castillo, P. Pelegrin, The NLRP3 and Pypin Inflammasomes: implications in the pathophysiology of autoinflammatory diseases, *Front Immunol.* 8 (2017) 43, <https://doi.org/10.3389/fimmu.2017.00043>.
- [260] M. Hoffmann, H. Kleine-Weber, S. Schroeder, et al., SARS-CoV-2 Cell Entry Depends on ACE2 and TMPRSS2 and Is Blocked by a Clinically Proven Protease Inhibitor, *Cell* 181 (2020) 271–280, <https://doi.org/10.1016/j.cell.2020.02.052>.
- [261] T. Liu, W. Cong, L. Ye, et al., Rational design of stapled peptides targeting phosphorylated GSK3beta for regulating osteoclast differentiation, *Rsc Adv.* 10 (2020) 7758–7763, <https://doi.org/10.1039/d0ra00008f>.
- [262] W. Cong, H. Shen, X. Liao, et al., Discovery of an orally effective double-stapled peptide for reducing ovariectomy-induced bone loss in mice, *Acta Pharm. Sin.* B (2023) 3770–3781, <https://doi.org/10.1016/j.apsb.2023.05.004>.
- [263] S. Maretto, S. Mammi, E. Bissacco, et al., Mono- and bicyclic analogs of parathyroid hormone-related protein.2. Conformational analysis of antagonists by CD NMR, and distance geometry calculations, *Biochem. -Us* 36 (1997) 3300–3307, <https://doi.org/10.1021/bi9619031>.
- [264] C. Yost, G.H. Farr, S.B. Pierce, et al., GBP, an inhibitor of GSK-3, is implicated in Xenopus development and oncogenesis, *Cell* 93 (1998) 1031–1041, [https://doi.org/10.1016/S0092-8674\(00\)81208-8](https://doi.org/10.1016/S0092-8674(00)81208-8).
- [265] Pharmacotherapy for Postmenopausal Osteoporosis (Reprinted from Medical Letter on Drugs and Therapeutics, vol 62, pg 105-112, 2020) 325 *Jama-J. Am. Med Assoc* 2021, 1888–1889, 10.1001/jama.2020.13841.
- [266] S. Minisola, C. Cipriani, G. Della Grotta, et al., Update on the safety and efficacy of teriparatide in the treatment of osteoporosis, 1759720×19877994, *Ther. Adv. Musculoskel* 11 (2019), <https://doi.org/10.1177/1759720×19877994>.
- [267] M. Chorev, R.F. Epanand, M. Rosenblatt, et al., Circular dichroism (CD) studies of antagonists derived from parathyroid hormone-related protein, *Int. J. Pept. Protein Res* 42 (1993) 342–345, <https://doi.org/10.1111/j.1399-3011.1993.tb00503.x>.
- [268] L. Peraro, Z.J. Zou, K.M. Makwana, et al., Diversity-oriented stapling yields intrinsically cell-penetrant inducers of autophagy, *J. Am. Chem. Soc.* 139 (2017) 7792–7802, <https://doi.org/10.1021/jacs.7b01698>.
- [269] T. Jayakody, S. Marwari, R. Lakshminarayanan, et al., Hydrocarbon stapled B chain analogues of relaxin-3 retain biological activity, *Peptides* 84 (2016) 44–57, <https://doi.org/10.1016/j.peptides.2016.08.001>.
- [270] E. Muratspahić, A.M. White, C.I. Ciotu, et al., Development of a selective peptide κ-opioid receptor antagonist by late-stage functionalization with cysteine staples, *J. Med Chem.* (2023) 11843–11854, <https://doi.org/10.1021/acs.jmedchem.3c00426>.
- [271] X.H. Liang, S. Jackson, M. Seaman, et al., Induction of autophagy and inhibition of tumorigenesis by beclin 1, *Nature* 402 (1999) 672–676, <https://doi.org/10.1038/45257>.
- [272] Z. Zhong, E. Sanchez-Lopez, M. Karin, Autophagy, inflammation, and immunity: a troika governing cancer and its treatment, *Cell* 166 (2016) 288–298, <https://doi.org/10.1016/j.cell.2016.05.051>.
- [273] S. Shoji-Kawata, R. Sumpter, M. Leveno, et al., Identification of a candidate therapeutic autophagy-inducing peptide, *Nature* 494 (2013) 201–206, <https://doi.org/10.1038/nature11866>.
- [274] A.K. Cardozo, V. Buchillier, M. Mathieu, et al., Cell-permeable peptides induce dose- and length-dependent cytotoxic effects, *Bba-Biomembr.* 1768 (2007) 2222–2234, <https://doi.org/10.1016/j.bbamem.2007.06.003>.
- [275] B.M. McGowan, S.A. Stanley, K.L. Smith, et al., Effects of acute and chronic relaxin-3 on food intake and energy expenditure in rats, *Regul. Pept.* 136 (2006) 72–77, <https://doi.org/10.1016/j.regpep.2006.04.009>.
- [276] S.W. Sutton, J. Shelton, C. Smith, et al., Metabolic and Neuroendocrine Responses to RXFP3 Modulation in the Central Nervous System, *Relaxin Relat. Pept.: Fifth Int. Conf.* 1160 (2009) 242–249, <https://doi.org/10.1111/j.1749-6632.2008.03812.x>.
- [277] J. Munro, O. Skrobot, M. Sanyoura, et al., Relaxin polymorphisms associated with metabolic disturbance in patients treated with antipsychotics, *J. Psychopharmacol.* 26 (2012) 374–379, <https://doi.org/10.1177/0269881111408965>.
- [278] H. Yamamoto, H. Shimokawa, T. Haga, et al., The expression of relaxin-3 in adipose tissue and its effects on adipogenesis, *Protein Pept. Lett.* 21 (2014) 517–522, <https://doi.org/10.2174/0929866520666131217101424>.
- [279] M. Matsumoto, M. Kamohara, T. Sugimoto, et al., The novel G-protein coupled receptor SALPR shares sequence similarity with somatostatin and angiotensin receptors, *Gene* 248 (2000) 183–189, [https://doi.org/10.1016/S0378-1119\(00\)00123-2](https://doi.org/10.1016/S0378-1119(00)00123-2).
- [280] S. Marwari, A. Poulsen, N. Shih, et al., Intranasal administration of a stapled relaxin-3 mimetic has anxiolytic- and antidepressant-like activity in rats, *Brit J. Pharm.* 176 (2019) 3899–3923, <https://doi.org/10.1111/bph.14774>.
- [281] F.I. Carroll, W.A. Carlezon, Jr, Development of κ opioid receptor antagonists, *J. Med Chem.* 56 (2013) 2178–2195, <https://doi.org/10.1021/jm301783x>.
- [282] M.L. Dalefield, B. Scouller, R. Bibi, et al., The Kappa Opioid Receptor: a promising therapeutic target for multiple pathologies, *Front. Pharm.* 13 (2022) 837671, <https://doi.org/10.3389/fphar.2022.837671>.